



University of Tennessee, Knoxville

## TRACE: Tennessee Research and Creative Exchange

---

Doctoral Dissertations

Graduate School


---

12-2012

### Condensed Matter from Gauge/Gravity Duality

Jason Edward Therrien  
jtherrie@utk.edu

Follow this and additional works at: [https://trace.tennessee.edu/utk\\_graddiss](https://trace.tennessee.edu/utk_graddiss)

 Part of the [Condensed Matter Physics Commons](#), and the [Elementary Particles and Fields and String Theory Commons](#)

---

#### Recommended Citation

Therrien, Jason Edward, "Condensed Matter from Gauge/Gravity Duality. " PhD diss., University of Tennessee, 2012.  
[https://trace.tennessee.edu/utk\\_graddiss/1567](https://trace.tennessee.edu/utk_graddiss/1567)

This Dissertation is brought to you for free and open access by the Graduate School at TRACE: Tennessee Research and Creative Exchange. It has been accepted for inclusion in Doctoral Dissertations by an authorized administrator of TRACE: Tennessee Research and Creative Exchange. For more information, please contact [trace@utk.edu](mailto:trace@utk.edu).

To the Graduate Council:

I am submitting herewith a dissertation written by Jason Edward Therrien entitled "Condensed Matter from Gauge/Gravity Duality." I have examined the final electronic copy of this dissertation for form and content and recommend that it be accepted in partial fulfillment of the requirements for the degree of Doctor of Philosophy, with a major in Physics.

George Siopsis, Major Professor

We have read this dissertation and recommend its acceptance:

Adolfo Eguiluz, Norman Mannella, Henry Simpson

Accepted for the Council:

Carolyn R. Hodges

Vice Provost and Dean of the Graduate School

(Original signatures are on file with official student records.)

# Condensed Matter from Gauge/Gravity Duality

A Dissertation

Presented for the

Doctor of Philosophy

Degree

The University of Tennessee, Knoxville

Jason Edward Therrien

December 2012

© by Jason Edward Therrien, 2012  
All Rights Reserved.

*This dissertation is dedicated to my loving wife. I couldn't have done it without you.*

# Acknowledgements

Throughout my academic career, I have recieved support from many people. I would like to thank

- Colleagues, for all the discussions over the years.
- Professors, for sharing their love of physics with me.
- The Department of Energy and the University of Tennessee, Department of Physics and Astronomy, for funding
- My numerous collaborators
  - George Siopsis (UT)
  - Jim Alsup (UM-Flint)
  - Suphot Musiri (Srinakharinwirot University)
  - Suman Ganguli (UT)
  - Jimmy Hutasoit (Penn State)
- My advisor, George Siopsis, for his  $\infty$  patience over the years and for all the knowledge he has shared with me.
- My wife, Meredith, without her I don't know where I would be.

# Abstract

Currently strongly coupled systems present the greatest challenge to theoretical physics. For years conventional methods of approach have failed to describe these systems analytically. In recent years it has been shown that there is a duality between weakly coupled and strongly coupled systems, the Gauge Theory/Gravity Duality. In this dissertation I will discuss how the AdS/CFT is used to describe strongly coupled condensed matter systems as well as present the work done by the author and collaborators.

# Contents

<b>1</b>	<b>Introduction</b>	<b>1</b>
1.1	Introduction . . . . .	1
1.1.1	AdS/CFT . . . . .	2
1.1.2	History . . . . .	3
1.1.3	Heavy Ion Collisions . . . . .	4
1.1.4	AdS/CFT and Condensed Matter . . . . .	5
1.2	Superconductivity . . . . .	6
1.2.1	Weak Coupling . . . . .	6
1.2.2	Strong Coupling . . . . .	7
1.2.3	Ginzburg-Landau Theory . . . . .	7
1.2.4	Thesis Outline . . . . .	9
<b>2</b>	<b>Phase Transitions</b>	<b>11</b>
2.1	Probe Limit: $q \rightarrow \infty$ . . . . .	14
2.1.1	Anisotropy . . . . .	15
2.2	The Limit of Neutral Scalar Hair: $q \rightarrow 0$ . . . . .	25
2.2.1	The Critical Temperature . . . . .	26
<b>3</b>	<b>Superconducting Phase</b>	<b>35</b>
3.1	Immediately below $T_c$ . . . . .	35
3.2	The Limit $T \rightarrow 0$ . . . . .	37
3.2.1	Probe Limit . . . . .	37



3.2.2	Anisotropy . . . . .	53
3.2.3	$T \ll T_c$ . . . . .	62
3.2.4	As $q \rightarrow 0$ . . . . .	64
<b>4</b>	<b>Transport</b>	<b>68</b>
4.1	Probe Limit . . . . .	70
4.1.1	BF Bound . . . . .	76
4.2	as $q \rightarrow 0$ . . . . .	85
<b>5</b>	<b>Conclusion</b>	<b>88</b>
	<b>Bibliography</b>	<b>91</b>
	<b>Appendices</b>	<b>99</b>
	A Operators and the AdS/CFT Correspondence . . . . .	99
	B Hawking Temperature . . . . .	101
	<b>Vita</b>	<b>103</b>

# List of Tables

1.1 A few examples of the AdS/CFT Dictionary . . . . . 3

# List of Figures

1.1	A comparison of $\frac{\eta}{s}$ for different liquids. The red line corresponds to the lower bound(12)	5
2.1	The critical temperature $T_c$ <i>vs</i> the scaling dimension $\Delta$ for $d = 3$ (left panel) and $d = 4$ (right panel). Data points represent exact values; solid line is obtained by minimizing (2.21) with the trial function (2.22).	16
2.2	Critical temperature $T_c$ for $\delta = 1$ and $\Delta = 2$ obtained numerically. For $\Delta > 3/2$ , there is a critical modulation $Q^*$ , at which $T_c$ discontinuously drops to zero. Here, $Q^* = 0.288 \mu$ . The lower branch in $Q < Q^*$ regime is unstable.	19
2.3	The critical temperature as a function of $Q_c$ for $\Delta = 1$ . The black lines are obtained by numerical analysis and the dashed red lines, which are closer to the numerical results, are obtained by perturbative method.	24
2.4	The critical temperature as a function of $Q/\mu$ for $\Delta = 1$ . The black solid lines, dashed red lines and the dashed blue lines are obtained by numerical analysis, perturbative method and variational method, respectively.	24
2.5	The critical temperature $T_c$ as a function of $q^2$ found by a numerical solution (dashed) and an analytic one based on hypergeometric functions (solid) for $\Delta = 1$ (left panel) and $\Delta = 2$ (right panel). $T_c \rightarrow 0$ as $q^2 \rightarrow -\frac{1}{4}$ .	29
2.6	The critical coupling constant $q^2$ <i>vs.</i> $\Delta$ (boundary of the shaded region).	32

2.7	The critical temperature <i>vs.</i> the coupling constant $q^2$ for $\Delta = 0.634, 0.578, 0.525, 0.501$ (curves become steeper as $\Delta$ decreases). . . . .	33
2.8	The critical temperature $T_c$ found by a variational method (dashed) compared to numerical results (solid), for $\Delta = 1$ (left panel) and $\Delta = 2$ (right panel). . . . .	34
3.1	The parameter $\gamma$ that determines the condensate near the critical temperature <i>vs.</i> the dimension of the condensate $\Delta$ (eq. (3.6)). . . . .	36
3.2	The eigenvalue $\hat{\mathcal{A}}$ defined in (3.19) as a function of $\Delta$ [solid line] compared with the estimate (3.21) [dashed line]. . . . .	41
3.3	The parameter $\alpha$ that determines the approximation (3.22) to the scalar field as a function of $\Delta$ . . . . .	42
3.4	The condensate at zero temperature as a function of $\Delta$ . The solid line is our analytic estimate whereas the dashed line is the exact numerical result. . . . .	44
3.5	This figure is taken from (25). They have used $\lambda$ as the dimension of the operator that condenses(I have used $\Delta$ ) The left and right figures are qualitatively similar. The BF bound is saturated for $\lambda = 3/2$ and 2 for $d=3$ and 4 respectively. In (25) they claim that at the BF bound the condensate increases linearly as $\frac{T}{T_c} \rightarrow 0$ . . . . .	45
3.6	The field $F$ for $\Delta = 1.2$ (left panel), 1.4 (middle panel), 1.5 (right panel) and $d = 3$ . Solid curves are first-order analytic expression (3.44), and dashed curves are exact numerical results (almost indistinguishable) at $T/T_c \approx 0.1$ . . . . .	45
3.7	The field $F$ for $\Delta = 1.6$ (left panel), 1.8 (middle panel), 2 (right panel) and $d = 4$ . Solid curves are first-order analytic expression (3.44), and dashed curves are exact numerical results (almost indistinguishable) at $T/T_c \approx 0.2$ . . . . .	46

3.8	The field $F$ for $\Delta = 1.2$ (left panel), 1.4 (middle panel), 1.5 (right panel) and $d = 3$ . Solid curves are first-order analytic expression (3.44), and dashed curves are exact numerical results (almost indistinguishable) at $T/T_c \approx 0.1$ . . . . .	48
3.9	The field $F$ for $\Delta = 1.6$ (left panel), 1.8 (middle panel), 2 (right panel) and $d = 4$ . Solid curves are first-order analytic expression (3.44), and dashed curves are exact numerical results (almost indistinguishable) at $T/T_c \approx 0.2$ . . . . .	48
3.10	The second order correction to the scalar field $F$ for $d = 3$ , $\Delta = 1.4$ at $b = 20$ ( $T/T_c \sim 0.1$ ) (solid line) and $b = 200$ ( $T/T_c \sim 0.01$ ) (dashed line). . . . .	49
3.11	The second order correction to the scalar field $F$ for $d = 3$ , $\Delta = 1.4$ as a function of temperature at the mid-point, $z = \frac{1}{2}$ , (left panel) and the horizon, $z = 1$ , (right panel). The horizontal axis corresponds to the temperature range $0.01 \lesssim \frac{T}{T_c} \lesssim 0.1$ with $T$ decreasing to the right. . . . .	50
3.12	The parameter $\gamma$ in the low temperature expression (3.54) for the condensate <i>vs</i> $\Delta$ . Curve on left (right) is for $d = 3$ ( $d = 4$ ). . . . .	50
3.13	The ratio $\frac{\langle \mathcal{O}_\Delta \rangle^{(1)}}{\langle \mathcal{O}_\Delta \rangle^{(0)}} \frac{Q_c^2}{\lambda^2 \delta (1-\delta)}$ as a function $\Delta$ . . . . .	55
3.14	The ratio $\frac{\langle \mathcal{O}_\Delta \rangle^{(2)}}{\langle \mathcal{O}_\Delta \rangle^{(0)}} \frac{Q_c^2}{\lambda^2 \delta^2}$ as a function $\Delta$ . . . . .	56
3.15	The expectation value of the condensate for $\delta = 1$ and $\Delta = 1$ for $Q_c = 6, 33$ and $55$ . The solid black lines and the dashed blue lines depict the numerical and analytical results, respectively. . . . .	61
3.16	The energy gap for $q^2 = 0$ , and $\Delta = 1, 1.5, 1.7$ (left to right). The thin line is our first-order analytic result, the thick one is from numerics. . . . .	67
3.17	Left panel: energy gap <i>vs</i> temperature for $\Delta = 1.5$ $q^2 = 0.38$ (lower curve), $q^2 = 0$ (middle curve), and $q^2 = -.125$ (upper curve). Right panel: energy gap <i>vs</i> $q^2$ at temperature $T = .95T_c$ (asymptote at $q^2 = -0.375$ ). . . . .	67

4.1	The real and imaginary parts of the conductivity at low temperatures for $\Delta = 2$ . . . . .	73
4.2	The imaginary part of the conductivity in $d = 3$ using the expression (3.44) for the scalar field (dotted line) compared with the exact numerical solution (solid line) at $\frac{T}{T_c} \approx .1$ . . . . .	80
4.3	The imaginary part of the conductivity <i>vs.</i> frequency in $d = 3$ using the expression (3.44) for $F$ at $\frac{T}{T_c} \approx .05$ (left), $.04$ (right). As the temperature decreases, poles move toward the real axis. . . . .	80
4.4	Comparison of the imaginary part of the conductivity in $d = 3$ using the expression (3.44) for $F$ at $\frac{T}{T_c} \approx .01$ (dotted line) and the $b \rightarrow \infty$ limit (4.57) (solid line). . . . .	81
4.5	The imaginary part of the conductivity in $d = 4$ using the expression (3.44) for the scalar field (dotted line) compared with the exact numerical solution (solid line) at $\frac{T}{T_c} \approx .17$ . . . . .	83
4.6	The imaginary part of the conductivity <i>vs.</i> frequency in $d = 4$ using the expression (3.44) for $F$ at $\frac{T}{T_c} \approx .1$ (left), $.04$ (right). . . . .	84
4.7	The imaginary part of the conductivity in the (unphysical) limit $b \rightarrow \infty$ in $d = 4$ (4.67). . . . .	84
4.8	Real and imaginary parts of the conductivity. . . . .	86
4.9	Comparison of analytic and numerical results on the real and imaginary parts of the conductivity (left and right panel, respectively). . . . .	86
4.10	Left panel: the potential determining the conductivity for $q = 0$ at various temperatures below $T_c$ . Right panel shows detail near the horizon. . . . .	87

# Chapter 1

## Introduction

### 1.1 Introduction

The AdS\*/CFT<sup>†</sup> correspondence, which was discovered in the late 90's, was initially used to describe strongly coupled systems in Heavy Ion physics. Recently it has been shown that we can also use this correspondence to describe condensed matter systems as well. In this thesis proposal I will review what the AdS/CFT is and its history. I will give a very brief overview of the history and theory of Superconductivity. I will show some of the major results when this correspondence is used to describe a system that superconducts. Finally I will discuss my work so far, as well as a future program of research.

---

\*AdS stands for Anti de Sitter space. In the vacuum Einstein's equations are  $R_{\mu\nu} - \frac{1}{2}Rg_{\mu\nu} + \Lambda g_{\mu\nu} = 0$  where  $R_{\mu\nu}$  and  $R$  are the Ricci Tensor and Scalar, respectively,  $g_{\mu\nu}$  is the metric, and  $\Lambda$  is the cosmological constant that defines the global structure of the space. If it is zero the space is flat, if it is positive the space is de Sitter space(a Lorentzian sphere), and if it is negative the space is Anti de Sitter(a Lorentzian hyperbolic space).

<sup>†</sup>A conformal field theory is a theory that is invariant under conformal transformations, e.g. rotations and dilations. As a result the theory is scale invariant and  $\beta(g) = E \frac{\partial g}{\partial E} = 0$ , where  $g$  is the coupling constant of the theory.

### 1.1.1 AdS/CFT

In recent years much research has been done in the area of gauge theory/string theory duality, where the string theory is a weakly coupled theory and the gauge theory that it is dual to is strongly coupled. The most successful of these is the AdS/CFT duality. Some examples are

- type IIB on  $AdS_3 \times S^3 \times T^4$
- M-theory on  $AdS_4 \times S^7$
- type IIB on  $AdS_5 \times S^5$
- M-theory on  $AdS_7 \times S^4$

These theories are all dual to a superconformal field theory in 2,3,4, and 6 dimensions, respectively. The equivalence between a gravitational theory in the bulk and a gauge theory in the boundary requires that both theories have exactly the same symmetries. If the space is empty then it is at zero temperature and so is the boundary CFT. If we wish to explore the thermodynamic properties of the boundary CFT then we must introduce thermodynamics in the bulk. It's long been known that black holes have temperature and entropy, so if we place a black hole in the bulk we introduce temperature into the system. The temperature of the black hole is then the temperature of the dual field theory. The duality is made holographic since the partition functions of each theory are equivalent(1)

$$Z_{AdS} = Z_{CFT} \tag{1.1}$$

This means that all of the information of the black hole becomes translated at the boundary. The AdS/CFT dictionary (2)(3) tells us how fields in the bulk translate to observables in the CFT.



**Table 1.1:** A few examples of the AdS/CFT Dictionary

Bulk	CFT
Scalar Field- $\psi$	An observable- $\langle \mathcal{O} \rangle$
Gauge Field- $A_\mu$	A current - $J_\mu$
Metric- $g_{\mu\nu}$	Stress Tensor- $T_{\mu\nu}$

In this manner all of the physics in one system is included in the other system (this works both ways, while most research is currently directed at describing strongly correlated CFT's, this could also be used to make predictions about quantum gravity).

### 1.1.2 History

In 1993 't Hooft laid the ground work for gauge/gravity dualities(4) along with Susskind in 1994(5). While these papers concerned a 3 dimensional space that is entirely described by a 2 dimensional space, the idea of the world existing as a Hologram took a foot hold in the string theory community. The first gauge/string duality was proposed by Banks, Fischler, Shenker and Susskind, who showed that M-theory was dual to  $N = \infty$  supersymmetric matrix quantum mechanics(6). In 1997 it was shown by Maldacena(7) that the large N limit of certain field theories was dual to a quantum theory of gravity. In particular he was able to show that  $\mathcal{N} = 4$  SU(N) Super Yang-Mills in 4 dimensions was dual to  $AdS_5 \times S^5$ . In the case of  $\mathcal{N} = 4$  Super Yang-Mills the supergroup is  $SU(2,2|4)^\dagger$ , which is the same supergroup that describes type IIB string theory, and thus these 2 theories are dual to each other. Witten was then able to make this correspondence more precise(3), and showed how correlators in the dual CFT arose from the Gravity Action. In the large N limit the theory in the bulk is classical, and the higher order corrections to the CFT,  $\frac{1}{N^2}, \frac{1}{N^3}, \dots$ , correspond to quantum corrections and require quantum corrections to the theory in the bulk. Because of this we can use classical gravity in bulk to do our calculations.

---

<sup>†</sup>A superalgebra  $SU(m|n)$  contains the subalgebra  $SU(m) \times SU(n) \times U(1)$ . If  $n=m$   $U(1)$  decouples.

So far this duality has found applications in Heavy Ion Collisions resulting in quark gluon plasmas, and in strongly correlated condensed matter systems, mainly superconductivity, though there have been other applications.

### 1.1.3 Heavy Ion Collisions

For the last several decades scientists have tried to create a state of matter thought to occur in the earliest stages of our universe, the Quark Gluon Plasma. In the last decade though scientists at the Relativistically Heavy Ion Collider at Brookhaven claim to have created a QGP (they are the first so far and we are still waiting on independent confirmation from the LHC). Standard attempts to describe the QGP using QCD have failed because the QGP forms at a temperature where the quarks are still strongly correlated and is deep within the non-perturbative regime of QCD. Since it is a strongly coupled system AdS/CFT is used to investigate the system. In 2001 Policastro, Son, and Starinets(8) showed that the duality between type IIB and SYM could be used to calculate the shear viscosity of a strongly coupled fluid which is applied in the context of quark gluon plasmas. You will note that SYM and QCD are in fact two different theories and realistically we would want to have a theory that was dual to QCD. People have been working on this, but currently this program has not born much fruit(9; 10). There are good reasons though to use SYM to describe the QGP. In this regime QCD and SYM have several features in common that make SYM an attractive model to describe QGP(11). One of the more interesting results to come from this study is that there is a lower bound on the ratio of viscosity to entropy density of a strongly coupled fluid(12)

$$\frac{\eta}{s} \geq \frac{1}{4\pi} \tag{1.2}$$

It has been shown that the QGP seen at RHIC does not violate(and actually comes very close to) this bound(13).

For further reading a few reviews are (14; 11; 15)

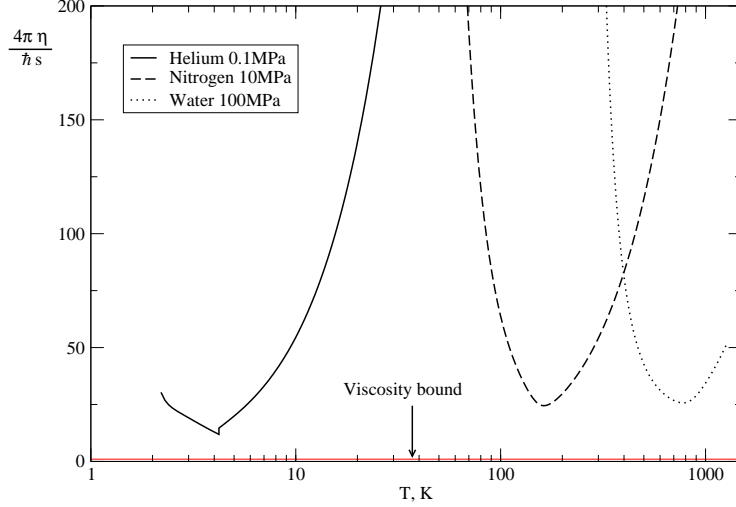


**Figure 1.1:** A comparison of  $\frac{\eta}{s}$  for different liquids. The red line corresponds to the lower bound(12)

#### 1.1.4 AdS/CFT and Condensed Matter

Starting in 2007 the AdS/CFT was applied to quantum critical transport(16) showing that the AdS/CFT could be useful in exploring transport properties in 2+1 dimensional systems. This led to a few papers exploring the Hall effect(17) and the application to the Nernst effect(18; 19; 20). In 2008 Gubser showed that with a charged scalar field could you could break gauge invariance of a black hole, suggesting that it could superconduct(22). Following up on this Hartnoll, Herzog, and Horowitz(23) showed that in the absence of backreaction that this model did in fact have a second order phase transition and were able to demonstrate that the model was able to support AC current that were qualitatively like those found in superconductors, and that the DC conductivity was infinite. Then depending on which boundary condition you chose, defining the theory that lives on the boundary, the absence of backreaction caused the theory to have two different behaviors as  $T \rightarrow 0$ . In the probe limit as  $T \rightarrow 0$  one of the theories has a divergent energy gap. It was later shown that this was fixed when backreaction was allowed and the full Einstein equations were solved(24).

While these papers were able to go to low temperatures, in both cases the numerics broke down, in most cases at  $\frac{T}{T_c} \sim .1$  and the ground state was inaccessible. Two papers appeared at roughly the same time in which the problems were fixed numerically(25; 26) and later on the ground state of the probe limit was investigated analytically by us(27). With the ground state accessible, exploration of the Fermi surface has begun(29).

After it was discovered that these systems could in fact superconduct the next question was what kind of superconductor were they? In the BCS theory of weakly coupled superconductors,  $2E_g = 3.54T_c$  at  $T=0$ . It is well known that strongly coupled superconductors have a much larger value of  $E_g$ . (30) showed that this was in fact the case with holographic superconductors. Another question was: what happens when a magnetic field is applied? Most high  $T_c$  superconductors (all of the cuprates-the most studied class of strongly coupled superconductors) are type-II superconductors. It was shown (24; 32; 33) that holographic superconductors were in fact type-II. These studies were done with a 2+1 holographic superconductor, and the problem has not been looked at in 3+1 dimensions(34). So far the program has been very promising.

## 1.2 Superconductivity

### 1.2.1 Weak Coupling

Conventional superconductors were discovered at the turn of the 20<sup>th</sup> century. These consisted of mainly type-I superconductors, where below the critical temperature the superconducting state can be completely destroyed by an applied magnetic field. In 1950, Ginzburg and Landau proposed the GL-theory of superconductivity, and in 1952 Abrikosov showed that another type of superconductor can exist, one in which there is a mixed state that occurs between a lower critical magnetic field and an upper magnetic field. These are known as type-II superconductors. While Landau's theory explained a lot about superconductivity, it was not a quantum theory and did not

explain the mechanism which causes the phase transition (in fact it doesn't care, GL theory is still used today to describe strongly correlated superconductors as well). In 1954 Leon Cooper had the initial insight that allowed the problem to be solved microscopically (46). He said that given the Hamiltonian of two electrons

$$H = -\frac{\hbar^2}{2m} (\nabla_1^2 + \nabla_2^2) + V(r_1, r_2) \quad (1.3)$$

we can approximate the potential as a constant and no matter how small that constant is there is always at least one bound state and the electrons form (Cooper) pairs. This assumes the electrons have energy no more than  $E_F + \hbar\omega_D$ , where  $\omega_D$  is the Debye frequency which defines the maximum frequency at which a lattice can vibrate (and therefore the maximum speed with which phonons can propagate). Since the transition temperature is directly proportional to the Debye energy, there is a maximum theoretical limit on  $T_c$  for weakly coupled superconductors.

### 1.2.2 Strong Coupling

In the 1980's it was discovered that superconductors existed with  $T_c$ 's higher than the theoretical maximum predicted by BCS theory. Because of this (and other factors) the binding mechanism is thought to be different in these materials. The cuprates, the most well studied of these HTc superconductors, is effectively a 2+1 dimensional system. For more than 2 decades it has withstood efforts to create a model that explains the binding mechanism and the normal state of the system which isn't a Fermi liquid(36).

### 1.2.3 Ginzburg-Landau Theory

In the Ginzburg-Landau Theory of Superconductivity(37) the initial assumption is that there is some complex order parameter which minimizes the free energy of the system. We care not how the order parameter arose, just that it was due to a second

order phase transition. Following from the Landau theory of second order phase transitions we can write down the free energy density of the system.

$$f = f_n + \frac{1}{4m} \left| (\nabla - i2q\vec{A})\psi \right|^2 + \alpha |\psi|^2 + \beta |\psi|^4 \quad (1.4)$$

We include terms up to the fourth order and the first spatial derivative<sup>§</sup>.  $f_n$  is the free energy density of the normal state. Varying  $f$  with respect to  $\psi$  we get

$$\left( 2\beta |\psi|^2 + \alpha + \frac{1}{4m} \left| \nabla - i2q\vec{A} \right|^2 \right) \psi = 0 \quad (1.5)$$

Note there is a surface term that gives a boundary condition.  $\frac{\delta f}{\delta \vec{A}}$  gives the current

$$\vec{j} = \frac{qi}{2m} \left( \psi^* \left( \nabla - i2q\vec{A} \right) \psi \right) \quad (1.6)$$

These are the celebrated Ginzburg-Landau equations.

If we consider a spatially homogeneous system with a very weak magnetic field, then  $\nabla\psi=0$  and eqn.(1.5) has the solution  $|\psi|^2 = -\frac{\alpha}{\beta}$ . Note that the trivial solution,  $\psi = 0$  must be approached as  $T \rightarrow T_c$  and therefore  $\alpha$  is a function of  $T - T_c$ . We can derive the London equation

$$\nabla \times \nabla \times \vec{B} = \nabla^2 \vec{B} = c \nabla \times \vec{j} = 4\pi \frac{2q^2}{m} \frac{\alpha}{\beta} \vec{B} \quad (1.7)$$

and therefore the penetration depth is

$$\delta = \left( \frac{\beta m}{8\pi q \alpha} \right)^{\frac{1}{2}} \quad (1.8)$$

---

<sup>§</sup>A few motivations for choosing a free energy density of this form are the free energy must be real and cannot depend on the phase of  $\psi$

Note that at  $T_c$  the penetration depth diverges and magnetic lines fully penetrate the sample. The correlation length of the bound electrons is given by

$$\xi(T) = \frac{1}{2} \left( \frac{1}{m |T - T_c|} \right)^{\frac{1}{2}} \quad (1.9)$$

We can derive the Ginzburg Landau parameter from this. It is the ratio of these two numbers.

$$\kappa = \frac{\delta}{\xi} = \frac{m}{q} \left( \frac{\beta m}{2\pi} \right)^{\frac{1}{2}} \quad (1.10)$$

This parameter defines what type of superconductor is described. For  $\kappa < \frac{1}{\sqrt{2}}$  it is type-I, and for  $\kappa \geq \frac{1}{\sqrt{2}}$  it is type-II.  $\kappa$  is independent of the temperature.

It was shown by Gor'kov in 1959 (38) that G-L theory can be derived from BCS theory.

## 1.2.4 Thesis Outline

### Outline of Chapter 2

In this chapter we will begin by introducing the problem that we are interested studying and build the frame work needed to study the problem using the AdS/CFT correspondence. We will span the parameter space and show that an instability arises in our system that leads to a second order phase transition. We will first look at the probe limit in an isotropic space, and will later allow our matter field to be anisotropic corresponding to a charge density wave. We will then look at the extremal limit of Reissner-Nordstrom AdS where isotropic fields are allowed to back react on the geometry.

### Outline of Chapter 3

We will begin by looking just below  $T_c$  to learn about the transition from the normal state to the superconducting state. Then, we will look at the system in the low temperature limit. We wish to study two particular regimes of our system. In both

regimes numerical results are not adequate to describe these systems, and we use analytical tools to derive new results. Specifically, we are interested in determining when the backreaction from our matter fields on the geometry can no longer be ignored. We will then look at what happens when the charge of the scalar, which is thought to be analagous to a Cooper pair, vanishes.

#### **Outline of Chapter 4**

Using the results from Chapter 3, we will apply an electromagnetic perturbation to the system. This will allow us to study the linear response of the system and determine its transport properties.

#### **Outline of Chapter 5**

Finally we will conclude with a summary and outlook for future work.



# Chapter 2

## Phase Transitions

Let us consider the system given by the action

$$S = \int d^{d+1} \sqrt{-g} \left[ \frac{R + d(d-1)/l^2}{16\pi G} - \frac{1}{4} F_{\mu\nu} F^{\mu\nu} - |(\partial_\mu - iqA_\mu)\Psi|^2 - m^2 |\Psi|^2 \right] \quad (2.1)$$

where  $F = dA$ ,  $l$  is the AdS radius, which we can set to one, and  $G$  is the gravitational constant.

We shall work with the metric ansatz

$$ds^2 = \frac{1}{z^2} \left[ -f(z) e^{-\chi(z)} dt^2 + d\vec{x}^2 + \frac{dz^2}{f(z)} \right] \quad (2.2)$$

where  $z \in (0, 1]$  with  $z=0$  corresponding to the AdS boundary, and  $z$  has been scaled such that  $z=1$  corresponds to the black hole horizon,  $f(1) = 0$ .  $\vec{x} \in \mathbb{R}^{d-1}$ . For now let us concentrate on isotropic electric and scalar fields

$$A = \Phi(z) dt, \quad \Psi = \Psi(z) \quad (2.3)$$

The equations of motion that follow from this action are given by

$$\begin{aligned}
\Psi'' + \left[ \frac{f'}{f} - \frac{\chi'}{2} - \frac{d-1}{z} \right] \Psi' + \left[ \frac{q^2 \Phi^2 e^\chi}{f^2} - \frac{m^2}{z^2 f} \right] \Psi &= 0 \\
\Phi'' + \left[ \frac{\chi'}{2} - \frac{d-3}{z} \right] \Phi' - \frac{2q^2 \Psi^2}{z^2 f} \Phi &= 0 \\
-\frac{d-1}{2} \chi' + z \Psi'^2 + \frac{z q^2 \Phi^2 \Psi^2}{f^2} e^\chi &= 0 \\
\frac{f}{2} \Psi'^2 + \frac{z^2}{4} \Phi'^2 e^\chi - \frac{d-1}{2} \frac{f'}{z} + \frac{d(d-1)}{2} \frac{f-1}{z^2} + \frac{m^2 \Psi^2}{2z^2} + \frac{q^2 \Psi^2 \Phi^2 e^\chi}{2f} &= 0 \quad (2.4)
\end{aligned}$$

The  $d=3$  and  $4$  cases are of particular interest because they correspond to in plane (cuprates and pnictides) and bulk superconductivity, respectively.

Near the boundary ( $z \rightarrow 0$ ) we must recover the AdS metric, therefore we have

$$\chi \rightarrow 0, \quad f \rightarrow 1 \quad (2.5)$$

Integrating the equations of motion for the scalar and electric potential leads to

$$\Psi \approx \Psi^{(\pm)} z^{\Delta_{\pm}}, \quad \Phi \approx \mu - \rho z^{d-2} \quad (2.6)$$

where  $\Psi^{(\pm)}$  are two integration constants corresponding to two expectation values of conformal dimension  $\Delta_{\pm}$ ,  $\mu$  is the chemical potential and  $\rho$  is the charge density.  $\Delta$  is related to the mass of the scalar field

$$\Delta_{\pm} = \frac{d}{2} \pm \sqrt{\frac{d^2}{4} + m^2} \quad (2.7)$$

and

$$\langle \mathcal{O}_{\Delta_{\pm}} \rangle = \sqrt{2} \Psi^{(\pm)} \quad (2.8)$$

Where the normalization factor of  $\sqrt{2}$  is chosen to conform to existing literature. For  $m^2 < -\frac{d^2}{4}$  (Breitenlohner-Freedman (BF) bound (42)),  $\Delta_{\pm}$  have an imaginary part and the system is unstable. For  $-\frac{d^2}{4} \leq m^2 < -\frac{d^2}{4} + 1$ , both modes are normalizable.

While a linear combination of these modes is allowed by the field equations, it turns out that any such combination is unstable (47). However, if the horizon has negative curvature, such linear combinations lead to stable configurations in certain cases (39). Thus, the system is labeled uniquely by the dimension  $\Delta = \Delta_{\pm}$ . For  $m^2 \geq -\frac{d^2}{4} + 1$ , only the mode of scaling dimension  $\Delta_+$  is normalizable. It follows that  $\Delta = \Delta_- > \frac{d-2}{2}$  (unitarity bound)(40). At the horizon we require that

$$\Phi(1) = 0 \tag{2.9}$$

This gauge choice is made so that  $A = \Phi dt$  is regular at the horizon (22).

Finally we demand regularity of  $\Psi$  as  $z \rightarrow 1$ . This can be achieved by applying Eq. (2.9) to the scalar equation of motion giving

$$f'(1)\Psi'(1) = m^2\Psi(1) \tag{2.10}$$

This leaves us with a one parameter family of solutions. We find it convient to allow that parameter to be

$$\frac{T}{T_c} \propto \rho^{\frac{1}{1-d}} \tag{2.11}$$

Where T is given by the Hawking temperature of the black hole

$$T = -\frac{(f(z)e^{-\chi(z)/2})'}{4\pi} \Big|_{z=1} \tag{2.12}$$

If instead of an isotropic ansatz we choose

$$\Psi = \Psi(z, x) \quad A = A(z, x)dt \tag{2.13}$$

we have the following equations of motion

$$A'' - \frac{2\Psi^2}{z^2 h} A + \frac{\partial_x^2 A}{r_+^2 h} = 0, \quad (2.14)$$

$$\Psi'' + \left( \frac{h'}{h} - \frac{2}{z} \right) \Psi' + \left( \frac{A^2}{r_+^2 h^2} - \frac{m^2}{z^2 h} \right) \Psi + \frac{\partial_x^2 \Psi}{r_+^2 h} = 0, \quad (2.15)$$

## 2.1 Probe Limit: $q \rightarrow \infty$

In the probe limit the matter fields decouple from gravity, ie they no longer effect the geometry and we can work in a fixed background. Expanding in large  $q$  we have

$$\begin{aligned} \Psi &= \frac{1}{q} \left[ \Psi_0 + \frac{\Psi_1}{q^2} + \dots \right] \\ \Phi &= \frac{1}{q} \left[ \Phi_0 + \frac{\Phi_1}{q^2} + \dots \right] \\ f &= f_0 + \frac{f_1}{q^2} + \dots \\ \chi &= \chi_0 + \frac{\chi_1}{q^2} + \dots \end{aligned} \quad (2.16)$$

It is convenient to write

$$\Psi(z) = \frac{1}{\sqrt{2q}} b^\Delta z^\Delta F(z), \quad b = \langle q \mathcal{O}_\Delta \rangle^{1/\Delta} \quad (2.17)$$

In the probe limit\* we have

$$f_0 = 1 - z^d, \quad \chi_0 = 0 \quad (2.18)$$

and the equations of motion become

$$\begin{aligned} -F_0'' + \frac{1}{z} \left[ \frac{d}{1 - z^d} - 1 - 2\Delta \right] F_0' + \frac{\Delta^2 z^{d-2}}{1 - z^d} F_0 - \frac{1}{(1 - z^d)^2} \Phi_0^2 F_0 &= 0 \\ \Phi_0'' - \frac{d-3}{z} \Phi_0' - \frac{b^{2\Delta} z^{2(\Delta-1)}}{1 - z^d} F_0^2 \Phi_0 &= 0 \end{aligned} \quad (2.19)$$

---

\*When talking about the probe limit we will often drop the subscript "0"

For  $T > T_c$  a solution to these equations exist,  $F = 0$ ,  $\Phi = \lambda(1 - z^{d-2})$  with  $\lambda$  being an integration constant. As we approach  $T_c$  we can treat  $F$  as a perturbation and we can find  $\lambda$  by solving the eigenvalue problem given by

$$-F_0'' + \frac{1}{z} \left[ \frac{d}{1-z^d} - 1 - 2\Delta \right] F_0' + \frac{\Delta^2 z^{d-2}}{1-z^d} F_0 = \lambda^2 \frac{(1-z^{d-2})^2}{(1-z^d)^2} F_0 \quad (2.20)$$

With this redefinition our boundary conditions become  $F(0) = 1$  and  $F'(0) = 0$  for all  $\Delta$ .  $\lambda^2$  minimizes the expression

$$\lambda^2 = \frac{\int dz z^{2\Delta-d+1} \{ (1-z^d) F_0'(z)^2 + \Delta^2 z^{d-2} F_0(z)^2 \}}{\int dz z^{2\Delta-d+1} \frac{(1-z^{d-2})^2}{1-z^d} F_0(z)^2} \quad (2.21)$$

We can obtain an estimate of the eigenvalue by using the trial function

$$F_0 = F_\alpha \equiv 1 - \alpha z^{d-1} \quad (2.22)$$

This obeys our boundary conditions,  $F_\alpha(0) = 1$ ,  $F_\alpha'(0) = 0$  and  $F$  is regular at the horizon. From figure 2.1 we see that the trial function provides a very good approximation for solution obtained from direct numeric integration. Of interest is that the limit,  $\Delta \rightarrow \Delta_{BF} = \frac{d}{2}$  is well defined and we are able to saturate the BF bound.

### 2.1.1 Anisotropy

If instead of a homogenous system we consider one in which the charge density is no longer constant, but instead being sourced by a modulated charge density wave we are able to study the effects of inhomogeneity in our system. This modulation is done as an outside perturbation. This differs from the case of charge density waves studied in AdS/CFT (60), for which a mechanism exists that allows for SDW to exist from

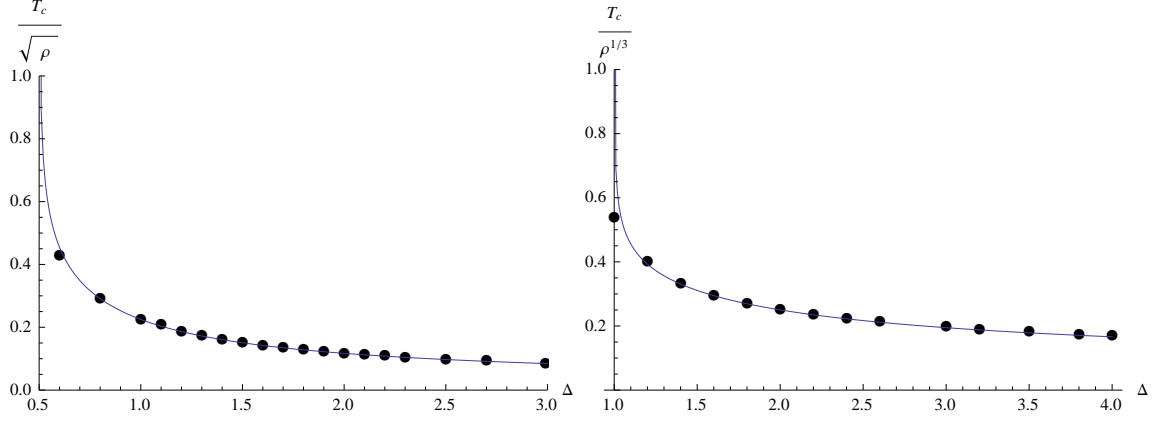


**Figure 2.1:** The critical temperature  $T_c$  vs the scaling dimension  $\Delta$  for  $d = 3$  (left panel) and  $d = 4$  (right panel). Data points represent exact values; solid line is obtained by minimizing (2.21) with the trial function (2.22).

first principles. We shall pick as our ansatz

$$\Phi(z, x) = \mu \sum_{n \geq 0} \delta^{(n)} \Phi^{(n)}(z) \cos nQx$$

$$\Psi = \frac{\langle \mathcal{O}_\Delta \rangle^{(0)}}{\sqrt{2}} \frac{z^\Delta}{r_+^\Delta} \sum_{n \geq 0} F^{(n)}(z) \cos nQx \quad (2.23)$$

$$(2.24)$$

with

$$\sum_{n \geq 0} \delta^{(n)} = 1, \quad (2.25)$$

And with each mode subject to our previous boundary conditions.

For our analysis, we will only concetrate on 2 Fourier modes, then  $\delta^{(1)} = \delta$  and  $\delta^{(0)} = 1 - \delta$ . This way  $\delta$  controls the amount of in homogeniety in the system, with  $\delta = 0$  corresponding to the homogenous case. Above  $T_c$  the order parameter vanishes, but the modulation is still present, therefore we can use the solutions to the field equation

$$\Phi^{(n)''} - \frac{n^2 Q^2 \Phi^{(n)}}{r_+^2 h} = 0. \quad (2.26)$$

to provide solutions for  $\Psi$  using either a variational method or perturbation theory.

## Variational Method

The equation of motion for the scalar field can be written as

$$\begin{aligned}
hz^{2\Delta-2} F^{(n)''} &+ (hz^{2\Delta-2})' F^{(n)'} + [(h-1)\Delta^2 - n^2 Q_c^2 z^2] z^{2\Delta-4} F^{(n)} \\
&= -\mu_c^2 \frac{z^{2\Delta-2}}{h} \left[ (1-\delta)^2 A^{(0)2} F^{(n)} - \delta(1-\delta) A^{(0)} A^{(1)} (F^{(n-1)} + F^{(n+1)}) \right. \\
&\quad \left. + \frac{\delta^2}{4} A^{(1)2} (F^{(n-2)} + 2F^{(n)} + F^{(n+2)}) \right], \tag{2.27}
\end{aligned}$$

where  $\mu_c (Q_c)$  is the chemical potential (wavenumber) in units of the horizon radius at the critical point,

$$\mu_c = \frac{\mu}{r_{+c}}, \quad Q_c = \frac{Q}{r_{+c}}. \tag{2.28}$$

Looking at the  $n = 0$  equation, the eigenvalue  $\mu_c$  minimizes the expression

$$\mu_c^2 = \frac{\int_0^1 dz z^{2\Delta-4} \{hz^2 (F^{(0)'} )^2 - (h-1)\Delta^2 (F^{(0)})^2\}}{\int_0^1 dz \frac{z^{2\Delta-2}}{h} F^{(0)} \{ (1-\delta)^2 A^{(0)2} F^{(0)} - 2\delta(1-\delta) A^{(0)} A^{(1)} F^{(1)} + \frac{\delta^2}{2} A^{(1)2} (F^{(0)} + F^{(2)}) \}}. \tag{2.29}$$

Since at large  $Q$ , it is expected (and numerical study confirms) that  $F^{(0)} \gg F^{(1)}, F^{(2)}$ , the above expression reduces to

$$\begin{aligned}
\mu_c^2 &= \frac{\int_0^1 dz z^{2\Delta-4} \{hz^2 (F^{(0)'} )^2 - (h-1)\Delta^2 (F^{(0)})^2\}}{\int_0^1 dz \frac{z^{2\Delta-2}}{h} (F^{(0)})^2 \{ (1-\delta)^2 A^{(0)2} + \frac{\delta^2}{2} A^{(1)2} \}} \\
&\approx \frac{\int_0^1 dz z^{2\Delta-4} \{hz^2 (F^{(0)'} )^2 - (h-1)\Delta^2 (F^{(0)})^2\}}{\int_0^1 dz \frac{z^{2\Delta-2}}{h} (1-\delta)^2 A^{(0)2} (F^{(0)})^2 + \frac{\Gamma(2\Delta-1)}{2^{2\Delta}} \frac{\delta^2}{Q_c^{2\Delta-1}}} \tag{2.30}
\end{aligned}$$

In the absence of a homogeneous term in the chemical potential ( $\delta = 1$ ), Eq. (2.30) becomes

$$\mu_c^2 = \frac{2^{2\Delta}}{\Gamma(2\Delta-1)} Q_c^{2\Delta-1} \int_0^1 dz z^{2\Delta-4} \{hz^2 (F^{(0)'} )^2 - (h-1)\Delta^2 (F^{(0)})^2\} \tag{2.31}$$

Using the trial function  $F^{(0)} = 1 - \alpha z^2$ , we obtain

$$\mu_c^2 = \frac{2^{2\Delta}}{\Gamma(2\Delta - 1)} \left( \frac{2\Delta^2 - 3\Delta + 6}{2(2\Delta + 1)} \alpha^2 - \frac{\Delta^2}{\Delta + 1} \alpha + \frac{\Delta}{2} \right) Q_c^{2\Delta-1}. \quad (2.32)$$

The minimum is attained at

$$\alpha = \frac{\Delta^2(2\Delta + 1)}{(\Delta + 1)(2\Delta^2 - 3\Delta + 6)}, \quad (2.33)$$

which results in the estimate

$$\mu_c^2 = \frac{2^{2\Delta-1}\Delta}{\Gamma(2\Delta - 1)} \frac{2\Delta^2 + 9\Delta + 6}{(\Delta + 1)^2(2\Delta^2 - 3\Delta + 6)} Q_c^{2\Delta-1}. \quad (2.34)$$

Recall that for the above derivation to be valid, we needed  $Q_c \gtrsim 1$  (i.e.,  $Q \gtrsim T_c$ ).

Therefore,  $\mu_c \gtrsim 1$ . Since

$$\frac{Q}{\mu} = \frac{Q_c}{\mu_c} \sim \mu_c^{\frac{3-2\Delta}{2\Delta-1}} \quad (2.35)$$

it follows that for  $\Delta > \frac{3}{2}$ ,  $Q/\mu \lesssim 1$ , suggesting that there is a critical value of  $Q$  above which there is no phase transition. This sudden drop in the critical temperature has been observed in the numerical studies, see Fig. 2.2.

For  $\Delta < \frac{3}{2}$ , we deduce the estimate of the critical temperature,

$$\frac{T_c}{\mu} = \frac{3}{4\pi} \left[ \frac{2^{2\Delta-1}\Delta}{\Gamma(2\Delta - 1)} \frac{2\Delta^2 + 9\Delta + 6}{(\Delta + 1)^2(2\Delta^2 - 3\Delta + 6)} \right]^{\frac{1}{2\Delta-3}} \left( \frac{Q}{\mu} \right)^{-\frac{2\Delta-1}{3-2\Delta}}. \quad (2.36)$$

For  $\Delta = 1$ , we have  $\mu_c^2 = 1.7 Q_c$  and

$$\frac{T_c}{\mu} = \frac{0.14}{Q/\mu}. \quad (2.37)$$

Thus the critical temperature has a power law behavior in the large  $Q$  limit. Of course, this is only an estimate of  $T_c$ . Nevertheless, the exponent of  $Q$  is confirmed by the perturbative method to be discussed later, which yields not only the exponent but also the multiplicative coefficient accurately in the case  $\delta = 1$ . We shall also



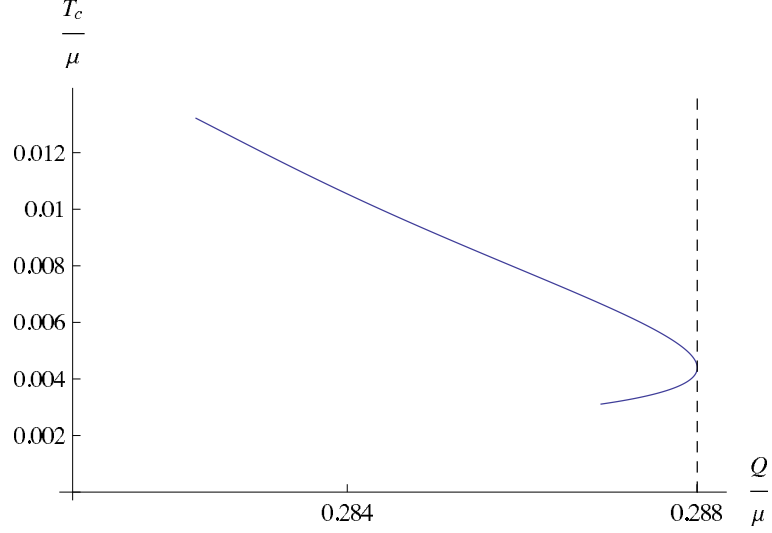


**Figure 2.2:** Critical temperature  $T_c$  for  $\delta = 1$  and  $\Delta = 2$  obtained numerically. For  $\Delta > 3/2$ , there is a critical modulation  $Q^*$ , at which  $T_c$  discontinuously drops to zero. Here,  $Q^* = 0.288 \mu$ . The lower branch in  $Q < Q^*$  regime is unstable.

compare this with the numerical results to assess the accuracy of the results of the variational method.

In the presence of a homogeneous term in the chemical potential ( $\delta \neq 1$ ), Eq. (2.30) becomes

$$\mu_c^2 = \frac{\int_0^1 dz z^{2\Delta-4} \{hz^2(F^{(0)'})^2 - (h-1)\Delta^2 (F^{(0)})^2\}}{\int_0^1 dz \frac{z^{2\Delta-2}}{h} (1-\delta)^2 (1-z)^2 (F^{(0)})^2} - \frac{\int_0^1 dz z^{2\Delta-4} \{hz^2(F^{(0)'})^2 - (h-1)\Delta^2 (F^{(0)})^2\}}{\left[\int_0^1 dz \frac{z^{2\Delta-2}}{h} (1-\delta)^2 (1-z)^2 (F^{(0)})^2\right]^2} \frac{\Gamma(2\Delta-1)}{2^{2\Delta}} \frac{\delta^2}{Q_c^{2\Delta-1}} \quad (2.38)$$

where we have approximated the second integral in the denominator by evaluating the integrand near the horizon. We note that the subleading term is not exponentially suppressed as suggested, based on numerical calculations (58), but is a power law in  $Q$ . This is to be contrasted with the  $1/\log Q$  behavior seen in the weak coupling BCS calculation (59).

Since the second term in the last line is subleading, we can find the eigenvalue  $\mu_c$  by first minimizing the leading term using a trial function

$$F^{(0)} = 1 - \alpha z^2. \quad (2.39)$$

For  $\Delta = 1$ , the minimum is attained at  $\alpha \approx 0.24$ , which yields

$$\mu_c^2 = \frac{1.27}{(1 - \delta)^2} - \frac{0.94 \delta^2}{(1 - \delta)^4 Q_c}. \quad (2.40)$$

The critical temperature is

$$\frac{T_c}{\mu} \approx 0.21 (1 - \delta) + \frac{0.078 \delta^2}{Q/\mu}. \quad (2.41)$$

We note that in obtaining the last line of Eq. (2.38), we have assumed that the first term of the denominator is much greater than the second one. Obviously, this assumption is not always valid. In particular, it is easy to see that the limit  $\delta \rightarrow 1$  does not commute with the large  $Q$  limit.

## Perturbation Theory

To gain more insight, let us solve the equation of motion for  $F^{(0)}$  by treating the electrostatic potential as a perturbation to a leading order solution, which is nothing but that of a scalar field on an AdS Schwarzschild black hole without any background  $U(1)$  gauge field

$$F_0^{(0)''} + \left( \frac{h'}{h} + \frac{2(\Delta - 1)}{z} \right) F_0^{(0)'} - \frac{\Delta^2 z}{h} F_0^{(0)} = 0. \quad (2.42)$$

Here,  $F_0^{(0)}$  is the leading term of the solution. Strictly speaking, this perturbation is valid only when  $\delta \approx 1$ , however, as we shall see in a bit, the result is a good approximation even when  $\delta$  is far away from unity.

The solution that satisfies the correct boundary conditions at  $z = 0$  is

$$F_0^{(0)} = {}_2F_1\left(\frac{\Delta}{3}, \frac{\Delta}{3}, \frac{2\Delta}{3}; z^3\right), \quad (2.43)$$

where  ${}_2F_1$  is the Gauss hypergeometric function. There is another solution, which corresponds to the solution with the correct boundary conditions for  $\Delta \rightarrow 3 - \Delta$

$$\tilde{F}_0^{(0)} = z^{3-2\Delta} {}_2F_1\left(\frac{3-\Delta}{3}, \frac{3-\Delta}{3}, \frac{2(3-\Delta)}{3}; z^3\right). \quad (2.44)$$

Using perturbation theory, we obtain the next leading order solution, which is given by

$$\begin{aligned} F_1^{(0)}(z) &= \frac{\mu_c^2}{3-2\Delta} \left( F_0^{(0)}(z) \int_0^z \frac{dz'}{z'^{2-2\Delta}} \tilde{F}_0^{(0)} \frac{\mathcal{A}}{h} F_0^{(0)} - \tilde{F}_0^{(0)}(z) \int_0^z \frac{dz'}{z'^{2-2\Delta}} F_0^{(0)} \frac{\mathcal{A}}{h} F_0^{(0)} \right) \\ &\equiv \frac{\mu_c^2}{3-2\Delta} \left( F_0^{(0)}(z) \tilde{a}(z) - \tilde{F}_0^{(0)}(z) a(z) \right), \end{aligned} \quad (2.45)$$

where

$$\mathcal{A}(z) = (1-\delta)^2 A^{(0)2} + \frac{\delta^2 A^{(1)2}}{2}. \quad (2.46)$$

As both  $F_0^{(0)}$  and  $\tilde{F}_0^{(0)}$  diverge logarithmically at the horizon, we obtain the following singularity for the full solution

$$\begin{aligned} F^{(0)}(z \rightarrow 1) &= F_0^{(0)}(z \rightarrow 1) + F_1^{(0)}(z \rightarrow 1) + \dots \\ &\approx \log(1-z) \left\{ \frac{\Gamma\left(\frac{2\Delta}{3}\right)}{\Gamma^2\left(\frac{\Delta}{3}\right)} \left[ 1 + \frac{\mu_c^2 \tilde{a}(1)}{3-2\Delta} \right] - \frac{\Gamma\left(\frac{2(3-\Delta)}{3}\right)}{\Gamma^2\left(\frac{3-\Delta}{3}\right)} \frac{\mu_c^2 a(1)}{3-2\Delta} \right\}, \end{aligned} \quad (2.47)$$

where

$$\begin{aligned} a(1) &\approx (1-\delta)^2 a_0^{(0)} + \frac{\Gamma(2\Delta-1)}{2^{2\Delta}} \frac{\delta^2}{Q_c^{2\Delta-1}}, \\ \tilde{a}(1) &\approx (1-\delta)^2 \tilde{a}_0^{(0)} + \frac{1}{8} \frac{\delta^2}{Q_c^2}, \end{aligned} \quad (2.48)$$

with

$$\begin{aligned} a_0^{(0)} &= \int_0^1 \frac{dz}{z^{2-2\Delta}} F_0^{(0)} \frac{(1-z)^2}{h} F_0^{(0)}, \\ \tilde{a}_0^{(0)} &= \int_0^1 \frac{dz}{z^{2-2\Delta}} \tilde{F}_0^{(0)} \frac{(1-z)^2}{h} F_0^{(0)}. \end{aligned} \quad (2.49)$$

In obtaining Eq. (2.48), we have approximated the subleading integrals by evaluating the integrand near the boundary  $z = 0$ .

Requiring regularity at the horizon, we obtain

$$\begin{aligned} \frac{1}{\mu_c^2} &= \frac{1}{3-2\Delta} \left( \frac{\Gamma^2\left(\frac{\Delta}{3}\right)}{\Gamma\left(\frac{2\Delta}{3}\right)} \frac{\Gamma\left(\frac{2(3-\Delta)}{3}\right)}{\Gamma^2\left(\frac{3-\Delta}{3}\right)} a(1) - \tilde{a}(1) \right) \\ &= \left( \frac{\Gamma^2\left(\frac{\Delta}{3}\right)}{\Gamma\left(\frac{2\Delta}{3}\right)} \frac{\Gamma\left(\frac{2(3-\Delta)}{3}\right)}{\Gamma^2\left(\frac{3-\Delta}{3}\right)} a_0^{(0)} - \tilde{a}_0^{(0)} \right) \frac{(1-\delta)^2}{3-2\Delta} + \frac{\Gamma^2\left(\frac{\Delta}{3}\right)}{\Gamma\left(\frac{2\Delta}{3}\right)} \frac{\Gamma\left(\frac{2(3-\Delta)}{3}\right)}{\Gamma^2\left(\frac{3-\Delta}{3}\right)} \frac{\Gamma(2\Delta-1)}{2^{2\Delta}(3-2\Delta)} \frac{\delta^2}{Q_c^{2\Delta-1}}, \end{aligned} \quad (2.50)$$

where we have dropped the term proportional to  $1/Q_c^2$  on the last line. Both terms in Eq. (2.50) are small, but to connect this result with the result from variational method Eqs. (2.40) and (2.36), we make two different approximations in which one is a lot larger than the other.

When the first term is significantly larger than the second one, for  $\Delta = 1$ , we have

$$\mu_c^2 = \frac{1.19}{(1-\delta)^2} - \frac{0.91 \delta^2}{(1-\delta)^4 Q_c}, \quad (2.51)$$

which agrees well with Eq. (2.40). We would like to emphasize that this agreement is valid even when  $\delta$  is far away from unity.

When the second term is significantly larger than the first, we have

$$\mu_c^2 = \frac{\Gamma\left(\frac{2\Delta}{3}\right)}{\Gamma^2\left(\frac{\Delta}{3}\right)} \frac{\Gamma\left(\frac{3-\Delta}{3}\right)}{\Gamma\left(\frac{2(3-\Delta)}{3}\right)} \frac{2^{2\Delta}(3-2\Delta)}{\Gamma(2\Delta-1)} \frac{Q_c^{2\Delta-1}}{\delta^2}. \quad (2.52)$$

For  $\Delta = 1$ ,  $\delta = 1$ , we then have  $\mu_c^2 = 1.55 Q_c$  and

$$\frac{T_c}{\mu} = \frac{0.15}{Q/\mu}, \quad (2.53)$$

which agrees with the previous result obtained by variational method Eq. (2.37).

We would like to note that for  $\delta = 1$  and  $\Delta > 3/2$ , Eq. 2.52 does not have any solutions. This is related to the fact that for  $\delta = 1$  and  $\Delta > 3/2$ , there is a critical  $Q^*$  such that  $T_c(Q > Q^*) = 0$ , as we have mentioned earlier.

Let us also comment on the  $\Delta = 1/2$  unitarity limit, which is singular. To approach it, we introduce a cutoff  $\Lambda$  in  $Q$ -space. From Eq. (2.50), we have

$$\frac{1}{\mu_c^2(Q)} - \frac{1}{\mu_c^2(\Lambda)} = \frac{\Gamma^2\left(\frac{\Delta}{3}\right)}{\Gamma\left(\frac{2\Delta}{3}\right)} \frac{\Gamma\left(\frac{2(3-\Delta)}{3}\right)}{\Gamma^2\left(\frac{3-\Delta}{3}\right)} \frac{\Gamma(2\Delta-1)}{2^{2\Delta}(3-2\Delta)} \delta^2 (Q^{1-2\Delta} - \Lambda^{1-2\Delta}). \quad (2.54)$$

If  $\Delta > 1/2$ , we can safely take the limit  $\Lambda \rightarrow \infty$ , in which  $\Lambda^{1-2\Delta} \rightarrow 0$  and  $\mu_c(\Lambda)$  has a finite limit. This is not so for the case of  $\Delta = 1/2$ . Taking the limit  $\Delta \rightarrow 1/2$ , we have

$$\lim_{\Delta \rightarrow \frac{1}{2}} \left[ \frac{1}{\mu_c^2(Q)} - \frac{1}{\mu_c^2(\Lambda)} \right] = \frac{\Gamma^2\left(\frac{1}{6}\right)}{\Gamma\left(\frac{1}{3}\right)} \frac{\Gamma\left(\frac{5}{3}\right)}{\Gamma^2\left(\frac{5}{6}\right)} \frac{\delta^2}{4} \log \frac{\Lambda}{Q}, \quad (2.55)$$

which shows that the limit  $\Lambda \rightarrow \infty$  is not well defined and that for  $\Delta = 1/2$ , the chemical potential is no longer a physical quantity. A well defined physical quantity would be

$$\frac{d}{d \log Q} \left[ \frac{1}{\mu_c^2(Q)} \right] = - \frac{\Gamma^2\left(\frac{1}{6}\right)}{\Gamma\left(\frac{1}{3}\right)} \frac{\Gamma\left(\frac{5}{3}\right)}{\Gamma^2\left(\frac{5}{6}\right)} \frac{\delta^2}{4}. \quad (2.56)$$

Lastly, let us compare the critical temperatures obtained by the variational and perturbative methods with the numerical result. This is depicted in Fig. 2.3. The agreement between the results obtained by analytical methods and the numerical results for  $Q_c \gtrsim 3$  is remarkable. We also show the critical temperature as a function of  $Q/\mu$  for different values of  $\delta$  in Fig. 2.4.

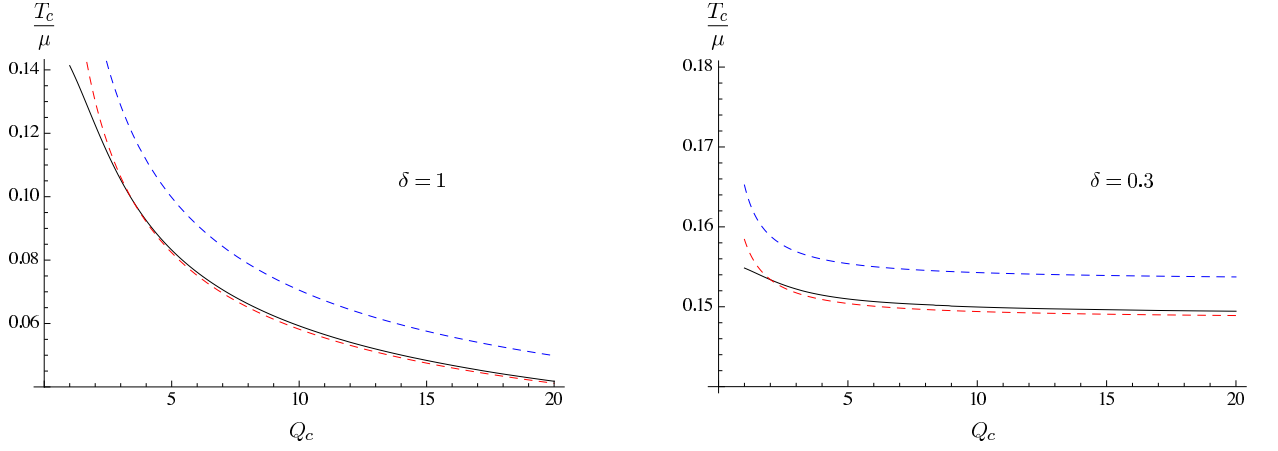


**Figure 2.3:** The critical temperature as a function of  $Q_c$  for  $\Delta = 1$ . The black lines are obtained by numerical analysis and the dashed red lines, which are closer to the numerical results, are obtained by perturbative method.

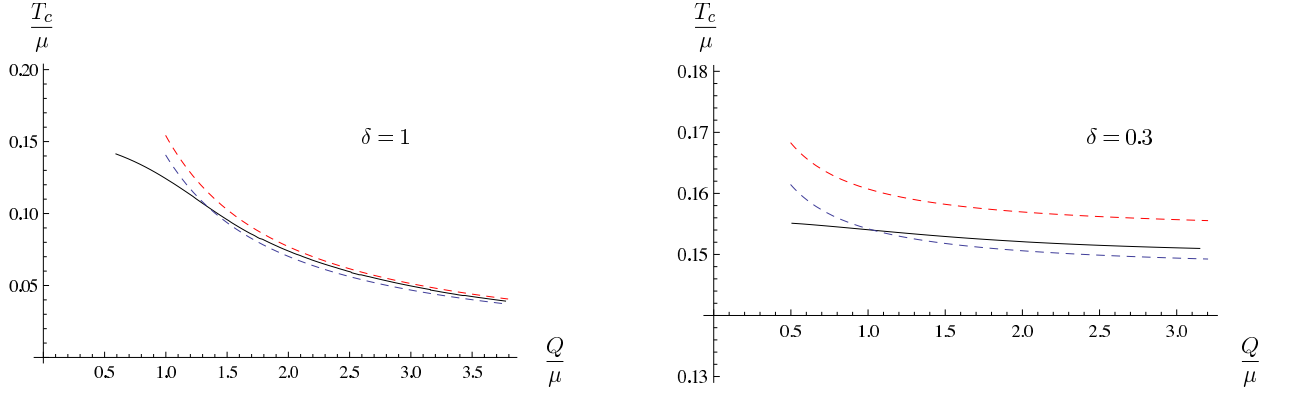


**Figure 2.4:** The critical temperature as a function of  $Q/\mu$  for  $\Delta = 1$ . The black solid lines, dashed red lines and the dashed blue lines are obtained by numerical analysis, perturbative method and variational method, respectively.

## 2.2 The Limit of Neutral Scalar Hair: $q \rightarrow 0$

The other limit of interest is  $q \rightarrow 0$ . In the probe limit, we found that a variational method produced extremely accurate results when it came to finding the critical temperatures. For values of  $q^2 \gg 0$  numerical integration allows for accurate results. However, as  $q \rightarrow q_c$  this is no longer the case and we must leverage analytical methods. In the following we outline two different analytical methods. The first is most accurate for larger values of  $\Delta$ . The second method seems to be accurate for all values of  $\Delta$ .

In this limit one naïvely expects  $T_c \rightarrow 0$ . Since the  $q$  is thought to be analogous to the charge of a Cooper pair (24), one would expect if the charge vanishes that you no longer have something analogous to a cooper pair. In initial studies it was shown, via numerics, that  $T_c \approx 0$  when  $q = 0$ . However, the numerics weren't enough to determine whether it was zero or not. Restricting our discussion to  $d=3$ , we consider a more general action

$$S = \int d^4x \sqrt{-g} \left[ \frac{R + 6/L^2}{16\pi G} - \frac{1}{4} F^{\mu\nu} F_{\mu\nu} - |D_\mu \phi|^2 - m^2 |\phi|^2 \right], \quad (2.57)$$

where  $D_\mu = \partial_\mu - iqA_\mu$ . We consider a complex scalar field

$$\phi = \frac{1}{\sqrt{2}} \psi e^{iq\theta}. \quad (2.58)$$

where  $\psi$  and  $\theta$  are real. The action then becomes

$$S = \frac{1}{2} \int d^4x \sqrt{-g} \left[ R + 6 - \frac{1}{2} F^{\mu\nu} F_{\mu\nu} - \partial_\mu \psi \partial^\mu \psi + q^2 \psi^2 (\partial_\mu \theta - A_\mu)^2 - m^2 \psi^2 \right]. \quad (2.59)$$

This action is invariant under the local U(1) transformations

$$A_\mu \rightarrow A_\mu + \partial_\mu \omega, \quad \theta \rightarrow \theta + \omega \quad (2.60)$$

We can fix the gauge by setting  $\theta = 0$ . This action is more general than our previous one, because we are allowed to continue  $q^2$  to negative values. This doesn't change the boundary conditions.

The Hawking temperature is

$$\frac{T}{\rho} = -\frac{f'(1)}{4\pi\sqrt{-\Phi'(0)}}e^{-\chi(1)/2} \quad (2.61)$$

As before, below  $T_c$  the equations of motion admit non-vanishing solutions for the scalar field and  $\chi$ . Above  $T_c$ , the system has a well known solution, a Reissner-Nordström black hole given by

$$f(z) = 1 - (1 + \frac{\rho^2}{4})z^3 + \frac{\rho^2}{4}z^4, \quad \Phi(z) = \rho(1 - z) \quad (2.62)$$

whose Hawking temperature is given by

$$\frac{T}{\rho} = \frac{1}{4\pi\sqrt{\rho}}(3 - \frac{\rho^2}{4}) \quad (2.63)$$

### 2.2.1 The Critical Temperature

To find the critical temperature we will solve the equation of motion of  $\Psi$  in the RN background.

$$\Psi'' + \left[ \frac{f'}{f} - \frac{2}{z} \right] \Psi' + \left[ \frac{q^2 \Phi^2}{f^2} - \frac{m^2}{z^2 f} \right] \Psi = 0 \quad (2.64)$$

We know from numerics, see (24), that the regime that we are interested in,  $q \rightarrow 0$  is near extremality

$$\frac{\rho^2}{4} = 3, \quad T = 0 \quad (2.65)$$

The near horizon solution to Eq.(2.64) behaves as

$$\Psi \sim (1 - z)^{\delta_{\pm}}, \quad \delta_{\pm} = -\frac{1}{2} \pm \frac{i}{\sqrt{3}} \sqrt{q^2 - \frac{3 + 2m^2}{4}} \quad (2.66)$$



This near horizon behaviour is due to the  $AdS_2 \times \mathbb{R}^2$  geometry near the horizon of our black hole. In this limit the BF bound is given by

$$q^2 \geq \frac{3 + 2m^2}{4} \quad (2.67)$$

as long as  $q$  and  $m$  satisfy this relationship there are potential instabilities that can lead to condensation of  $\Psi$ .

**$m^2 = -2$**

Let us concentrate on a particular value of  $m^2$  for now, the results are qualitatively similar to what is found other values of  $m^2$  but are simplified considerably. Let us consider a critical temperature near extremality

$$\frac{\rho^2}{4} = 3 - \epsilon, \quad T = T_0 = \frac{\epsilon}{4\pi} \quad (2.68)$$

where  $\epsilon \leq 1$ .

To find  $T_c$ , and therefore  $\epsilon$  we need to solve the system in 2 regimes, near and far horizon regimes. In the far field limit, the background is approximated by the extremal background, and solutions are

$$\begin{aligned} \Psi = \Psi_{\text{far}} &= \mathcal{C} \frac{z}{z - z_0} \left( \frac{z - z_0^*}{z - z_0} \right)^{\frac{2\sqrt{2}-i}{2\sqrt{3}}q} \left( \frac{1 - z}{z - z_0} \right)^{\delta_+} \\ &\times F \left( -\delta_- + 2\sqrt{\frac{2}{3}}q, -\delta_- - \frac{iq}{\sqrt{3}}; -2\delta_-; 2z_0^2 \frac{1 - z}{z - z_0} \right) + \text{c.c} \end{aligned} \quad (2.69)$$

where  $z_0, z_0^*$  are the 2 non real roots of  $f(z)$ . The multiplicative constant  $\mathcal{C}$  is complex, we can fix its phase, but  $|\mathcal{C}|$  will remain arbitrary since the field equation is linear in  $\Psi$ .

To find the near horizon solution one must exercise care. We begin by making the coordinate transformation

$$z = 1 - \frac{\epsilon}{6}\zeta \quad (2.70)$$

The horizon is at  $\zeta = 0$ .

The metric becomes

$$ds^2 = \frac{1}{6\zeta^2} \left[ -\epsilon^2 \zeta(1 + \zeta) dt^2 + \frac{d\zeta^2}{\zeta(1 + \zeta)} \right] + d\vec{x}^2 + \dots \quad (2.71)$$

where we only consider terms that are linear in  $\epsilon$ . The Hawking temperature is obviously unchanged by this transformation. The electrostatic potential reads

$$\Phi = \frac{\rho\epsilon}{6}\zeta + \dots \quad (2.72)$$

we can expand the field equation near the horizon in  $\epsilon$ , throwing away second order terms and higher

$$\zeta(1 + \zeta)\Psi'' + (2\zeta + 1)\Psi' + \frac{1}{3} \left[ 1 + q^2 \frac{\zeta}{1 + \zeta} \right] \Psi \quad (2.73)$$

where here primes denotes differentiation with respect to  $\zeta$ . The acceptable solution near the horizon (the other is not regular) is

$$\Psi_{near}(\zeta) = A(1 + \zeta)^{iq/\sqrt{3}} F(-\delta_+, -\frac{iq}{\sqrt{3}}, -\delta_-, -\frac{iq}{\sqrt{3}}; 1; -\zeta) \quad (2.74)$$

This is a real solution ( $\text{Im}(\Psi_{near}) = 0$ ) and can be shown using the identity

$$F(\alpha, \beta; \gamma; x) = (1 - x)^{\gamma - \alpha - \beta} F(\gamma - \alpha, \gamma - \beta; \gamma; x) \quad (2.75)$$

Now that we possess a full solution set we need to fix the integration constants. Our boundary conditions are found by matching the solutions at an arbitrary point (it turns out that it doesn't matter where, as long as it's near the horizon),  $\Psi_{far}(z \rightarrow 0) \approx z^\Delta$ ,

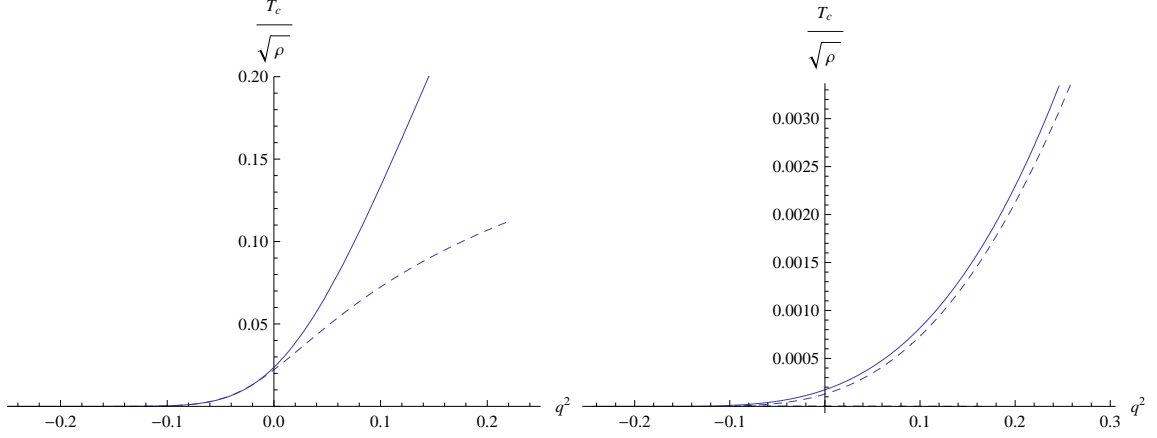


**Figure 2.5:** The critical temperature  $T_c$  as a function of  $q^2$  found by a numerical solution (dashed) and an analytic one based on hypergeometric functions (solid) for  $\Delta = 1$  (left panel) and  $\Delta = 2$  (right panel).  $T_c \rightarrow 0$  as  $q^2 \rightarrow -\frac{1}{4}$ .

and that  $\Psi_{near}(\zeta = 0)$  is regular. This will give us a solution that is unique up to an arbitrary normilization since the  $\Psi$  satisfies a linear equation of motion.

To match the solutions we should expand  $\Psi_{near}$  in the limit that  $\zeta \rightarrow \infty$  and  $\Psi_{far}$  in the limit that  $z \rightarrow 1$ . We have

$$\Psi_{far} \sim \mathcal{C}(1 - z_0)^{\delta_-} \left( \frac{1 - z_0^*}{1 - z_0} \right)^{\frac{2\sqrt{2}-i}{2\sqrt{3}}q} (1 - z)^{\delta_+} + \text{c.c.} \quad (2.76)$$

and

$$\Psi_{near} \approx A \frac{\Gamma(-1 - 2\delta_-)}{\Gamma(-\delta_- - \frac{iq}{\sqrt{3}})\Gamma(-\delta_- + \frac{iq}{\sqrt{3}})} \zeta^{\delta_+} + \text{c.c.}, \quad (2.77)$$

Using (2.70), we deduce the relation

$$\mathcal{C} = A \frac{\Gamma(-1 - 2\delta_-)}{\Gamma(-\delta_- + \frac{iq}{\sqrt{3}})\Gamma(-\delta_- - \frac{iq}{\sqrt{3}})} \left( \frac{\epsilon}{6} \right)^{-\delta_+} (1 - z_0)^{-\delta_-} \left( \frac{1 - z_0}{1 - z_0^*} \right)^{\frac{2\sqrt{2}-i}{2\sqrt{3}}q}. \quad (2.78)$$

Finally by choosing either  $\Delta_+$  or  $\Delta_-$  we can uniquely determine  $\epsilon$  as a function of  $q^2$

As you can see from figure (2.5), as expected  $T_c$  goes to zero as  $q \rightarrow q_c$ . One thing to note is that the small  $\epsilon$  approximation breaks down when  $\Delta \rightarrow \Delta_U = \frac{d-2}{2}$ .

## The Variational Method: A better result

For other values of  $\Delta$  there does exist closed form analytical solutions in the form of Heun functions. However these prove to be too unwieldy and we have to employ different methods to find solutions.

With this in mind we shall analyze this limit using a variational method. To that end Hartnoll et al.(24) attempted this type of analysis and were able to obtain good results for  $\Delta = 1$ , but due to their choice of trial function were unable to find a good solution for  $\Delta = 2$ . We have greatly improved upon this, and have found a trial function which works for all allowed values of  $\Delta$ .

As before we start by rewriting  $\Psi$

$$\Psi = \frac{\langle \mathcal{O} \rangle}{\sqrt{2}} z^\Delta F(z) \quad (2.79)$$

We will treat  $q^2$  as the eigen value and for a given  $\rho$  we have

$$q^2 = \frac{\mathcal{N}}{\mathcal{D}} \quad (2.80)$$

where

$$\mathcal{N} = \int dz z^{2\Delta-2} \left[ f F'^2 + \Delta z (\Delta + \Delta \frac{\rho^2}{4} (1-z) - \frac{\rho^2}{4} z) F^2 \right], \quad \mathcal{D} = \rho^2 \int dz z^{2\Delta-2} \frac{(1-z)^2}{f} F^2 \quad (2.81)$$

We will work with a trial function of the form

$$F_{\alpha,\beta} = 1 - \frac{\alpha z^2}{(z_- - z)^\beta} \quad (2.82)$$

It turns out that for any value of  $\Delta$  and  $\alpha$  that  $\beta$  is always  $\frac{1}{2}$  for the values of  $q$  and  $m$  satisfying our instability conditions, so we end up with a one parameter family of solutions.

The critical point  $q_c^2$  can be found by considering the extremal case ( $\rho^2 = 12$ ). Substituting the trial function 2.82 into 2.81, we obtain

$$\begin{aligned}\mathcal{N} &= -\frac{3-2\Delta(3-\Delta)}{2}\alpha^2 \ln(z_- - 1) + n_0(\alpha) + \mathcal{O}(\sqrt{z_- - 1}) , \\ \mathcal{D} &= -2\alpha^2 \ln(z_- - 1) + d_0(\alpha) + \mathcal{O}(\sqrt{z_- - 1}) .\end{aligned}\quad (2.83)$$

The functions  $n_0(\alpha)$  and  $d_0(\alpha)$  can be found explicitly, but will not be needed for our purposes.

In the extremal limit  $z_- \rightarrow 1$ , we obtain from Eq. 2.80,

$$q^2 = \frac{3-2\Delta(3-\Delta)}{4} + \mathcal{O}\left(\frac{1}{-\ln(z_- - 1)}\right) , \quad (2.84)$$

and therefore  $q_c^2$ , which is given by (2.84) in the limit  $z_- \rightarrow 1$ , is in agreement with expectations from geometrical considerations at the horizon (Eq. (2.67)).

The above conclusion is valid as long as  $\alpha \neq 0$ . In general, setting  $\alpha = 0$ , one obtains a value of the ratio (2.80) which is higher than the minimum, validating the above conclusion. However, for sufficiently small  $\Delta$ , the value of the ratio (2.80) at  $\alpha = 0$  is lower than the value (2.84). In this case, the minimum is attained at  $\alpha = 0$ . We deduce the critical point (in the limit  $z_- \rightarrow 1$ ),

$$q_c^2 = \frac{n_0(0)}{d_0(0)} = -3\Delta(\Delta - 1)(2\Delta - 1) \frac{\Im z_0}{\Im_{z_0} \frac{1}{F}(2\Delta - 1, 1; 2\Delta; \frac{1}{z_0})} . \quad (2.85)$$

The two possible critical coupling constants  $q_c^2$  are plotted in figure 2.6 as functions of the scaling dimension  $\Delta$ . The two critical lines meet at  $\Delta_0$  which solves

$$\frac{3-2\Delta_0(3-\Delta_0)}{4} = -3\Delta_0(\Delta_0 - 1)(2\Delta_0 - 1) \frac{\Im z_0}{\Im_{z_0} \frac{1}{F}(2\Delta_0 - 1, 1; 2\Delta_0; \frac{1}{z_0})} . \quad (2.86)$$

Numerically,

$$\Delta_0 \approx 0.64 . \quad (2.87)$$

For  $\Delta > \Delta_0$ , the critical point is given by (2.67), whereas for  $\Delta < \Delta_0$ , it is given by (2.85). We have instability in the shaded region of figure 2.6 (above the minimum of the two critical lines for each  $\Delta$ ). Notice that even in the range  $\Delta < \Delta_0$ , we have  $q_c^2 < 0$ , with  $q_c^2 = 0$  at the unitarity bound  $\Delta = 0.5$ . Therefore Reissner-Nordström black holes are unstable against neutral hair down to the unitarity bound, contrary to what one would expect by geometrical considerations at the horizon. This result is confirmed by a numerical calculation of the critical temperature as a function of  $q^2$  for various values of  $\Delta$  (figure 2.7).

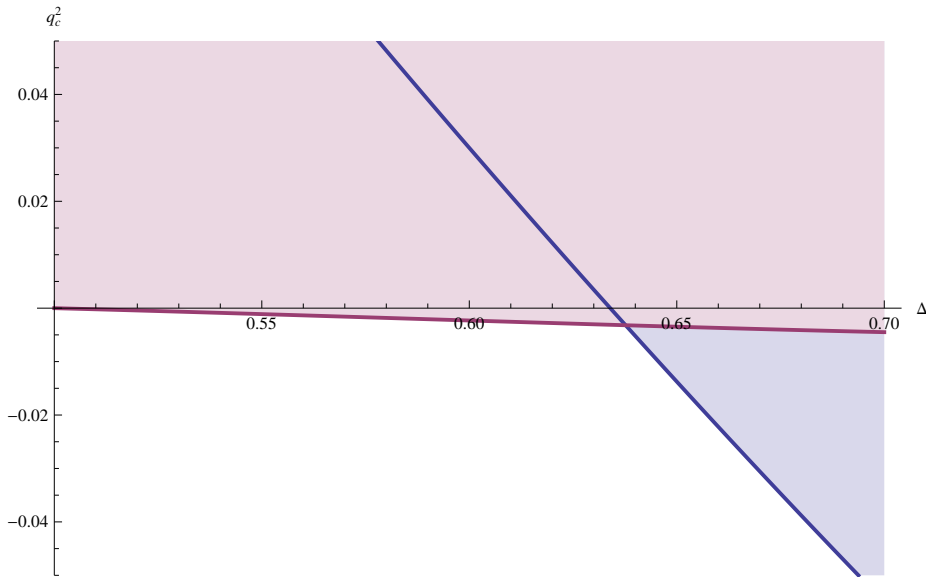


**Figure 2.6:** The critical coupling constant  $q^2$  vs.  $\Delta$  (boundary of the shaded region).

The above results show conclusively that we have instability for all  $q^2 > q_c^2$ . Indeed, for a given  $q^2 > q_c^2$ , define the action

$$S = \mathcal{N} - q^2 \mathcal{D} , \quad (2.88)$$

with  $\mathcal{N}$  and  $\mathcal{D}$  given in 2.81. The action  $S$  is extremized ( $\delta S = 0$ ) by the solutions of the wave equation (2.64). It becomes negative for trial functions corresponding to

eigenvalues (coupling constants)  $\tilde{q}^2 < q^2$ , since

$$S = (\tilde{q}^2 - q^2)\mathcal{D} < 0 . \quad (2.89)$$

This shows that we have instability above the critical point ( $q^2 > q_c^2$ ). By the same argument, below the critical point ( $q^2 < q_c^2$ ), we have  $S > 0$ , since  $\tilde{q}^2 > q_c^2 > q^2$  for all trial functions, therefore no instability against scalar hair.

We obtain analytic expressions for the critical temperature as a function of  $q^2$  for given  $\Delta$  by using (2.12). These expressions are compared with numerical data in figure 2.8. We obtain excellent agreement (the curves are almost indistinguishable) both near and away from the critical point, as shown in figure 2.8. The variational method is superior to the numerical solution as we approach the critical point ( $T_c \rightarrow 0$ ), because the latter becomes unstable there.

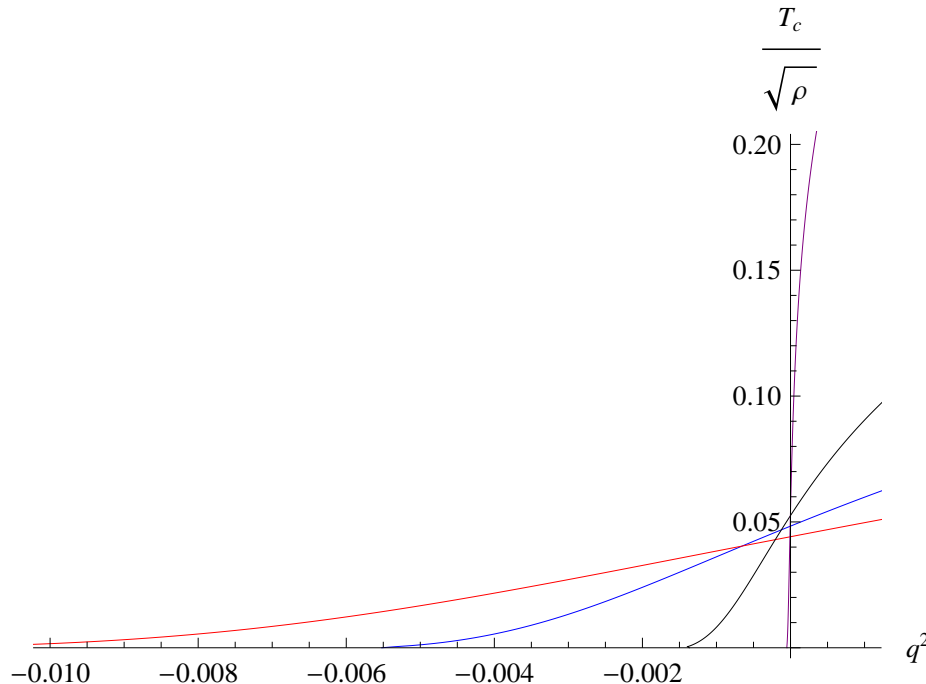


**Figure 2.7:** The critical temperature *vs.* the coupling constant  $q^2$  for  $\Delta = 0.634, 0.578, 0.525, 0.501$  (curves become steeper as  $\Delta$  decreases).

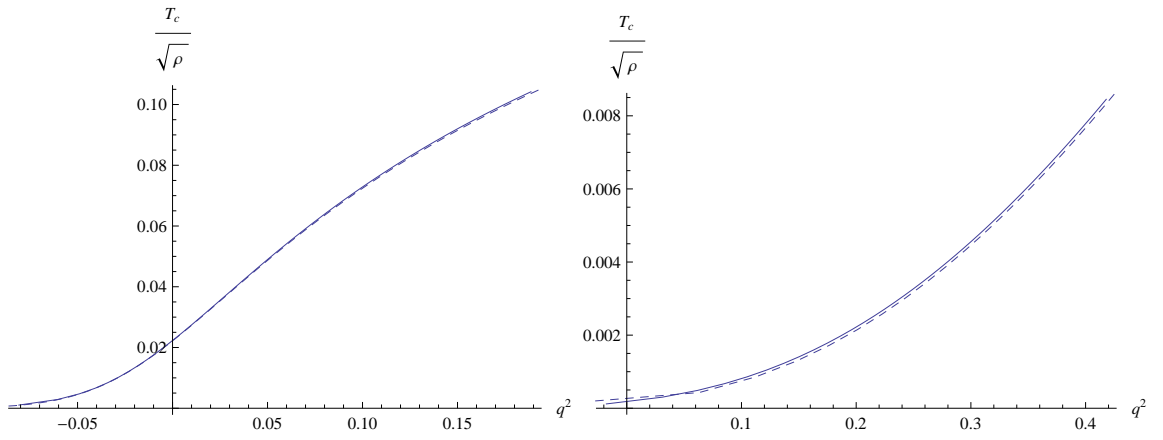


**Figure 2.8:** The critical temperature  $T_c$  found by a variational method (dashed) compared to numerical results (solid), for  $\Delta = 1$  (left panel) and  $\Delta = 2$  (right panel).



# Chapter 3

## Superconducting Phase

We are interested in what happens to the system as in the superconducting phase. For  $\frac{T}{T_c} \gg 0$  numerics produce results with few errors, however as  $\frac{T}{T_c} \rightarrow 0$  numerical errors grow large enough that the results can't be trusted. We will be using analytical techniques to explore the system in the probe limit, with anisotropy, and in the extremal limit with back reaction. We will then compare our results to numerics.

### 3.1 Immediately below $T_c$

Near  $T_c$  the order parameter is small, so we can expand the electric potential  $\Phi$  in it, let

$$\Phi = \lambda(1 - z^{d-2}) + \frac{\langle \mathcal{O}_\Delta \rangle^2}{2} \chi(z) \quad (3.1)$$

$$\chi'' - \frac{d-3}{z} \chi' = z^{2(\Delta-2)} \mathfrak{h}(z) F^2(z) \quad \text{where} \quad \mathfrak{h}(z) = \frac{\sum_{n=1}^{d-2} z^n}{\sum_{n=1}^{d-1} z^n} \quad (3.2)$$

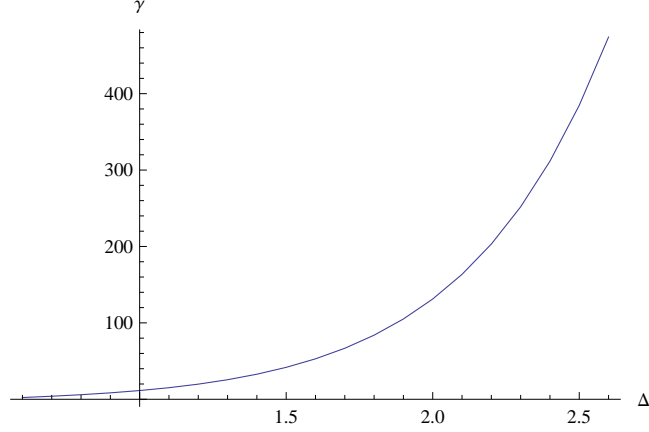


**Figure 3.1:** The parameter  $\gamma$  that determines the condensate near the critical temperature *vs.* the dimension of the condensate  $\Delta$  (eq. (3.6)).

With  $\chi(1) = \chi'(1) = 0$ , to find the temperature we need to find  $\rho = \rho_0 + \frac{\langle \mathcal{O}_\Delta \rangle^2}{2} \rho_2$  from eqn (2.6), to this end we can rewrite our equation as

$$(z^{d-3}\chi')' = \lambda z^{(2\Delta-1-d)}\mathfrak{h}(z)F^2(z) \quad (3.3)$$

$$\chi' = z^{d-3} \int dz \lambda z^{(2\Delta-1-d)}\mathfrak{h}(z)F^2(z) \quad (3.4)$$

It follows then that

$$\rho_2 = \int dz \lambda z^{(2\Delta-1-d)}\mathfrak{h}(z)F^2(z) \quad (3.5)$$

therefore the condensate near the critical temperature is

$$\langle \mathcal{O}_\Delta \rangle \approx \gamma T_c^\Delta \left(1 - \frac{T}{T_c}\right) \quad , \quad \gamma = \frac{2}{\sqrt{\mathcal{C}}} \left(\frac{4\pi}{d}\right)^\Delta \quad (3.6)$$

Using the trial functions (2.22), for  $\Delta = 1$   $d = 3$ , we obtain from (3.5),  $\mathcal{C} \approx 0.54$  and  $\gamma \approx 11.4$  to be compared with the exact  $\gamma = 9.3$  (23). Similarly, for  $\Delta = 2$   $d = 3$ , we find  $\mathcal{C} \approx 0.07$  and  $\gamma \approx 133$  to be compared with the exact  $\gamma = 144$  (23). In fig. 3.1 we plot the analytic prediction (3.6) for the parameter  $\gamma$  as a function of the dimension of the condensate  $\Delta$  with  $d = 3$ . Notice that  $\gamma$  diverges as  $\Delta \rightarrow 3$ .

## 3.2 The Limit $T \rightarrow 0$

### 3.2.1 Probe Limit

In the probe limit we seek solutions to (2.19) for all values of  $\frac{T}{T_c}$ . The energy gaps exhibit three different types of behavior depending on the conformal dimension of the condensate. For  $\Delta_+$  the matter fields do not significantly backreact on the geometry, for  $\Delta_-$  backreaction does effect the system and care should be taken. Finally for  $\Delta_{BF}$ , numerics suggest that  $E_g$  remains finite as  $T \rightarrow 0$ , but instead of approaching a constant value, it increases linearly.

In our original paper (27) we concentrated on  $d = 3$  and were able to find approximate solutions that provided very good results when compared to numerics. In (28) we generalized our solutions to  $d$  dimensions using an iterative method.

### Approximation

We will be concentrating on  $d = 3$ , we will generalize to other dimensions later with using an iterative method. As  $T \rightarrow 0$ , we expect a simple scaling,  $\Psi = \Psi(bz)$ ,  $\Phi = \Phi(bz)$  where  $b \rightarrow \infty$ . Then scaling  $z \rightarrow z/b$  and letting  $b \rightarrow \infty$ , the field equations (2.19) simplify, since the dominant contribution comes from the neighborhood of the boundary ( $z = 0$ ). Thus at low temperature we obtain the simplified system of equations

$$\begin{aligned} -F'' + \frac{2(1-\Delta)}{z}F' - \frac{\Phi^2}{r_+^2}F &= 0 \\ \Phi'' - \frac{\langle \mathcal{O}_\Delta \rangle^2}{r_+^{2\Delta}}F^2 z^{2(\Delta-1)}\Phi &= 0 \end{aligned} \tag{3.7}$$

where we restored the original coordinate  $z$  (before scaling).

This system of coupled non-linear equations is to be solved subject to the boundary condition at the horizon

$$3F'(1) + \Delta^2 F(1) = 0 \tag{3.8}$$

as well as those at the boundary,  $F(0) = 1$  and  $F'(0) = 0$ .

For  $\Delta = \Delta_- < 3/2$ , numerical results indicate that  $F \rightarrow 1$  as  $T \rightarrow 0$ . Using this the solution to the field equation (3.7) for  $\Phi$  is

$$\Phi(z) = \mathcal{A} r_+ \sqrt{z} K_{\frac{1}{2\Delta}}(b^\Delta z^\Delta) \quad , \quad b^\Delta = \frac{\langle \mathcal{O}_\Delta \rangle}{\Delta r_+^\Delta} \quad (3.9)$$

The other solution is rejected because it is large at the horizon, contradicting the boundary condition (2.9). Notice that at the horizon  $\Phi(1) \sim e^{-b^\Delta}$ , which is an exponentially small error in the  $T \rightarrow 0$  ( $b \rightarrow \infty$ ) limit.

From the behavior of  $\Phi$  (eq. (3.9)) near the boundary ( $z = 0$ ), using (2.6), we deduce

$$\frac{\rho}{r_+^2} = -\frac{\Gamma(-\frac{1}{2\Delta})}{2^{1+\frac{1}{2\Delta}}} \mathcal{A} b \quad (3.10)$$

The field equation (3.7) for  $F$  becomes

$$-F'' + \frac{2(1-\Delta)}{z} F' - \mathcal{A}^2 b z (K_{\frac{1}{2\Delta}}(b^\Delta z^\Delta))^2 F = 0 \quad (3.11)$$

Using perturbation theory, we obtain the solution

$$F(z) = 1 - \mathcal{A}^2 b \int_0^z dz' z'^{2(1-\Delta)} \int_0^{z'} dz'' z'' (K_{\frac{1}{2\Delta}}(b^\Delta z''^\Delta))^2 \quad (3.12)$$

Applying the boundary condition (2.6) at the horizon, we obtain

$$\mathcal{A}^2 = \frac{\Delta^2 b^{2(2-\Delta)}}{3b\mathcal{F}'_\Delta(b) + \Delta^2 \mathcal{F}_\Delta(b)} \quad , \quad \mathcal{F}_\Delta(x) = \int_0^x dx' x'^{2(1-\Delta)} \int_0^{x'} dx'' x'' (K_{\frac{1}{2\Delta}}(x''^\Delta))^2 \quad (3.13)$$

For large  $b$ , the denominator scales like  $b^{3-2\Delta}$ , showing that  $\mathcal{A} \sim \sqrt{b}$ . Then eq. (3.10) implies  $\rho/r_+^2 \sim b^{3/2}$ . Since  $\langle \mathcal{O}_\Delta \rangle \sim (r_+ b)^\Delta$  (see eq. (4.46)), it follows that

$$\frac{\langle \mathcal{O}_\Delta \rangle^{1/\Delta}}{T_c} \sim b^{1/4} \sim \left( \frac{T}{T_c} \right)^{-1/3} \quad (3.14)$$

showing that the condensate diverges as  $\langle \mathcal{O}_\Delta \rangle \sim T^{-\Delta/3}$  for  $\Delta$  in the range  $1/2 < \Delta < 3/2$  signaling the breakdown of the probe-limit approximation at low temperatures.

Turning to the case  $\Delta = \Delta_+ > 3/2$ , notice that as we switch from  $\Delta = \Delta_-$  to  $\Delta = \Delta_+$ , the boundary conditions at  $z = 0$  change, but not at the horizon. Thus, for a given  $m$ , the electrostatic potential  $\Phi$  has the same asymptotic behavior for both  $\Delta_+$  and  $\Delta_-$ . In terms of the scalar field, this implies  $F \approx 1$  near the boundary ( $z = 0$ ), but away from the boundary

$$F(z) \approx \left( \frac{bz}{\alpha} \right)^{3-2\Delta} \quad (3.15)$$

asymptotically ( $z \gtrsim 1/b$ , where  $b \gg 1$  is to be determined). Then in the asymptotic regime, eq. (3.7) for  $\Phi$  has solution (cf. eq. (3.9))

$$\Phi(z) = \mathcal{A} r_+ \sqrt{bz} K_{\frac{1}{2(3-\Delta)}}(b^{3-\Delta} z^{3-\Delta}) \quad , \quad b^\Delta = \frac{\langle \mathcal{O}_\Delta \rangle \alpha^{2\Delta-3}}{(3-\Delta) r_+^\Delta} \quad (3.16)$$

Notice that a singularity appears to develop at  $\Delta = 3$  indicating the onset of a quantum phase transition.

Near the boundary, we deduce the estimate for the ratio  $\rho/r_+^2$ ,

$$\frac{\rho}{r_+^2} = - \frac{\Gamma(-\frac{1}{2(3-\Delta)})}{2^{1+\frac{1}{2(3-\Delta)}}} \mathcal{A} b \quad (3.17)$$

However, this is not a good estimate. In fact, it diverges at  $\Delta = 5/2$ . We shall improve on this estimate by better accounting for the behavior of  $F$  near the boundary (where eq. (3.15) ought to be replaced by  $F \approx 1$ ).

The field equation (3.7) for  $F$  is

$$-F'' + \frac{2(1-\Delta)}{z} F' - \mathcal{A}^2 b z (K_{\frac{1}{2(3-\Delta)}}(b^{3-\Delta} z^{3-\Delta}))^2 F = 0 \quad (3.18)$$

Unlike with  $\Delta < 3/2$ , in this case the term involving the electrostatic potential  $\Phi$  cannot be treated as a perturbation. By rescaling  $z \rightarrow z/b$ , eq. (3.18) becomes

$$-F''' + \frac{2(1-\Delta)}{z}F' - \hat{\mathcal{A}}^2 z (K_{\frac{1}{2(3-\Delta)}}(z^{3-\Delta}))^2 F = 0 \quad , \quad \hat{\mathcal{A}} = \frac{\mathcal{A}}{b} \quad (3.19)$$

With

$$\mathcal{A} \sim b \quad (3.20)$$

Eq. (3.19) is independent of temperature and provides a good approximation to  $F$  and the corresponding eigenvalue  $\hat{\mathcal{A}}$  at  $T = 0$ . It ought to be solved in the interval  $(0, \infty)$  subject to the boundary conditions  $F(0) = 1$ ,  $F'(0) = 0$ ,  $F \rightarrow 0$  as  $z \rightarrow \infty$  (see eq. (3.15)). These conditions determine the eigenvalue  $\hat{\mathcal{A}}$ .

To estimate  $\hat{\mathcal{A}}$ , note that

$$\hat{\mathcal{A}}^2 = \frac{\int_0^\infty dz \, z^{2(\Delta-1)} [F'(z)]^2}{\int_0^\infty dz \, z^{2\Delta-1} [K_{\frac{1}{2(3-\Delta)}}(z^{3-\Delta}) F(z)]^2} \quad (3.21)$$

The eigenfunction  $F(z)$  minimizes this expression. We may substitute the trial function

$$F_\alpha(z) = \left(\frac{\alpha}{z}\right)^{2\Delta-3} \tanh\left(\frac{z}{\alpha}\right)^{2\Delta-3} \quad (3.22)$$

which obeys the correct boundary conditions. It interpolates smoothly between a constant value ( $F = 1$ ) near the boundary and the power behavior (3.15) away from the boundary. The parameter  $\alpha$  is fixed by minimizing the ratio (3.21). Similar functions have been considered before (56; 57) but without a determination of the parameter  $\alpha$ . In fig. 3.2 we compare the analytic estimate of the eigenvalue  $\hat{\mathcal{A}}$  using the trial functions (3.22) with exact numerical results. The agreement between the two is excellent. Notice that the limit  $\Delta \rightarrow 3$  is singular.  $\hat{\mathcal{A}} \rightarrow 0$  in this limit. Also, the parameter  $\alpha$  labeling the trial function that minimizes (3.21), which is plotted in fig. 3.9 as a function of the dimension  $\Delta$ , diverges as  $\Delta \rightarrow 3$ .

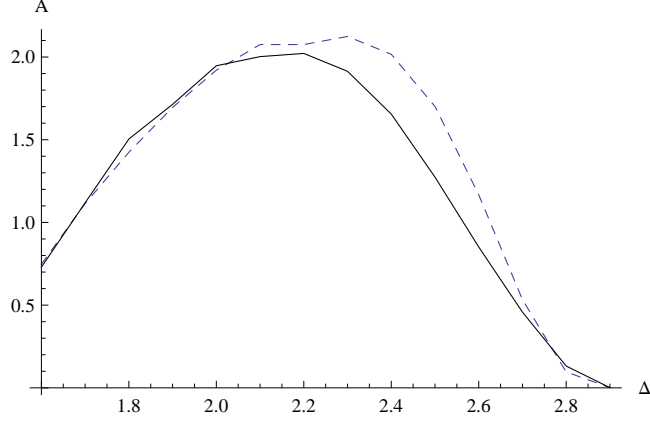


**Figure 3.2:** The eigenvalue  $\hat{\mathcal{A}}$  defined in (3.19) as a function of  $\Delta$  [solid line] compared with the estimate (3.21) [dashed line].

For  $\Delta = 2$  the minimum is obtained for  $\alpha \approx 0.8$  which yields  $\hat{\mathcal{A}} \approx 1.92$ . In this case,  $\hat{\mathcal{A}}$  can be found exactly because eq. (3.19) can be solved analytically. We find explicitly

$$F(z) = \frac{\pi}{2z} \left[ Y_0 \left( \sqrt{\frac{\pi}{2}} \hat{\mathcal{A}} \right) J_0 \left( \sqrt{\frac{\pi}{2}} \hat{\mathcal{A}} e^{-z} \right) - J_0 \left( \sqrt{\frac{\pi}{2}} \hat{\mathcal{A}} \right) Y_0 \left( \sqrt{\frac{\pi}{2}} \hat{\mathcal{A}} e^{-z} \right) \right] \quad (3.23)$$

which obeys the correct boundary conditions at  $z = 0$ . Demanding  $F \rightarrow 0$  as  $z \rightarrow \infty$  then yields

$$J_0 \left( \sqrt{\frac{\pi}{2}} \hat{\mathcal{A}} \right) = 0 \quad (3.24)$$

showing that

$$\hat{\mathcal{A}} = \frac{\mathcal{A}}{b} = \xi_0 \sqrt{\frac{2}{\pi}} \quad , \quad \xi_0 \approx 2.4 \quad (3.25)$$

where  $\xi_0$  is the first root of the Bessel function  $J_0$ . Numerically,  $\hat{\mathcal{A}} = 1.91$ , in good agreement with our earlier estimate.

Restoring  $b$ ,

$$F(z) = \frac{\pi}{2bz} Y_0(\xi_0) J_0(\xi_0 e^{-bz}) \quad (3.26)$$

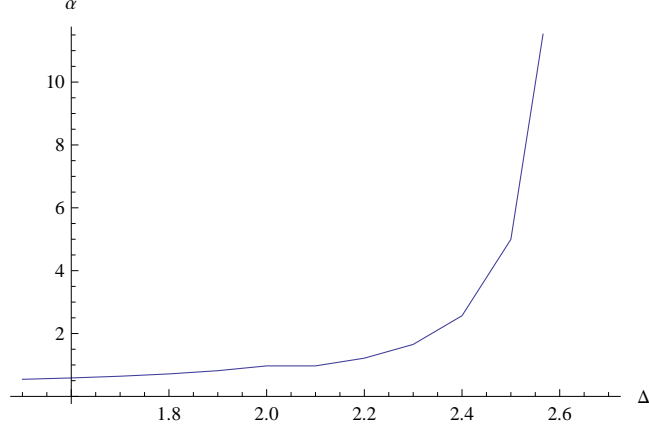


**Figure 3.3:** The parameter  $\alpha$  that determines the approximation (3.22) to the scalar field as a function of  $\Delta$ .

F

so  $F(z) = 1 + \mathcal{O}(z^2)$ , as desired. Away from the boundary ( $z \gtrsim 1/b$ ),

$$F(z) \approx \frac{\pi Y_0(\xi_0)}{2bz} \quad (3.27)$$

which upon comparison with (3.15) yields

$$\alpha = \frac{\pi Y_0(\xi_0)}{2} \approx 0.8 \quad (3.28)$$

in excellent agreement with our earlier estimate.

To calculate the condensate at  $T = 0$ , we need a better estimate of the ratio (3.17). To this end, we shall solve eq. (3.7) for  $\Phi$  perturbatively using (3.16) with  $\Delta = 2$  as our zeroth-order solution. We obtain

$$\begin{aligned} \Phi(z) = \sqrt{\frac{\pi}{2}} \mathcal{A} r_+ e^{-bz} & \left[ 1 + \frac{\alpha}{2} - \frac{\pi \alpha^2}{\sin \pi \alpha} e^{2bz} + \frac{\alpha}{2} F(-\alpha, 1; 1 - \alpha; -e^{2bz/\alpha}) \right. \\ & \left. + \frac{\alpha^2}{2(1 - \alpha)} e^{2bz/\alpha} F(1 - \alpha, 1, 2 - \alpha; -e^{2bz/\alpha}) \right] \quad (3.29) \end{aligned}$$



We deduce the ratio

$$\frac{\sqrt{\rho}}{r_+} \approx b\sqrt{\xi_0} \left[ 1 - \frac{\delta}{2} \right] \quad , \quad \delta = \alpha + \frac{\pi\alpha^2}{\sin \pi\alpha} + \frac{\alpha^2}{2}\psi\left(\frac{1-\alpha}{2}\right) - \frac{\alpha^2}{2}\psi\left(-\frac{\alpha}{2}\right) \Big|_{\alpha=\pi Y_0(\xi_0)/2} \quad (3.30)$$

improving the zeroth-order result  $\sqrt{\rho}/r_+ \approx \sqrt{\xi_0} b$  (eqs. (3.17) with  $\Delta = 2$  and (3.25)).

Numerically,  $\delta = 0.58$  and the condensate at  $T = 0$  is

$$\frac{\sqrt{\langle \mathcal{O}_2 \rangle}}{T_c} \approx \frac{1 + \frac{\delta}{2}}{0.118\sqrt{\alpha\xi_0}} \approx 7.9 \quad (3.31)$$

in good agreement with the exact result  $\langle \mathcal{O}_2 \rangle^{1/2} = 8.3T_c$ .

To generalize to arbitrary  $\Delta > 3/2$ , substitute the approximation to the function  $F_\alpha(z)$  (eq. (3.22)),

$$F_\alpha(z) \approx \begin{cases} 1 & , \quad z \leq \alpha \\ (\alpha/z)^{2\Delta-3} & , \quad z > \alpha \end{cases} \quad (3.32)$$

into the field equation for the electrostatic potential  $\Phi$  and solve it to find a better approximation for  $\Phi$  than (3.16). After rescaling,  $z \rightarrow z/b$ , for  $z > \alpha$  we obtain

$$\Phi = \Phi_>(z) = \hat{\mathcal{A}}br_+ \sqrt{z} K_{\frac{1}{2(3-\Delta)}}(z^{3-\Delta}) \quad (3.33)$$

whereas for  $z \leq \alpha$ ,

$$\Phi = \Phi_<(z) = \mathcal{B}_+ \sqrt{z} I_{\frac{1}{2\Delta}} \left( \frac{3-\Delta}{\Delta} \frac{z^\Delta}{\alpha^{2\Delta-3}} \right) + \mathcal{B}_- \sqrt{z} I_{-\frac{1}{2\Delta}} \left( \frac{3-\Delta}{\Delta} \frac{z^\Delta}{\alpha^{2\Delta-3}} \right) \quad (3.34)$$

providing the estimate for  $\rho$  improving on (3.17),

$$\rho = -\frac{\mathcal{B}_+ br_+}{\Gamma(1 + \frac{1}{2\Delta})} \left( \frac{3-\Delta}{2\Delta\alpha^{2\Delta-3}} \right)^{\frac{1}{2\Delta}} \quad (3.35)$$

The coefficients  $\mathcal{B}_\pm$  are found by matching the two expressions at  $z = \alpha$ . For  $\Delta = 2$  we obtain  $\mathcal{B}_+ \approx -1.73br_+$ ,  $\mathcal{B}_- \approx 1.96br_+$ , therefore  $\rho \approx 1.43b^2r_+^2$  and  $\sqrt{\langle \mathcal{O}_2 \rangle}/T_c \approx 7.9$ , as before. Fig. 3.4 shows the dependence of the condensate on the dimension  $\Delta$ . Our

analytic estimate is in good agreement with the exact numerical value for most of the range of  $\Delta$ . It becomes increasingly unreliable as  $\Delta \rightarrow 3$ . This is expected from our estimate of the electrostatic potential (3.34) which is singular in the limit  $\Delta \rightarrow 3$ .

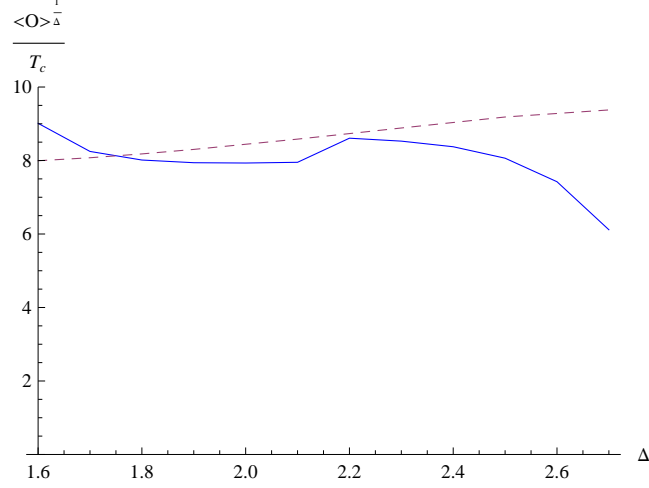


**Figure 3.4:** The condensate at zero temperature as a function of  $\Delta$ . The solid line is our analytic estimate whereas the dashed line is the exact numerical result.

### Iterative Solution

Another analytical method that we can use to solve our system is iteration. We find solutions in  $d$  dimensions, but only consider the  $\Delta_-$  theory. We will solve

$$\begin{aligned} -F_0^{(n+1)''} + \frac{1}{z} \left[ \frac{d}{1-z^d} - 1 - 2\Delta \right] F_0^{(n+1)'} + \frac{\Delta^2 z^{d-2}}{1-z^d} F_0^{(n+1)} &= \frac{\mu^2}{(1-z^d)^2} [\hat{\Phi}_0^{(n+1)}]^2 F_0^{(n)} \\ \hat{\Phi}_0^{(n+1)''} - \frac{d-3}{z} \hat{\Phi}_0^{(n+1)'} - \frac{b^2 \Delta z^{2(\Delta-1)}}{1-z^d} [F_0^{(n)}]^2 \hat{\Phi}_0^{(n+1)} &= 0 \end{aligned} \quad (3.36)$$

Where

$$b = \langle q \mathcal{O}_\Delta \rangle^{1/\Delta} \quad (3.37)$$

Motivated by numerics we shall start with

$$F_0^{(0)}(z) = 1 \quad , \quad \hat{\Phi}_0^{(0)}(z) = 0 \quad (3.38)$$

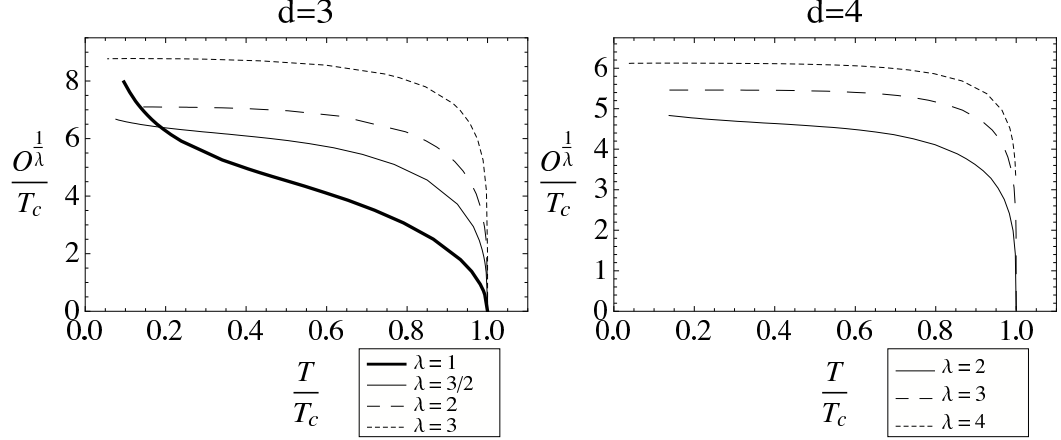


**Figure 3.5:** This figure is taken from (25). They have used  $\lambda$  as the dimension of the operator that condenses (I have used  $\Delta$ ) The left and right figures are qualitatively similar. The BF bound is saturated for  $\lambda = 3/2$  and 2 for  $d=3$  and 4 respectively. In (25) they claim that at the BF bound the condensate increases linearly as  $\frac{T}{T_c} \rightarrow 0$ .

We defined

$$\Phi_0(z) = \mu \hat{\Phi}_0(z) \quad , \quad \hat{\Phi}_0(0) = 1 \quad (3.39)$$

where  $\mu$  is the chemical potential. We need to fix the integration constants for  $F$  as

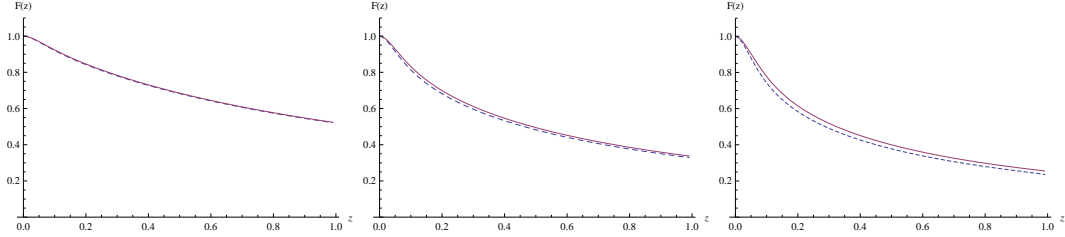


**Figure 3.6:** The field  $F$  for  $\Delta = 1.2$  (left panel), 1.4 (middle panel), 1.5 (right panel) and  $d = 3$ . Solid curves are first-order analytic expression (3.44), and dashed curves are exact numerical results (almost indistinguishable) at  $T/T_c \approx 0.1$ .

well the eigenvalue  $\mu$ . We can do this by imposing the boundary conditions at the horizon,  $F^{(m)}(0) = 1$  and that  $F^{(m)} \sim z^{d-2m}$  terms are absent, and impose that  $F^{(m)}$  be regular at the horizon. At  $n$ th order the solution to the scalar equation of motion

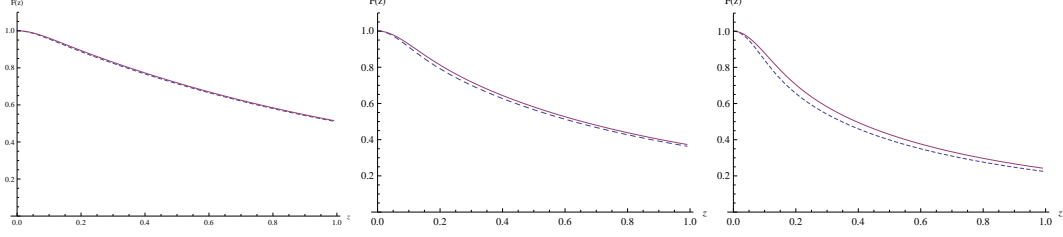


**Figure 3.7:** The field  $F$  for  $\Delta = 1.6$  (left panel), 1.8 (middle panel), 2 (right panel) and  $d = 4$ . Solid curves are first-order analytic expression (3.44), and dashed curves are exact numerical results (almost indistinguishable) at  $T/T_c \approx 0.2$ .

is given by

$$F_0^{(n+1)}(z) = \mathcal{F}_1(z) \left[ 1 + \mu^2 \int_0^z \frac{dz'}{1 - (z')^d} (z')^{2\Delta+1-d} \mathcal{F}_2(z') [\hat{\Phi}_0^{(n+1)}(z')]^2 F_0^{(n)}(z') \right] - \mathcal{F}_2(z) \mu^2 \int_0^z \frac{dz'}{1 - (z')^d} (z')^{2\Delta+1-d} \mathcal{F}_1(z') [\hat{\Phi}_0^{(n+1)}(z')]^2 F_0^{(n)}(z') \quad (3.40)$$

where

$$\mathcal{F}_1(z) = F\left(\frac{\Delta}{d}, \frac{\Delta}{d}; \frac{2\Delta}{d}; z^d\right), \quad \mathcal{F}_2(z) = \frac{z^{d-2\Delta}}{d-2\Delta} F\left(1 - \frac{\Delta}{d}, 1 - \frac{\Delta}{d}; 2 - \frac{2\Delta}{d}; z^d\right) \quad (3.41)$$

where we have used the boundary conditions at  $z=0$ . We can use the third boundary condition at  $z=1$  to fix the chemical potential.

For  $n=0$  we find that

$$\hat{\Phi}_0^{(1)}(z) = \frac{2}{\Gamma(\nu)(2\Delta)^\nu} (bz)^{\frac{d-2}{2}} \left[ K_\nu\left(\frac{(bz)^\Delta}{\Delta}\right) - \frac{K_\nu\left(\frac{b^\Delta}{\Delta}\right)}{I_\nu\left(\frac{b^\Delta}{\Delta}\right)} I_\nu\left(\frac{(bz)^\Delta}{\Delta}\right) \right], \quad \nu = \frac{d-2}{2\Delta} \quad (3.42)$$

This satisfies the boundary condition (2.9). Notice that the second Bessel function has an exponentially small coefficient,  $\mathcal{O}(\sim e^{-2b^\Delta/\Delta})$ , and can be neglected at low temperatures.

The charge density is found by using (2.6) to be

$$\frac{\rho_0}{b^{d-2}} = -\frac{\mu}{(2\Delta)^{2\nu}} \quad (3.43)$$

For the scalar field we obtain eq. (3.40) with  $n = 0$ ,

$$F_0^{(1)}(z) = \mathcal{F}_1(z) \left[ 1 + \mu^2 \int_0^z \frac{dz'}{1 - (z')^d} (z')^{2\Delta+1-d} \mathcal{F}_2(z') [\hat{\Phi}_0^{(1)}(z')]^2 \right] - \mathcal{F}_2(z) \mu^2 \int_0^z \frac{dz'}{1 - (z')^d} (z')^{2\Delta+1-d} \mathcal{F}_1(z') [\hat{\Phi}_0^{(1)}(z')]^2 \quad (3.44)$$

satisfying the correct boundary conditions at  $z = 0$ . At the horizon ( $z = 1$ ), we have a logarithmic singularity which is found using

$$\mathcal{F}_1(z) \approx -\frac{\Gamma(\frac{2\Delta}{d})}{\Gamma^2(\frac{\Delta}{d})} \ln(1-z) \quad , \quad \mathcal{F}_2(z) \approx -\frac{\Gamma(2 - \frac{2\Delta}{d})}{(d-2\Delta)\Gamma^2(1 - \frac{\Delta}{d})} \ln(1-z) \quad (3.45)$$

Near the horizon, we deduce

$$F_0^{(1)}(z) \approx - \left[ \frac{\Gamma(\frac{2\Delta}{d})}{\Gamma^2(\frac{\Delta}{d})} (1 + \mu^2 a_2) - \frac{\Gamma(2 - \frac{2\Delta}{d})}{(d-2\Delta)\Gamma^2(1 - \frac{\Delta}{d})} \mu^2 a_1 \right] \ln(1-z) \quad (3.46)$$

where

$$a_i = \int_0^1 \frac{dz}{1-z^d} z^{2\Delta+1-d} \mathcal{F}_i(z) \left[ \hat{\Phi}_0^{(1)}(z) \right]^2 \quad , \quad i = 1, 2 \quad (3.47)$$

Demanding regularity at the horizon, we need

$$\frac{\Gamma(\frac{2\Delta}{d})}{\Gamma^2(\frac{\Delta}{d})} (1 + \mu^2 a_2) - \frac{\Gamma(2 - \frac{2\Delta}{d})}{(d-2\Delta)\Gamma^2(1 - \frac{\Delta}{d})} \mu^2 a_1 = 0 \quad (3.48)$$

which fixes the chemical potential  $\mu$ ,

$$\frac{1}{\mu^2} = \frac{\Gamma(2 - \frac{2\Delta}{d})\Gamma^2(\frac{\Delta}{d})}{(d-2\Delta)\Gamma(\frac{2\Delta}{d})\Gamma^2(1 - \frac{\Delta}{d})} a_1 - a_2 \quad (3.49)$$

as advertised.

Explicitly,

$$a_1 = \frac{1}{b^{2\Delta+2-d}} \frac{(d-2)\Gamma(1-\nu)}{(2\Delta)^{2\nu}\Gamma(\nu)} + \dots \quad , \quad a_2 = \frac{1}{b^2} \frac{\sqrt{\pi}\Delta^{\frac{d}{2}-1}\Gamma(\frac{1}{\Delta})\Gamma(\frac{d-1}{\Delta})\Gamma(\frac{d}{2\Delta})}{(d-2\Delta)\Gamma^2(\nu)2^{2\nu}\Gamma(\frac{d+\Delta}{2\Delta})} + \dots \quad (3.50)$$

Evidently, for  $\Delta < \frac{d}{2}$ ,  $a_2 \ll a_1$  for  $b \ll 1$ , therefore

$$\mu^2 \approx \mathcal{C} b^{2\Delta+2-d}, \quad \mathcal{C} = \frac{(d-2\Delta)(2\Delta)^{2\nu}\Gamma(\nu)\Gamma(\frac{2\Delta}{d})\Gamma^2(1-\frac{\Delta}{d})}{(d-2)\Gamma(1-\nu)\Gamma(2-\frac{2\Delta}{d})\Gamma^2(\frac{\Delta}{d})} \quad (3.51)$$

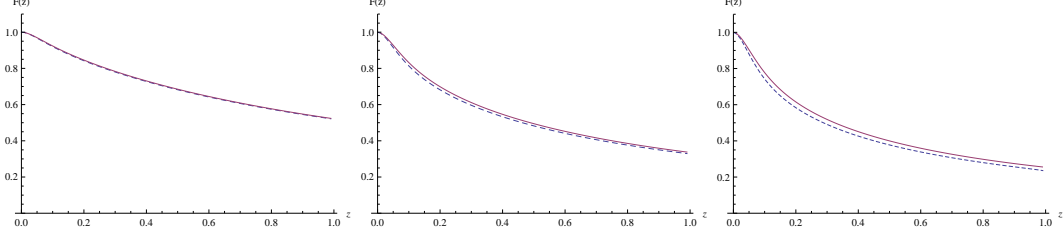


**Figure 3.8:** The field  $F$  for  $\Delta = 1.2$  (left panel),  $1.4$  (middle panel),  $1.5$  (right panel) and  $d = 3$ . Solid curves are first-order analytic expression (3.44), and dashed curves are exact numerical results (almost indistinguishable) at  $T/T_c \approx 0.1$ .

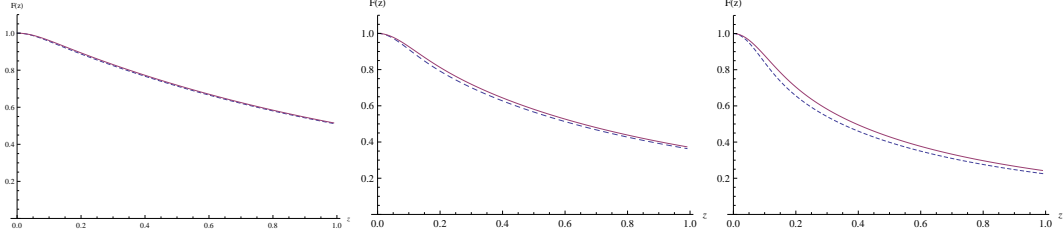


**Figure 3.9:** The field  $F$  for  $\Delta = 1.6$  (left panel),  $1.8$  (middle panel),  $2$  (right panel) and  $d = 4$ . Solid curves are first-order analytic expression (3.44), and dashed curves are exact numerical results (almost indistinguishable) at  $T/T_c \approx 0.2$ .

Before we consider the next iterative order, we note that at finite temperature, the first-order expression (3.44) is in excellent agreement with numerical results even at  $T/T_c \sim 0.1$ , which is the lowest temperature at which a numerical solution is available. This is shown in figs. 3.8 and 3.9 in which the corresponding curves are almost indistinguishable, implying that the next iterative order introduces negligible corrections to the first-order expression (3.44) for temperatures  $T/T_c \lesssim 0.1$ .

We can repeat the above steps for the next iterative order to calculate  $F_0^{(2)}$  and  $\hat{\Phi}_0^{(2)}$ . The resulting functions are very close to their first-order counterparts, showing that the iteration converges rather rapidly. In fact, the second order quantities are subleading in  $1/b$ . This is the case for all values of the scaling dimension

$\Delta < \frac{d}{2}$ . In fig. 3.10, we show the difference between first and second iterative order

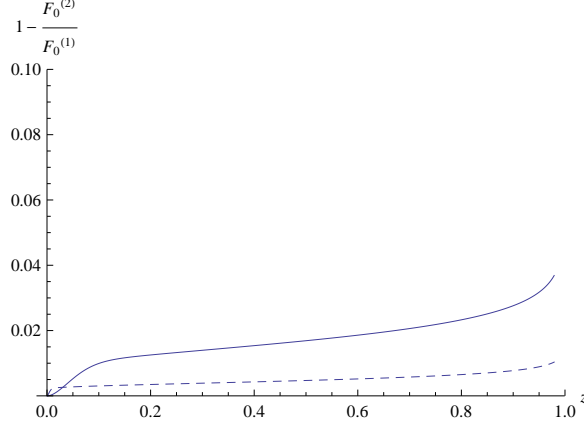


**Figure 3.10:** The second order correction to the scalar field  $F$  for  $d = 3$ ,  $\Delta = 1.4$  at  $b = 20$  ( $T/T_c \sim 0.1$ ) (solid line) and  $b = 200$  ( $T/T_c \sim 0.01$ ) (dashed line).

for  $d = 3$ ,  $\Delta = 1.4$  (all other values of  $\Delta$  are similar). The error,  $1 - \frac{F_0^{(2)}}{F_0^{(1)}}$ , is less than 5% in the entire interval  $[0, 1]$ . As the temperature decreases from  $T/T_c \sim 0.1$  to  $T/T_c \sim 0.01$ , the error decreases to less than 0.01. To demonstrate that the error is subleading in  $1/b$ , in fig. 3.11 we plot it at the mid-point ( $z = \frac{1}{2}$ ) as well as the horizon ( $z = 1$ ) (at  $z = 0$  the error vanishes by design). Evidently, it goes to zero as  $1/b$ , showing that the second iterative order introduces subleading corrections at low temperature.

For the charge density we deduce from (3.43)

$$\rho_0 \sim b^{\frac{d}{2} + \Delta - 1} \quad (3.52)$$

Using

$$\frac{\langle q \mathcal{O}_\Delta \rangle^{1/\Delta}}{T_c} \sim b \rho_0^{-\frac{1}{d-1}} \quad , \quad \frac{T}{T_c} \sim \rho_0^{-\frac{1}{d-1}} \quad (3.53)$$

we finally obtain for the energy gap

$$E_g = \frac{\langle q \mathcal{O}_\Delta \rangle^{1/\Delta}}{T_c} = \gamma \left( \frac{T}{T_c} \right)^{-\frac{d/2 - \Delta}{d/2 + \Delta - 1}} \quad (3.54)$$

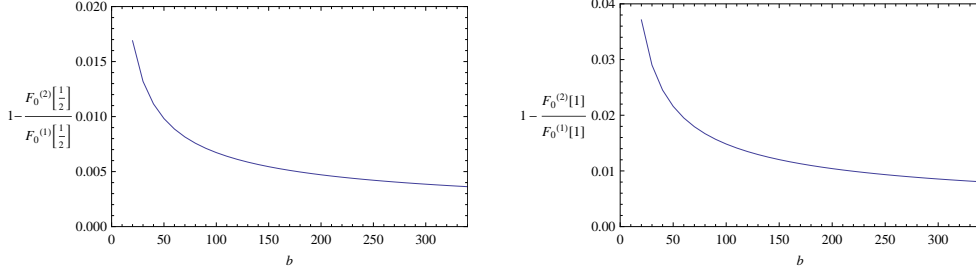


**Figure 3.11:** The second order correction to the scalar field  $F$  for  $d = 3$ ,  $\Delta = 1.4$  as a function of temperature at the mid-point,  $z = \frac{1}{2}$ , (left panel) and the horizon,  $z = 1$ , (right panel). The horizontal axis corresponds to the temperature range  $0.01 \lesssim \frac{T}{T_c} \lesssim 0.1$  with  $T$  decreasing to the right.

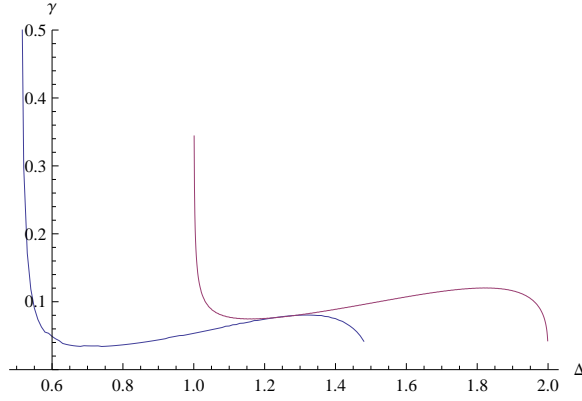


**Figure 3.12:** The parameter  $\gamma$  in the low temperature expression (3.54) for the condensate *vs*  $\Delta$ . Curve on left (right) is for  $d = 3$  ( $d = 4$ ).

showing that the condensate diverges at low temperatures (to be precise, in the regime  $1 \lesssim b \lesssim q^{1/\Delta}$ ). The exponent depends on the dimensions of the operator and spacetime. The expression for the exponent in (3.54) corrects an earlier analytic result (27). The constant of proportionality  $\gamma$  can be found analytically. It is plotted in fig. 3.12 *vs*  $\Delta$ . As  $\Delta$  approaches the BF bound,  $\gamma \rightarrow 0$ , showing that the power law behavior changes, as we discuss next.

Indeed, at the end point (BF bound),  $\Delta = \frac{d}{2}$ , we need to exercise care. Letting  $\Delta = \frac{d}{2} - \epsilon$ , we obtain from (3.49) and (3.50),

$$\frac{1}{\mu^2} = \frac{(d-2)\Gamma(\frac{2}{d})}{d^{2(1-\frac{2}{d})}\Gamma(1-\frac{2}{d})} \left[ \frac{1}{2\epsilon b^{2-2\epsilon}} - \frac{1}{2\epsilon b^2} + \dots \right] \quad (3.55)$$



and taking the limit  $\epsilon \rightarrow 0$ , we deduce at the BF bound

$$\frac{\mu^2}{b^2} = \frac{d^{2(1-\frac{2}{d})}\Gamma(1-\frac{2}{d})}{(d-2)\Gamma(\frac{2}{d})[\ln b + \beta_d + o(b^0)]} \quad (3.56)$$

where  $\beta_d$  is a constant that depends on the dimension and is easily computed (e.g., for  $d = 3$ ,  $\beta_3 \approx 1.75$ ).

Higher-order corrections are computed as before by considering the next iterative order. This introduces corrections that are subleading as  $b \rightarrow \infty$ . Already at  $T/T_c \sim 0.1$ , our first-order analytic results are almost indistinguishable from numerical results (see right panels of figs. 3.8 and 3.9), the discrepancy being  $\sim 1\%$ . Below that temperature, numerical results are not available. Nevertheless the error can be estimated by calculating the correction at the second iterative order, as before. One finds that the error tends to zero as  $b \rightarrow \infty$  in the entire interval  $[0, 1]$ .

For the charge density, we have

$$\rho_0 \sim b^{d-1}(\ln b)^{-1/2} \quad (3.57)$$

therefore the energy gap behaves as

$$E_g = \frac{\langle q\mathcal{O}_\Delta \rangle^{1/\Delta}}{T_c} \sim (\ln b)^{\frac{1}{2(d-1)}} \sim \left( \ln \frac{T_c}{T} \right)^{\frac{1}{2(d-1)}} \quad (3.58)$$

showing that the condensate diverges at the BF bound, albeit very mildly. This mild divergence was missed in earlier numerical studies (30).

The BF bound can also be approached from above. However, the calculation becomes considerably more involved, because for  $\Delta > d/2$ , as  $T \rightarrow 0$ , we have  $F_0 \approx 1$  near the boundary ( $z = 0$ ), but asymptotically ( $z \gtrsim 1/b$ ),  $F_0 \sim z^{d-2\Delta}$ , which does not have a smooth limit as  $T \rightarrow 0$ . Therefore, we cannot apply perturbation theory

and a different approach is called for (27). For example, one can approximate  $F_0$  by

$$F_0(z) = \begin{cases} 1 & , \quad z \leq \alpha \\ \left(\frac{z}{\alpha}\right)^{d-2\Delta} & , \quad z > \alpha \end{cases} \quad (3.59)$$

and find  $\alpha$  by a variational method. We shall not dwell on this further here.

Having understood the probe limit, we now turn to the first-order corections in a  $1/q^2$  expansion. For  $\Delta < d/2$ , it is necessary to include these corrections in order to obtain a physical system at low temperatures, because in the  $q \rightarrow \infty$  limit the condensate diverges as  $T \rightarrow 0$  (eqs. (3.54) and (3.58)).

At first order, we obtain for the functions determining the metric,

$$\begin{aligned} z f_1' - d f_1 &= \frac{(bz)^{2\Delta}}{4(d-1)} \left[ \left( m^2 + \Delta^2 f_0 + \frac{z^2 \Phi_0^2}{(bz)^{2\Delta}} \right) F_0^2 + 2\Delta z f_0 F_0 F_0' + z^2 f_0 F_0'^2 + \frac{z^4}{(bz)^{2\Delta}} \Phi_0'^2 \right] \\ z \chi_1' &= \frac{(bz)^{2\Delta}}{d-1} \left[ \left( \Delta^2 + \frac{z^2 \Phi_0^2}{f_0^2} \right) F_0^2 + 2\Delta z F_0 F_0' + z^2 F_0'^2 \right] \end{aligned} \quad (3.60)$$

They can be solved at low temperature using our zeroth-order results above. We obtain

$$f_1(z) = -\frac{\Delta}{4(d-1)} (bz)^{2\Delta} [2 - z^d - z^{d-2\Delta}] + \dots, \quad \chi_1(z) = -\frac{\Delta}{2(d-1)} (bz)^{2\Delta} + \dots \quad (3.61)$$

For the temperature, we deduce the first-order expression

$$T = \frac{d}{4\pi} \left[ 1 + \frac{\Delta^2}{2d(d-1)} \frac{b^{2\Delta}}{q^2} + \dots \right] \quad (3.62)$$

showing that the temperature receives a positive correction away from the probe limit. Moreover, it is now clear when the probe limit fails. Indeed, for the expansion in  $1/q^2$  to be valid, we ought to have

$$b \lesssim q^{1/\Delta} \quad (3.63)$$

justifying our earlier definition of the low energy regime ( $1 \lesssim b \lesssim q^{1/\Delta}$ ).

For a given  $q$ , (3.63) places a lower bound on the temperature. While zero temperature is unattainable for finite  $q$ , the temperature can be made arbitrarily low by choosing a sufficiently large  $q$ . It follows that, even though the probe limit ( $q \rightarrow \infty$ ) is not a physical system at zero temperature, its properties are a good approximation to corresponding properties of physical systems (of finite charge  $q$  and (low) temperature). The approximation becomes better with increasing  $q$  as the  $1/q^2$  corrections become smaller.

### 3.2.2 Anisotropy

#### Higher Modes

Before we begin discussion of the anisotropic system at low temperatures, we first need to establish that higher order modes don't contribute significantly. Using the perturbative method, we can also study the behavior of the subleading term of the condensate for  $1/2 < \Delta < 3/2$ . For  $\delta \neq 1$ , the  $n = 1$  mode does not vanish and at sub-leading order, it is given by

$$F_1^{(1)} = F_0^{(1)} \left[ \frac{\langle \mathcal{O}_\Delta \rangle^{(1)}}{\langle \mathcal{O}_\Delta \rangle^{(0)}} - \frac{\mu_c^2 \delta (1 - \delta)}{3 - 2\Delta} \int_0^z \frac{dz'}{z'^{2-2\Delta}} \tilde{F}_0^{(1)} \frac{A^{(0)} A^{(1)}}{h} F_0^{(0)} \right] + \tilde{F}_0^{(1)} \frac{\mu_c^2 \delta (1 - \delta)}{3 - 2\Delta} \int_0^z \frac{dz'}{z'^{2-2\Delta}} F_0^{(1)} \frac{A^{(0)} A^{(1)}}{h} F_0^{(0)}, \quad (3.64)$$

where  $F_0^{(1)}$  and  $\tilde{F}_0^{(1)}$  obey

$$\partial_z \left( h z^{2\Delta-2} \partial_z F_0^{(1)} \right) - (z\Delta^2 + Q_c^2) z^{2\Delta-2} F_0^{(1)} = 0, \quad (3.65)$$

with the boundary conditions  $F_0^{(1)}(z = 0) = 1$  and  $\tilde{F}_0^{(1)} \approx z^{3-2\Delta}$ . With  $\mu_c^2$  given by Eq. (2.50), the boundary value

$$F^{(1)}(z = 0) = \frac{\langle \mathcal{O}_\Delta \rangle^{(1)}}{\langle \mathcal{O}_\Delta \rangle^{(0)}} \quad (3.66)$$

is fully determined by demanding regularity at the horizon. To determine this, let us introduce the tortoise coordinate, defined as

$$\begin{aligned} r_* &= (3 - 2\Delta) \int_0^z \frac{dz'}{h z'^{2\Delta-2}} \\ &= \frac{3 - 2\Delta}{3} B\left(z^3; \frac{3 - 2\Delta}{3}, 0\right), \end{aligned} \quad (3.67)$$

where  $B(x; a, b)$  is the incomplete Euler beta function. We note that near the boundary  $r_*(z \rightarrow 0) = z^{3-2\Delta}$ . In this tortoise coordinate, the equation of motion for  $F_0^{(1)}$  and  $\tilde{F}_0^{(1)}$  can be rewritten in the Schrödinger form

$$-\partial_{r_*^2} F_0^{(1)} + V F_0^{(1)} = 0, \quad (3.68)$$

with the “potential”  $V$  given by

$$\begin{aligned} V &= \frac{Q_c^2 + z\Delta^2}{(3 - 2\Delta)^2} h z^{4(\Delta-1)} \\ &\approx \left(\frac{Q_c}{3 - 2\Delta}\right)^2 r_*^{\frac{4(\Delta-1)}{3-2\Delta}} \exp\left(-r_*^{\frac{3}{3-2\Delta}}\right). \end{aligned} \quad (3.69)$$

Rescaling the tortoise coordinate  $\tilde{r}_* = Q_c^{3-2\Delta} r_*$ , at large  $Q_c$ , we have

$$-\partial_{\tilde{r}_*^2} F_0^{(1)} + \left(\frac{1}{3 - 2\Delta}\right)^2 \tilde{r}_*^{\frac{4(\Delta-1)}{3-2\Delta}} F_0^{(1)} = 0, \quad (3.70)$$

whose solutions are given in terms of modified Bessel functions

$$F_0^{(1)} = \frac{\pi}{\Gamma\left(\frac{3-2\Delta}{2}\right)} \frac{2^{\frac{2\Delta-3}{2}}}{\sin \frac{\pi(3-2\Delta)}{2}} \sqrt{\tilde{r}_*} I_{\frac{2\Delta-3}{2}}\left(\tilde{r}_*^{\frac{1}{3-2\Delta}}\right), \quad (3.71)$$

and

$$\tilde{F}_0^{(1)} = \frac{\Gamma\left(\frac{5-2\Delta}{2}\right)}{Q_c^{3-2\Delta}} 2^{\frac{3-2\Delta}{2}} \sqrt{\tilde{r}_*} I_{\frac{3-2\Delta}{2}}\left(\tilde{r}_*^{\frac{1}{3-2\Delta}}\right). \quad (3.72)$$

These solutions satisfy the boundary conditions  $F_0^{(1)}(r_* = 0) = 1$  and  $\tilde{F}_0^{(1)}(r_* = 0) = \tilde{r}_*$  but they diverge at the horizon. Their ratio at large  $Q_c$  is then given by

$$\lim_{\tilde{r}_* \rightarrow \infty} \frac{\tilde{F}_0^{(1)}}{F_0^{(1)}} = \frac{\Gamma\left(\frac{5-2\Delta}{2}\right) \Gamma\left(\frac{3-2\Delta}{2}\right)}{\pi} 2^{3-2\Delta} \sin\left(\frac{\pi(3-2\Delta)}{2}\right) Q_c^{2\Delta-3}. \quad (3.73)$$

Substituting this into Eq. (3.64) and demanding the full solution to the  $n = 1$  mode be regular at the horizon, we obtain

$$\frac{\langle \mathcal{O}_\Delta \rangle^{(1)}}{\langle \mathcal{O}_\Delta \rangle^{(0)}} = \frac{\delta(1-\delta)}{3-2\Delta} \left[ 1 - \frac{\Gamma\left(\frac{5-2\Delta}{2}\right) \Gamma\left(\frac{3-2\Delta}{2}\right) \Gamma(2\Delta-1)}{\pi 2^{2\Delta-3}} \sin\left(\frac{\pi(3-2\Delta)}{2}\right) \right] \frac{\mu^2}{Q^2} \left[ 1 + \mathcal{O}\left(\frac{1}{Q_c}\right) \right]. \quad (3.74)$$

The leading order coefficient is plotted in Fig. 3.13. As this vanishes for  $\Delta = 1$  and  $\mu_c^2(\Delta = 1)$  is finite, the leading order is  $\mathcal{O}(\mu_c^2/Q_c^3)$ .

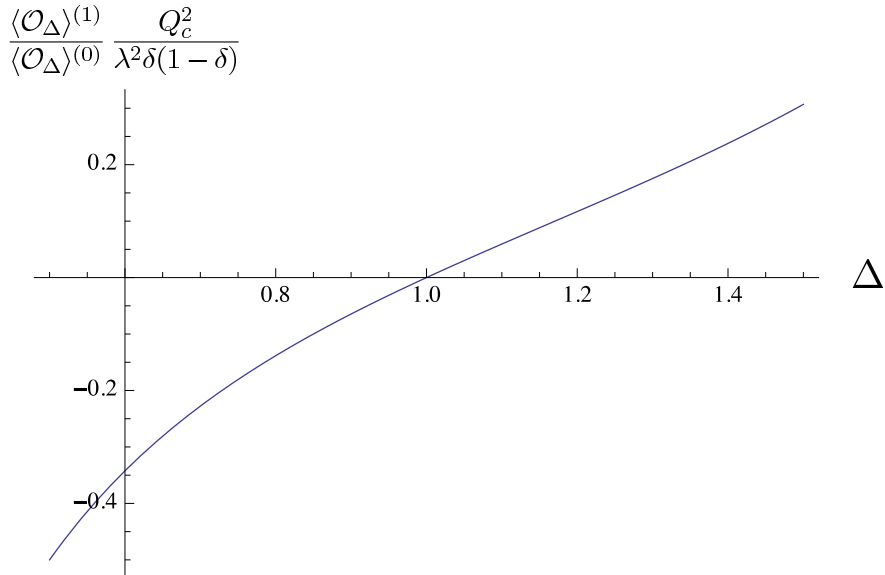


**Figure 3.13:** The ratio  $\frac{\langle \mathcal{O}_\Delta \rangle^{(1)}}{\langle \mathcal{O}_\Delta \rangle^{(0)}} \frac{Q_c^2}{\lambda^2 \delta (1-\delta)}$  as a function  $\Delta$ .

Similarly, we obtain

$$\frac{\langle \mathcal{O}_\Delta \rangle^{(2)}}{\langle \mathcal{O}_\Delta \rangle^{(0)}} = \frac{\delta^2}{4(3-2\Delta)} \left[ \frac{\Gamma\left(\frac{5-2\Delta}{2}\right) \Gamma\left(\frac{3-2\Delta}{2}\right) \Gamma(2\Delta-1)}{\pi 2^{2\Delta-1}} \sin\left(\frac{\pi(3-2\Delta)}{2}\right) - \frac{1}{4} \right] \frac{\mu^2}{Q^2} \left[ 1 + \mathcal{O}\left(\frac{1}{Q_c}\right) \right]. \quad (3.75)$$

The dependence of this ratio on  $\Delta$  is depicted in Fig. 3.14. Again, we see that for  $\Delta = 1$ , the bracketed quantity vanishes and the ratio is of order  $\mathcal{O}(\mu_c^2/Q_c^3)$ .

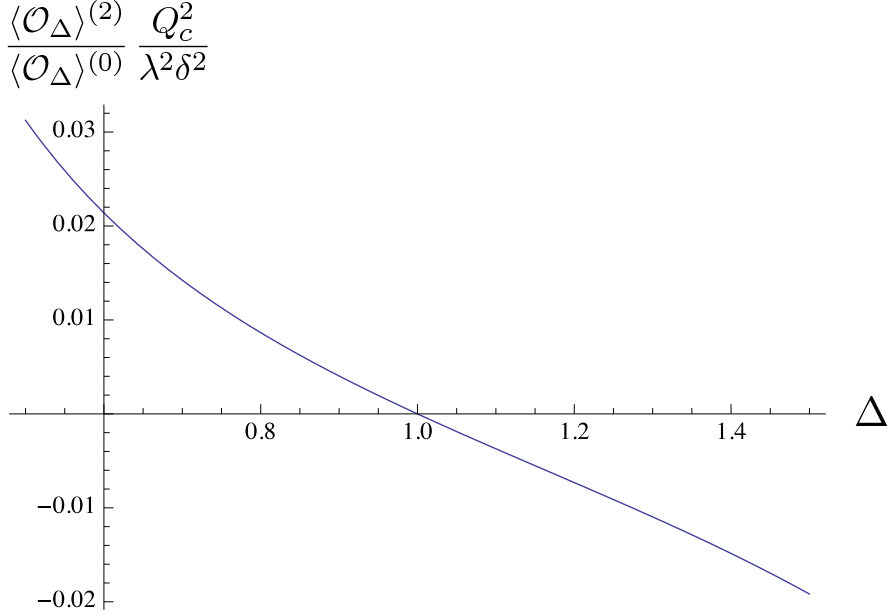


**Figure 3.14:** The ratio  $\frac{\langle \mathcal{O}_\Delta \rangle^{(2)}}{\langle \mathcal{O}_\Delta \rangle^{(0)}} \frac{Q_c^2}{\lambda^2 \delta^2}$  as a function  $\Delta$ .

It is easy to see that for  $\delta \neq 1$ , when  $\Delta \neq 1$

$$\frac{\langle \mathcal{O}_\Delta \rangle^{(n)}}{\langle \mathcal{O}_\Delta \rangle^{(0)}} = \mathcal{O}\left(\frac{\mu^{2[n/2]}}{Q^{2[n/2]}}\right), \quad (3.76)$$

where  $[n]$  denotes the largest integer  $\leq n$ , and

$$\frac{\langle \mathcal{O}_1 \rangle^{(n)}}{\langle \mathcal{O}_1 \rangle^{(0)}} = \mathcal{O}\left(\frac{\mu^{2[n/2]} T_c^{[n/2]}}{Q^{3[n/2]}}\right), \quad (3.77)$$

for  $\Delta = 1$ . For  $\delta = 1$ , the odd modes vanish while the result for the even modes stays the same. This result confirms that at large  $Q$ , higher modes are negligible.

### Below the Critical Temperature

Below the critical temperature,  $\Psi \neq 0$  and we have to include its contribution toward the electrostatic potential. From Eqs. 2.14 and 2.23, and by neglecting the higher modes, we have

$$A^{(n)''} - \left( \frac{n^2 Q^2}{r_+^2 h} + \frac{\langle \mathcal{O}_\Delta \rangle^{(0)^2} z^{2(\Delta-1)}}{r_+^{2\Delta} h} F^{(0)^2} \right) A^{(n)} = 0. \quad (3.78)$$

Rescaling  $\tilde{z} = \frac{Q}{r_+} z$ , we have

$$\partial_{\tilde{z}}^2 A^{(n)} - n^2 A^{(n)} = \frac{\langle \mathcal{O}_\Delta \rangle^{(0)^2} \tilde{z}^{2(\Delta-1)}}{Q^{2\Delta}} A^{(n)}, \quad (3.79)$$

where we have dropped terms of order  $1/Q^3$ .

$\Delta = 1$

The  $\Delta = 1$  case is a particularly easy one to solve and the solution is given by

$$A^{(n)} = \frac{\sinh \frac{\sqrt{n^2 Q^2 + \langle \mathcal{O}_1 \rangle^{(0)^2}}}{r_+} (1 - z)}{\sinh \frac{\sqrt{n^2 Q^2 + \langle \mathcal{O}_1 \rangle^{(0)^2}}}{r_+}}. \quad (3.80)$$

Substituting this into the equation of motion for the scalar field and demanding regularity at the horizon, we have

$$\frac{r_+^2}{\mu^2} = \frac{\Gamma^3\left(\frac{1}{3}\right)}{3\Gamma^3\left(\frac{2}{3}\right)} a(1) - \tilde{a}(1), \quad (3.81)$$

where  $a(1)$  and  $\tilde{a}(1)$  are defined in Eq. (2.45), but now with  $A^{(n)}$  ( $n = 0, 1$ ) given by (3.80).

For  $\delta = 1$ , we obtain

$$\frac{r_+}{\mu^2} = \frac{\Gamma^3\left(\frac{1}{3}\right)}{12\Gamma^3\left(\frac{2}{3}\right)} \frac{1}{\sqrt{Q^2 + \langle\mathcal{O}_1\rangle^{(0)2}}} . \quad (3.82)$$

Multiplying by  $\mu_c^2$ , and solving for the condensate, we obtain

$$\langle\mathcal{O}_1\rangle^{(0)} = Q \sqrt{\left(\frac{T_c}{T}\right)^2 - 1} , \quad (3.83)$$

showing that in the absence of a homogeneous term in the chemical potential, the condensate is proportional to the wavenumber  $Q$ .

Including a homogeneous term ( $\delta \neq 1$ ) changes this behavior. The case when the temperature is not too far away from the critical value, such that the expectation value of the condensate is small, will be treated when we study the case of general  $\Delta$ , but here let us assume that the condensate is large (low temperature regime). Then

$$\frac{r_+}{\mu^2} = \frac{\Gamma^3\left(\frac{1}{3}\right)}{3\Gamma^3\left(\frac{2}{3}\right)} \left[ \frac{(1-\delta)^2}{2\langle\mathcal{O}_1\rangle^{(0)}} + \frac{\delta^2}{4\sqrt{Q^2 + \langle\mathcal{O}_1\rangle^{(0)2}}} \right] . \quad (3.84)$$

Multiplying by  $\mu_c^2$ , we obtain for  $\delta \neq 1$  and  $\langle\mathcal{O}_1\rangle^{(0)} \lesssim Q$ ,

$$\frac{T}{T_c^2} = 1.54 \left( \frac{1}{\langle\mathcal{O}_1\rangle^{(0)}} + \frac{\delta^2}{2(1-\delta)^2} \frac{1}{Q} + \dots \right) . \quad (3.85)$$

Therefore,

$$\langle\mathcal{O}_1\rangle^{(0)} = 6.4 \frac{T_c^2}{T} + \mathcal{O}(1/Q) . \quad (3.86)$$

For  $Q \lesssim \langle\mathcal{O}_1\rangle^{(0)}$ , we similarly obtain at leading order

$$\langle\mathcal{O}_1\rangle^{(0)} = 6.4 \frac{1 - 2\delta + \frac{3\delta^2}{2}}{(1-\delta)^2} \frac{T_c^2}{T} . \quad (3.87)$$



Near  $T_c$

Let us now consider the case of general  $\Delta$ . For  $n = 0$ , the solution that satisfies the boundary conditions is given in terms of the modified Bessel function of the second kind

$$A^{(0)} = \frac{\langle \mathcal{O}_\Delta \rangle^{(0)} \frac{1}{2\Delta} 2^{\frac{2\Delta-1}{2\Delta}}}{\Gamma\left(\frac{1}{2\Delta}\right) r_+^{\frac{1}{2}} \Delta^{\frac{1}{2\Delta}}} \sqrt{z} K_{\frac{1}{2\Delta}} \left( \frac{\langle \mathcal{O}_\Delta \rangle^{(0)} z^\Delta}{\Delta r_+^\Delta} \right). \quad (3.88)$$

For  $n > 0$ , let us first consider a temperature not too far away below  $T_c$ , such that  $\langle \mathcal{O}_\Delta \rangle^{(0)}$  is small and the right hand side of Eq. (3.79) can be treated as perturbation. The solution is then expanded as

$$A^{(n)} = A_0^{(n)} + A_1^{(n)} + \dots, \quad (3.89)$$

where

$$\begin{aligned} A_0^{(n)} &= \frac{\sinh \frac{nQ}{r_+} (1-z)}{\sinh \frac{nQ}{r_+}}, \\ A_1^{(n)} &= -\frac{\langle \mathcal{O}_\Delta \rangle^{(0)2}}{r_+^{2\Delta-1} nQ} \left( A_0^{(n)} \int_0^1 dz' \frac{\sinh \frac{nQ}{r_+} z'}{(z')^{2(1-\Delta)}} A_0^{(n)} - \int_z^1 dz' \frac{\sinh \frac{nQ}{r_+} (z'-z)}{(z')^{2(1-\Delta)}} A_0^{(n)} \right) \\ &= -\frac{z^{2\Delta-1}}{2(2\Delta-1)} \frac{e^{-nQz/r_+}}{nQ} \frac{\langle \mathcal{O}_\Delta \rangle^{(0)2}}{r_+^{2\Delta-1}}. \end{aligned} \quad (3.90)$$

For small  $\langle \mathcal{O}_\Delta \rangle^{(0)}$ , the zero mode of the electrostatic potential can also be expanded as

$$A^{(0)} = 1 - z - \frac{(2\Delta-1)z^{2\Delta+1} - (2\Delta+1)z^{2\Delta} + 2z}{(2\Delta-1)2\Delta(2\Delta+1)} \frac{\langle \mathcal{O}_\Delta \rangle^{(0)2}}{r_+^{2\Delta}}. \quad (3.91)$$

It is easy to see that by substituting  $\Delta = 1$  into the above equations, we recover the result of Eq. (3.80) in this regime.

Substituting this into the equation of motion for the scalar and demanding regularity at the horizon, we obtain Eq. (3.81), but now with

$$\mathcal{A} = \frac{1}{2} \frac{\sinh^2 \frac{Q}{r_+} (1-z)}{\sinh^2 \frac{Q}{r_+}} - \frac{z^{2\Delta-1}}{2(2\Delta-1)} \frac{e^{-2Qz/r_+}}{Q} \frac{\langle \mathcal{O}_\Delta \rangle^{(0)2}}{r_+^{2\Delta-1}}, \quad (3.92)$$

for  $\delta = 1$ . We deduce

$$\frac{r_+^2}{\mu^2} = \frac{\Gamma^2\left(\frac{\Delta}{3}\right)}{\Gamma\left(\frac{2\Delta}{3}\right)} \frac{\Gamma\left(\frac{2(3-\Delta)}{3}\right)}{\Gamma^2\left(\frac{3-\Delta}{3}\right)} \frac{1}{2^{2\Delta}(3-2\Delta)} \frac{r_+^{2\Delta-1}}{Q^{2\Delta-1}} \left[ \Gamma(2\Delta-1) - \frac{\Gamma(4\Delta-2)}{2\Delta-1} \frac{1}{2^{2\Delta-1}} \frac{\langle \mathcal{O}_\Delta \rangle^{(0)^2}}{Q^{2\Delta}} \right]. \quad (3.93)$$

Multiplying by  $\mu_c^2$ , after some algebra, we obtain the condensate

$$\langle \mathcal{O}_\Delta \rangle^{(0)} = \sqrt{\frac{(2\Delta-1)2^{2\Delta-1}\Gamma(2\Delta-1)}{\Gamma(4\Delta-2)}} Q^\Delta \sqrt{1 - \left(\frac{T}{T_c}\right)^{3-2\Delta}}. \quad (3.94)$$

showing that for  $\delta = 1$ , in the large  $Q$  limit,

$$\langle \mathcal{O}_\Delta \rangle^{1/\Delta} \propto Q. \quad (3.95)$$

Similarly, in the case  $\delta \neq 1$ , we have

$$\begin{aligned} \frac{r_+^2}{\mu^2} = & \left( \frac{\Gamma^2\left(\frac{\Delta}{3}\right)}{\Gamma\left(\frac{2\Delta}{3}\right)} \frac{\Gamma\left(\frac{2(3-\Delta)}{3}\right)}{\Gamma^2\left(\frac{3-\Delta}{3}\right)} a_0^{(0)} - \tilde{a}_0^{(0)} \right) \frac{(1-\delta)^2}{3-2\Delta} + \frac{\Gamma^2\left(\frac{\Delta}{3}\right)}{\Gamma\left(\frac{2\Delta}{3}\right)} \frac{\Gamma\left(\frac{2(3-\Delta)}{3}\right)}{\Gamma^2\left(\frac{3-\Delta}{3}\right)} \frac{\Gamma(2\Delta-1)}{2^{2\Delta}(3-2\Delta)} \frac{\delta^2}{Q^{2\Delta-1}} \\ & + \left( \frac{\Gamma^2\left(\frac{\Delta}{3}\right)}{\Gamma\left(\frac{2\Delta}{3}\right)} \frac{\Gamma\left(\frac{2(3-\Delta)}{3}\right)}{\Gamma^2\left(\frac{3-\Delta}{3}\right)} a_1^{(0)} - \tilde{a}_1^{(0)} \right) \frac{(1-\delta)^2}{(2\Delta-3)\Delta(2\Delta-1)(2\Delta+1)} \frac{\langle \mathcal{O}_\Delta \rangle^{(0)^2}}{r_+^{2\Delta}}, \end{aligned} \quad (3.96)$$

where  $a_0^{(0)}$  and  $\tilde{a}_0^{(0)}$  are given by Eqs. 2.49, and

$$\begin{aligned} a_1^{(0)} &= \int_0^1 \frac{dz}{z^{1-2\Delta}} F_0^{(0)} \frac{(2\Delta-1)z^{2\Delta} - (2\Delta+1)z^{2\Delta-1} + 2}{z^2 + z + 1} F_0^{(0)}, \\ \tilde{a}_1^{(0)} &= \int_0^1 \frac{dz}{z^{2-2\Delta}} \tilde{F}_0^{(0)} \frac{(2\Delta-1)z^{2\Delta} - (2\Delta+1)z^{2\Delta-1} + 2}{z^2 + z + 1} F_0^{(0)}. \end{aligned} \quad (3.97)$$

Multiplying the above by  $\mu_c^2$ , we get for the condensate

$$\langle \mathcal{O}_\Delta \rangle^{(0)} = \gamma T^\Delta \sqrt{1 - \frac{T^2}{T_c^2}} \left[ 1 + \mathcal{O}\left(\frac{1}{Q^{2\Delta-1}}\right) \right], \quad (3.98)$$

where

$$\gamma = \left(\frac{4\pi}{3}\right)^\Delta \sqrt{\Delta(4\Delta^2 - 1)} \left( \frac{\frac{\Gamma^2\left(\frac{\Delta}{3}\right)}{\Gamma\left(\frac{2\Delta}{3}\right)} \frac{\Gamma\left(\frac{2(3-\Delta)}{3}\right)}{\Gamma^2\left(\frac{3-\Delta}{3}\right)} a_0^{(0)} - \tilde{a}_0^{(0)} }{\frac{\Gamma^2\left(\frac{\Delta}{3}\right)}{\Gamma\left(\frac{2\Delta}{3}\right)} \frac{\Gamma\left(\frac{2(3-\Delta)}{3}\right)}{\Gamma^2\left(\frac{3-\Delta}{3}\right)} a_1^{(0)} - \tilde{a}_1^{(0)} } \right)^{1/2}. \quad (3.99)$$

The expectation value of the condensate for  $\delta = 1$  and  $\Delta = 1$  obtained analytically is compared to the numerical results in Fig. 3.15.

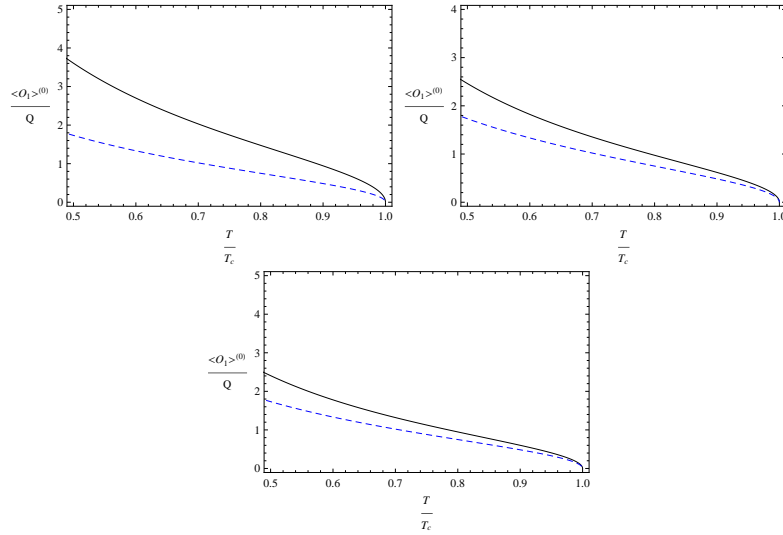


**Figure 3.15:** The expectation value of the condensate for  $\delta = 1$  and  $\Delta = 1$  for  $Q_c = 6, 33$  and  $55$ . The solid black lines and the dashed blue lines depict the numerical and analytical results, respectively.

We can also obtain the higher modes of the condensate using a similar calculation as the one in Section 3.2.2, but with the electrostatic potential given in Eqs. 3.91 and 3.90. The results are

$$\frac{\langle \mathcal{O}_\Delta \rangle^{(1)}}{\langle \mathcal{O}_\Delta \rangle^{(0)}} = \frac{\delta(1-\delta)}{3-2\Delta} \left[ 1 - \frac{\Gamma\left(\frac{5-2\Delta}{2}\right) \Gamma\left(\frac{3-2\Delta}{2}\right) \Gamma(2\Delta-1)}{\pi 2^{2\Delta-3}} \sin\left(\frac{\pi(3-2\Delta)}{2}\right) \right] \frac{\mu^2}{Q^2} \left[ 1 + \mathcal{O}\left(\frac{T}{Q}\right) \right], \quad (3.100)$$

and

$$\frac{\langle \mathcal{O}_\Delta \rangle^{(2)}}{\langle \mathcal{O}_\Delta \rangle^{(0)}} = \frac{\delta^2}{4(3-2\Delta)} \left[ \frac{\Gamma\left(\frac{5-2\Delta}{2}\right) \Gamma\left(\frac{3-2\Delta}{2}\right) \Gamma(2\Delta-1)}{\pi 2^{2\Delta-1}} \sin\left(\frac{\pi(3-2\Delta)}{2}\right) - \frac{1}{4} \right] \frac{\mu^2}{Q^2} \left[ 1 + \mathcal{O}\left(\frac{T}{Q}\right) \right]. \quad (3.101)$$

As before, for  $\Delta = 1$ , the  $\mathcal{O}(\mu^2/Q^2)$  terms vanish, and the  $n = 1, 2$  modes are suppressed by a factor of an order  $\mathcal{O}(\mu^2 T/Q^3)$  compared to the  $n = 0$  mode. For  $\delta = 1$ , the odd modes for the condensate vanish.

### 3.2.3 $T \ll T_c$

Lastly, let us consider a low temperature where the right hand side of Eq. (3.79) is a lot larger than unity. We then have

$$A^{(1)} = \frac{\langle \mathcal{O}_\Delta \rangle^{(0) \frac{1}{2\Delta}} 2^{\frac{2\Delta-1}{2\Delta}}}{\Gamma\left(\frac{1}{2\Delta}\right) r_+^{\frac{1}{2}} \Delta^{\frac{1}{2\Delta}}} \sqrt{z} K_{\frac{1}{2\Delta}} \left( \frac{\langle \mathcal{O}_\Delta \rangle^{(0)} z^\Delta}{\Delta r_+^\Delta} \right) = A^{(0)}. \quad (3.102)$$

Substituting this into the equation of motion for the scalar and demanding regularity at the horizon, we again obtain Eq. (3.81), but with

$$\begin{aligned} \mathcal{A} &= \left( 1 - 2\delta + \frac{3\delta^2}{2} \right) A^{(0)2} \\ &= \left( 1 - 2\delta + \frac{3\delta^2}{2} \right) \frac{\langle \mathcal{O}_\Delta \rangle^{(0) \frac{1}{\Delta}} 2^{\frac{2\Delta-1}{\Delta}}}{\Gamma^2\left(\frac{1}{2\Delta}\right) \Delta^{\frac{1}{\Delta}}} \frac{z}{r_+} K_{\frac{1}{2\Delta}}^2 \left( \frac{\langle \mathcal{O}_\Delta \rangle^{(0)} z^\Delta}{\Delta r_+^\Delta} \right). \end{aligned} \quad (3.103)$$

Furthermore, since  $\frac{1}{3} < \frac{1}{2\Delta} < 1$  is not an integer, we can express the modified Bessel function in terms of exponential and hypergeometric functions. The integral  $a(1)$  then becomes

$$\begin{aligned} a(1) &= \left( 1 - 2\delta + \frac{3\delta^2}{2} \right) \int_0^1 \frac{dz}{z^{2-2\Delta}} \frac{1}{h} e^{-\frac{2\langle \mathcal{O}_\Delta \rangle^{(0)} z^\Delta}{\Delta r_+^\Delta}} \left[ F_0^{(0)} {}_1F_1 \left( \frac{1}{2} - \frac{1}{2\Delta}; 1 - \frac{1}{\Delta}; \frac{2\langle \mathcal{O}_\Delta \rangle^{(0)} z^\Delta}{\Delta r_+^\Delta} \right) \right]^2 \\ &\approx \left( 1 - 2\delta + \frac{3\delta^2}{2} \right) \frac{\Gamma\left(\frac{2\Delta-1}{\Delta}\right)}{2^{\frac{2\Delta-1}{\Delta}} \Delta^{\frac{1-\Delta}{\Delta}}} \left( \frac{r_+^\Delta}{\langle \mathcal{O}_\Delta \rangle^{(0)}} \right)^{\frac{2\Delta-1}{\Delta}}, \end{aligned} \quad (3.104)$$

where we have approximated the integral by evaluating the integrand at  $z = 0$ . Similarly, we find  $\tilde{a}(1)$  to be of order  $(\langle \mathcal{O}_\Delta \rangle^{(0)})^{-2/\Delta}$ , which is negligible compared to  $a(1)$ . Therefore,

$$\frac{r_+^2}{\mu^2} = \frac{1 - 2\delta + \frac{3\delta^2}{2}}{3 - 2\Delta} \frac{\Gamma^2\left(\frac{\Delta}{3}\right)}{\Gamma\left(\frac{2\Delta}{3}\right)} \frac{\Gamma\left(\frac{2(3-\Delta)}{3}\right)}{\Gamma^2\left(\frac{3-\Delta}{3}\right)} \frac{\Gamma\left(\frac{2\Delta-1}{\Delta}\right)}{2^{\frac{2\Delta-1}{\Delta}} \Delta^{\frac{1-\Delta}{\Delta}}} \left(\frac{r_+^\Delta}{\langle \mathcal{O}_\Delta \rangle^{(0)}}\right)^{\frac{2\Delta-1}{\Delta}}. \quad (3.105)$$

Multiplying by  $\mu_c^2$ , for  $\delta = 1$ , we obtain the condensate

$$[\langle \mathcal{O}_\Delta \rangle^{(0)}]^{1/\Delta} = \left(2 \Delta^{\frac{1}{2\Delta-1}}\right)^{1-1/\Delta} \left[\frac{\Gamma\left(\frac{2\Delta-1}{\Delta}\right)}{\Gamma(2\Delta-1)}\right]^{\frac{1}{2\Delta-1}} \left(\frac{T_c}{T}\right)^{\frac{3-2\Delta}{2\Delta-1}} Q, \quad (3.106)$$

showing again that the gap,  $\langle \mathcal{O}_\Delta \rangle^{1/\Delta}$ , is proportional to  $Q$ .

For  $\delta \neq 1$ , similarly, we obtain the condensate at low temperature,

$$[\langle \mathcal{O}_\Delta \rangle^{(0)}]^{1/\Delta} = \gamma T_c \left(\frac{T_c}{T}\right)^{\frac{3-2\Delta}{2\Delta-1}} \left[1 + \mathcal{O}\left(\frac{1}{Q^{2\Delta-1}}\right)\right], \quad (3.107)$$

where

$$\gamma = \frac{4\pi}{3} \frac{1}{(2 \Delta^{\frac{1-\Delta}{2\Delta-1}})^{1/\Delta}} \left[ \frac{\left(1 - 2\delta + \frac{3\delta^2}{2}\right) \frac{\Gamma^2\left(\frac{\Delta}{3}\right) \Gamma\left(\frac{2(3-\Delta)}{3}\right) \Gamma\left(\frac{2\Delta-1}{\Delta}\right)}{\Gamma\left(\frac{2\Delta}{3}\right) \Gamma^2\left(\frac{3-\Delta}{3}\right)}}{\frac{\Gamma^2\left(\frac{\Delta}{3}\right) \Gamma\left(\frac{2(3-\Delta)}{3}\right)}{\Gamma\left(\frac{2\Delta}{3}\right) \Gamma^2\left(\frac{3-\Delta}{3}\right)} a_0^{(0)} - \tilde{a}_0^{(0)}} \right]^{\frac{1}{2\Delta-1}}, \quad (3.108)$$

where  $a_0^{(0)}$  and  $\tilde{a}_0^{(0)}$  are again defined in Eqs. (2.49).

We do not have a comparative plot for low temperature regime due to the fact that the numerical solution to the non-linear field equations become increasingly cumbersome as the temperature approaches zero.

By requiring regularity of the higher modes of the scalar field at the horizon, we can obtain the information concerning the higher modes of the condensate, as was

done in Section 3.2.2. The results are

$$\langle \mathcal{O}_\Delta \rangle^{(1)} = \frac{\delta(1-\delta)}{3-2\Delta} \frac{\Delta^{\frac{2-\Delta}{2}}}{2^{\frac{2}{\Delta}}} \Gamma\left(\frac{2}{\Delta}\right) \mu^2 [\langle \mathcal{O}_\Delta \rangle^{(0)}]^{1-\frac{2}{\Delta}}, \quad (3.109)$$

and

$$\langle \mathcal{O}_\Delta \rangle^{(2)} = \frac{\delta^2}{4(3-2\Delta)} \frac{\Delta^{\frac{2-\Delta}{2}}}{2^{\frac{2}{\Delta}}} \Gamma\left(\frac{2}{\Delta}\right) \mu^2 [\langle \mathcal{O}_\Delta \rangle^{(0)}]^{1-\frac{2}{\Delta}}. \quad (3.110)$$

It is easy to see that

$$\frac{\langle \mathcal{O}_\Delta \rangle^{(n)}}{\langle \mathcal{O}_\Delta \rangle^{(0)}} = \mathcal{O}\left([\langle \mathcal{O}_\Delta \rangle^{(0)}]^{-\frac{2[n/2]}{\Delta}}\right), \quad (3.111)$$

where  $[n]$  denotes the largest integer  $\leq n$ , but with the odd modes vanishing for  $\delta = 1$ .

### 3.2.4 As $q \rightarrow 0$

In this limit, our solution at  $T_c$  is near the extremal solution. Due to this we expect that a perturbative solution should converge rapidly, since the order parameter is small near the transition we can expand in it

$$\begin{aligned} \Psi &= \langle \mathcal{O}_\Delta \rangle \Psi_0 + \langle \mathcal{O}_\Delta \rangle^3 \Psi_1 + \dots \\ \Phi &= \Phi_0 + \langle \mathcal{O}_\Delta \rangle^2 \Phi_1 + \dots \\ \chi &= \chi_0 + \langle \mathcal{O}_\Delta \rangle^2 \chi_1 + \dots \\ g &= g_0 + \langle \mathcal{O}_\Delta \rangle^2 g_1 + \dots \end{aligned} \quad (3.112)$$

the charge density is found from the electric potential from a similar expansion

$$\rho = -\Phi'(0) = \rho_0 + \langle \mathcal{O}_\Delta \rangle^2 \rho_1 + \dots \quad (3.113)$$

The temperature of the hairy black hole (2.12) is expanded as

$$\frac{T}{\sqrt{\ell}} = \frac{T_0}{\sqrt{\rho_0}} [1 - \langle \mathcal{O}_\Delta \rangle^2 \mathcal{T}_1 + \dots], \quad (3.114)$$

around the critical temperature, where

$$\mathcal{T}_1 = -\frac{g'_1(1)}{g'_0(1)} + \frac{1}{2}\chi_1(1) + \frac{\rho_1}{2\rho_0} . \quad (3.115)$$

At zeroth order, we have

$$\Phi_0 = \rho_0(1 - z) , \quad \chi_0 = 0 , \quad g_0 = 1 - \left(1 + \frac{\rho_0^2}{4}\right)z^3 + \frac{\rho_0^2}{4}z^4 , \quad (3.116)$$

and  $\Psi_0$  obeys the wave equation in the background (3.116) and has already been calculated,

$$\Psi_0 = \frac{1}{\sqrt{2}}z^\Delta F(z) , \quad (3.117)$$

where  $F$  is normalized by  $F(0) = 1$ . We can find corrections at first order to the fields

$$\chi_1(z) = \int_0^z dz' \left[ z'(\Psi'_0(z'))^2 + q^2 \rho_0^2 \frac{z'(1-z')^2}{g_0^2(z')} (\Psi_0(z'))^2 \right] \quad (3.118)$$

$$\Phi_1(z) = - \int_z^1 dz' \Phi'_1(z') , \quad \Phi'_1(z) = -\rho_1 + \rho_0 \varphi(z) \quad (3.119)$$

$$g_1(z) = z^3 \left[ -\frac{\rho_0 \rho_1}{2}(1 - z) + \mathcal{G}(z) \right] \quad (3.120)$$

Where

$$\varphi(z) = \int_z^1 dz' \left[ \frac{z'}{2}(\Psi'_0(z'))^2 + q^2 \left( 2 \frac{1-z'}{z'^2 g_0(z')} + \rho_0^2 \frac{z'(1-z')^2}{2g_0^2(z')} \right) (\Psi_0(z'))^2 \right] \quad (3.121)$$

$$\mathcal{G}'(z) = \left( \frac{m^2}{2z^4} + \frac{q^2 \Phi_0^2(z)}{2z^2 g_0(z)} \right) \Psi_0^2(z) + \frac{g_0(z)}{2z^2} (\Psi'_0(z))^2 + \frac{\rho_0^2}{4} (\chi_1(z) - 2\varphi(z)) \quad (3.122)$$

Therefore at the horizon,

$$g'_1(1) = \frac{\rho_0^2}{4}\chi_1(1) + \frac{m^2}{2}\Psi_0^2(1) + \frac{\rho_0 \rho_1}{2} . \quad (3.123)$$

We are left with an unknown parameter,  $\rho_1$  which we can find from looking at the first order corrections to the scalar field equation,

$$\Psi_1'' + \left[ \frac{g_0'}{g_0} - \frac{2}{z} \right] \Psi_1' + \left[ \frac{q^2 \Phi_0^2}{g_0^2} - \frac{m^2}{z^2 g_0} \right] \Psi_1 = -\mathcal{H}_1 \Psi_0 , \quad (3.124)$$

where

$$\mathcal{H}_1 \Psi_0 = \left[ \frac{g_1'}{g_0} - \frac{g_1 g_0'}{g_0^2} - \frac{\chi_1'}{2} \right] \Psi_0' + \left[ \frac{m^2 g_1}{z^2 g_0^2} - \frac{2q^2 \Phi_0 (g_0 \Phi_1 - g_1 \Phi_0)}{g_0^3} \right] \Psi_0 . \quad (3.125)$$

If we take the inner product of the field equation with  $\Psi_0$  we are left with the condition

$$\int_0^1 \frac{dz}{z^2} g_0(z) \Psi_0(z) \mathcal{H}_1 \Psi_0(z) = 0 , \quad (3.126)$$

which is linear in  $\rho_1$  and it can easily be seen that

$$\rho_1 = \frac{\int_0^1 \frac{dz}{z^2} \left( \left[ (z^3 \mathcal{G})' - \frac{z^3 \mathcal{G} g_0'}{g_0} - g_0 \frac{\chi_1'}{2} \right] \Psi_0 \Psi_0' + \left[ \frac{m^2 z \mathcal{G}}{g_0} + \frac{2q^2 \rho_0^2 (1-z)(g_0 \varphi - z^3 (1-z) \mathcal{G})}{g_0^2} \right] \Psi_0^2 \right)}{\rho_0 \int_0^1 \frac{dz}{z^2} \left( \left[ \frac{z^2 (3-4z)}{2} - \frac{g_0' z^3 (1-z)}{2g_0} \right] \Psi_0 \Psi_0' + \left[ \frac{m^2 z (1-z)}{2g_0} - \frac{q^2 (1-z)^2 (2g_0 + \rho_0^2 z^3 (1-z))}{g_0^2} \right] \Psi_0^2 \right)} . \quad (3.127)$$

This provides us with everything we need to make an approximation of the energy gap below the critical temperature. The leading order behavior of the condensate below  $T_c$  is given by

$$\langle \mathcal{O}_\Delta \rangle = \frac{1}{\sqrt{\mathcal{T}_1}} \sqrt{1 - \frac{T}{T_c}} . \quad (3.128)$$

and thus at  $T = 0$  the first order approximation of the energy gap is

$$\frac{\langle \mathcal{O}_\Delta \rangle^{1/\Delta}}{T_c} = \frac{1}{T_0 \mathcal{T}_1^{1/(2\Delta)}} . \quad (3.129)$$

In figure 3.16 we compare our first order analytical results with  $q^2 = 0$  to numerical solutions to the full set of field equations (2.4). The solution we find with



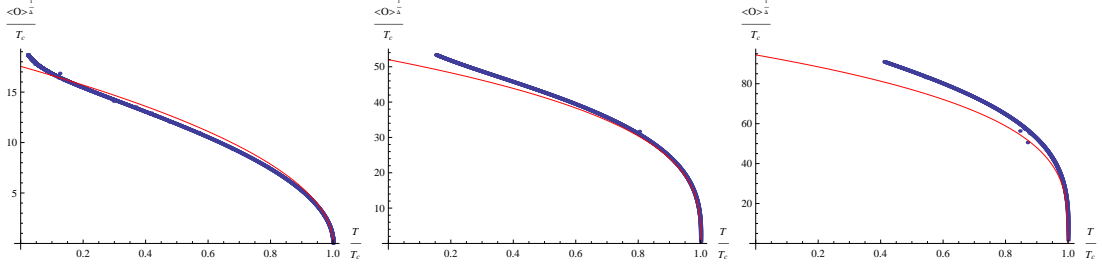


**Figure 3.16:** The energy gap for  $q^2 = 0$ , and  $\Delta = 1, 1.5, 1.7$  (left to right). The thin line is our first-order analytic result, the thick one is from numerics.

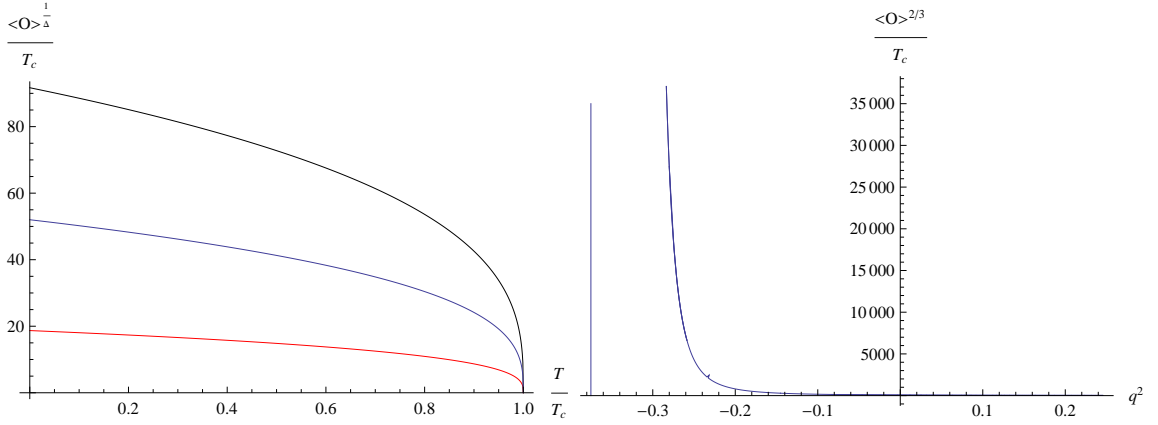


**Figure 3.17:** Left panel: energy gap *vs* temperature for  $\Delta = 1.5$   $q^2 = 0.38$  (lower curve),  $q^2 = 0$  (middle curve), and  $q^2 = -0.125$  (upper curve). Right panel: energy gap *vs*  $q^2$  at temperature  $T = 0.95T_c$  (asymptote at  $q^2 = -0.375$ ).

our approximation is in very good agreement with numerics. In figure 4.1, we plot the gap as a function of  $q^2$  and show that it diverges as  $q^2 \rightarrow q_c^2$  (i.e.,  $T_c \rightarrow 0$ ).

# Chapter 4

## Transport

Since we are interested in superconductivity, we need to study the transport properties of the system to get a more complete picture of what we are working with. To this end we shall look at the linear response of the system to an electromagnetic perturbation

$$\delta A_x \sim \delta g_{tx} \sim e^{i\omega t} \quad (4.1)$$

The field equations are

$$\begin{aligned} \left( A'_x g e^{\frac{-x}{2}} \right)' + \left( \frac{\omega^2 e^{\frac{x}{2}}}{g} - 2q^2 \frac{\Psi^2}{z^2} e^{\frac{-x}{2}} \right) A_x &= -\Phi' e^{\frac{x}{2}} (z^2 g'_{tx} + 2z g_{tx}) , \\ 2g_{tx} + z(\Phi' A_x + g'_{tx}) &= 0 , \end{aligned} \quad (4.2)$$

From this we can calculate the optical conductivity, given by the retarded 2 point Green's function

$$\sigma(\omega) = \frac{-iG_{J_x J_x}^R}{\omega} \quad (4.3)$$

In general we can calculate other Green's functions related to thermal conductivity and second sound, we will not consider them here. From the near boundary behavior of  $A_x$  we have

$$A_x \approx A_x^{(0)} + z A_x^{(1)} + \dots , \quad (4.4)$$

Where  $A_x$  is the solution of (4.2) with ingoing boundary conditions at the horizon. As discussed before, these leading terms tell us about the physics in the CFT. In this case

$$A_x^{(0)} = A_x \quad A_x^{(1)} = \langle J_x \rangle \quad (4.5)$$

$$\sigma = \frac{\langle J_x \rangle}{E_x} = -\frac{A_x^{(1)}}{i\omega A_x^{(0)}} . \quad (4.6)$$

Where we have used the fact that  $A_x$  has a simple time dependence. It is useful to rewrite eqn (4.2) in Schrödinger form

$$-\frac{d^2 A_x}{dz_*^2} + V A_x = \omega^2 A_x , \quad (4.7)$$

where  $z_*$  is a “tortoise” coordinate defined by

$$z_* = \int_0^z \frac{dz'}{g(z')} e^{\chi(z')/2} , \quad (4.8)$$

with  $z_* = 0$  at  $z = 0$ , and the potential is given by

$$V = g \left( 2q^2 \frac{\Psi^2}{z^2} e^{-\chi} + z^2 \Phi'^2 \right) . \quad (4.9)$$

With this change of coordinate performed, it is useful to think about this problem in terms of incident waves. The conductivity can be rewritten in terms of reflection coefficients (see (25))

$$\sigma = \frac{1 - \mathcal{R}}{1 + \mathcal{R}} \quad (4.10)$$

where  $\mathcal{R}$  is the reflection of incident wave with energy  $\omega$  off of the potential  $V$ . If  $\omega < \sqrt{V_{max}}$  our system is able to form ”cooper pairs” and the system superconducts, if the incident wave is of sufficiently high energy then our system doesn’t see the potential, and no superconductivity is present.

## 4.1 Probe Limit

In the probe limit the potential is very simple

$$V = 2f\Psi^2 \quad (4.11)$$

And since the form of  $f(z)$  is simple, we can find  $r_*$  explicitly

$$r_* = \int \frac{dr}{f(r)} = \frac{1}{6r_+} \left[ \ln \frac{(1-z)^3}{1-z^3} - 2\sqrt{3} \tan^{-1} \frac{\sqrt{3}z}{2+z} \right] \quad (4.12)$$

where the integration constant is fixed so that at the boundary  $r_* = 0$

To find solutions we shall replace  $V$  with its mean value  $\langle V \rangle$  in a self consistent manner. This allows us to solve the problem for the whole frequency spectrum. Applying the proper boundary conditions, the solution is

$$A = e^{-i\sqrt{\omega^2 - \langle V \rangle} r_*} \quad (4.13)$$

From which we can readily attain the conductivity

$$\sigma = \sqrt{1 - \frac{\langle V \rangle}{\omega^2}} \quad (4.14)$$

The mean value of the potential is found from

$$\langle V \rangle = \frac{\int_{-\infty}^0 dr_* V |A(r_*)|^2}{\int_{-\infty}^0 dr_* |A(r_*)|^2} \quad (4.15)$$

For  $\Delta < 3/2$ , in the low temperature limit the potential simplifies to

$$V \approx \frac{\langle \mathcal{O}_\Delta \rangle^2}{r_+^{2(\Delta-1)}} z^{2(\Delta-1)} (1-z^3) \quad (4.16)$$

where we used  $F(z) \approx 1$ . Moreover, since  $r_+ \rightarrow 0$ , the main contribution to the integrals in (4.15) is from the vicinity of the boundary where  $r_* \approx -z/r_+$ . We deduce

the leading contribution

$$\langle V \rangle \approx \frac{\langle \mathcal{O}_\Delta \rangle^2}{r_+^{2(\Delta-1)}} \frac{\int_0^\infty dz z^{2(\Delta-1)} |A(-z/r_+)|^2}{\int_0^\infty |A(-z/r_+)|^2} = \Gamma(2\Delta - 1) \langle \mathcal{O}_\Delta \rangle^2 \left[ -2i\sqrt{\omega^2 - \langle V \rangle} \right]^{2(1-\Delta)} \quad (4.17)$$

which determines  $\langle V \rangle$  implicitly as a function of  $\omega$ . We obtain the low-temperature high-frequency ( $\omega \gtrsim \langle \mathcal{O}_\Delta \rangle^{1/\Delta}$ ) conductivity

$$\sigma(\omega) = \sqrt{1 - \frac{\Gamma(2\Delta - 1) \langle \mathcal{O}_\Delta \rangle^2 (-2i)^{2(1-\Delta)}}{\omega^{2\Delta}}} \quad (4.18)$$

whereas for low frequencies, we have

$$\sigma(\omega) = \sqrt{1 - \frac{[2^{2(1-\Delta)} \Gamma(2\Delta - 1) \langle \mathcal{O}_\Delta \rangle^2]^{1/\Delta}}{\omega^2}} \quad (4.19)$$

In particular for  $\Delta = 1$  eq. (4.17) can be solved for all frequencies and the expression (4.18) for the conductivity, which coincides with (4.19), is valid in the entire spectrum,

$$\sigma(\omega) = \sqrt{1 - \frac{\langle \mathcal{O}_1 \rangle^2}{\omega^2}} \quad (4.20)$$

This expression is in excellent agreement with numerical results even down to low frequencies ( $\omega \ll \langle \mathcal{O}_1 \rangle$ ).

For  $\Delta > 3/2$ , the potential can be approximated by

$$V \approx (3 - \Delta)^2 b^2 r_+^2 (1 - z^3) (bz)^{2(2-\Delta)} \tanh^2 \left( \frac{bz}{\alpha} \right)^{2\Delta-3} \quad (4.21)$$

where  $b$  is given in (3.16). This expression can be used, as before, to find an estimate for  $\langle V \rangle$ . In particular, for  $\Delta = 2$ , we obtain

$$\hat{V} = 1 + 2\alpha\sqrt{\hat{V} - \hat{\omega}^2} + 2\alpha^2(\hat{V} - \hat{\omega}^2) \left[ \psi \left( \frac{\alpha}{2} \sqrt{\hat{V} - \hat{\omega}^2} \right) - \psi \left( \frac{1}{2} + \frac{\alpha}{2} \sqrt{\hat{V} - \hat{\omega}^2} \right) \right] \quad (4.22)$$

where

$$\hat{V} = \frac{\langle V \rangle}{\langle \mathcal{O}_2 \rangle \alpha} \quad , \quad \hat{\omega}^2 = \frac{\omega^2}{\langle \mathcal{O}_2 \rangle \alpha} \quad (4.23)$$

At high frequencies, this implies

$$\sigma(\omega) \approx \sqrt{1 + \frac{\langle \mathcal{O}_2 \rangle^2}{2\omega^4}} \quad (4.24)$$

showing that  $\sigma > 1$  for  $\omega \gtrsim \sqrt{\langle \mathcal{O}_2 \rangle}$ , whereas as  $\omega \rightarrow 0$ ,  $\hat{V} \approx 0.65$ , and the low-frequency conductivity is

$$\sigma(\omega) \approx 0.7i \frac{\sqrt{\langle \mathcal{O}_2 \rangle}}{\omega} \quad (4.25)$$

We shall improve on this estimate later by using a more accurate analytic technique which is better suited for low frequencies. We shall also obtain an exponentially small real part of the conductivity which survives in the limit  $\omega \rightarrow 0$ .

At intermediate frequencies, we may expand around  $\hat{V} = \hat{\omega}^2 = 1$ . We obtain

$$\sigma(\omega) \approx \sqrt{1 - \frac{\alpha \langle \mathcal{O}_2 \rangle}{\omega^2}} \quad (4.26)$$

for  $\omega/\sqrt{\langle \mathcal{O}_2 \rangle} \approx \sqrt{\alpha} \approx 0.9$ . We may also use perturbation theory to go beyond the leading order. Treating  $\delta V = V - \langle \mathcal{O}_2 \rangle \alpha$  as a perturbation, we obtain the wavefunction

$$A = e^{-i\sqrt{\omega^2 - \langle \mathcal{O}_2 \rangle \alpha} r_*} \left[ 1 + \frac{\alpha^2}{2\beta} - \frac{\alpha^2 \pi}{\sin \beta \pi} e^{2i\sqrt{\omega^2 - \langle \mathcal{O}_2 \rangle \alpha} r_*} + \frac{\alpha^2}{2\beta} F\left(\beta, 1; 1 + \beta; -e^{-2\sqrt{\langle \mathcal{O}_2 \rangle / \alpha} r_*}\right) - \frac{\alpha^2}{2(1 + \beta)} e^{-2\sqrt{\langle \mathcal{O}_2 \rangle / \alpha} r_*} F\left(1 + \beta, 1, 2 + \beta; -e^{-2\sqrt{\langle \mathcal{O}_2 \rangle / \alpha} r_*}\right) \right] \quad (4.27)$$

where

$$\beta = i\alpha \sqrt{\frac{\omega^2}{\langle \mathcal{O}_2 \rangle \alpha} - 1} \quad (4.28)$$

We deduce the conductivity

$$\sigma(\omega) \approx \sqrt{1 - \frac{\langle \mathcal{O}_2 \rangle \alpha}{\omega^2}} - \frac{i\sqrt{\langle \mathcal{O}_2 \rangle \alpha^3}}{\omega} \quad (4.29)$$

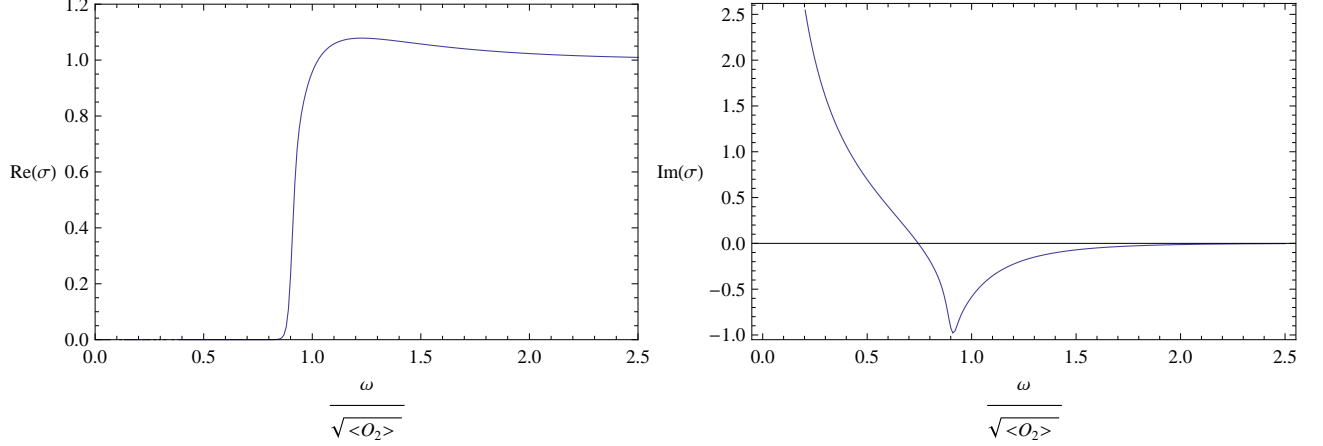


**Figure 4.1:** The real and imaginary parts of the conductivity at low temperatures for  $\Delta = 2$ .

improving on the leading order expression (4.26). The conductivity resulting from our analytic procedure (both real and imaginary parts) is plotted in fig. 4.1 for the entire spectrum.

At low frequencies, the above expressions do not properly account for the boundary condition at the horizon. To this end, define

$$A = (1 - z)^{-i\omega/(3r_+)} \mathcal{G}(z) \quad (4.30)$$

where  $\mathcal{G}$  is regular at the horizon ( $z = 1$ ). The wave equation (4.7) reads

$$-3(1-z^3)\mathcal{G}'' + (9z^2 - 2(1+z+z^2))\frac{i\omega}{r_+}\mathcal{G}' + \left[ \frac{6\Psi^2}{z^2} - (1+2z)\frac{i\omega}{r_+} - \frac{(2+z)(4+z+z^2)}{3(1+z+z^2)}\frac{\omega^2}{r_+^2} \right] \mathcal{G} = 0 \quad (4.31)$$

At the horizon we may expand  $\mathcal{G}$  in a Taylor series. We deduce the boundary condition

$$\mathcal{G}'(1) + \left[ \frac{2\Psi^2(1)}{3 - 2i\omega/r_+} - \frac{i\omega}{3r_+} \right] \mathcal{G}(1) = 0 \quad (4.32)$$

At low temperature, for  $\Delta = 1$ , we have  $\Psi \approx \frac{\langle \mathcal{O}_1 \rangle}{\sqrt{2}r_+} z$ . We may rescale  $z \rightarrow z/b$ , where  $b = \langle \mathcal{O}_1 \rangle / r_+$  and then let  $b \rightarrow \infty$ . We obtain the approximate solution

$$A = \left( c_+ e^{+\langle \mathcal{O}_1 \rangle^2 z/r_+} + c_- e^{-\langle \mathcal{O}_1 \rangle^2 z/r_+} \right) e^{-\frac{i\omega z}{3r_+}} \quad (4.33)$$

which is valid for low frequencies ( $\omega \ll \langle \mathcal{O}_1 \rangle$ ). We deduce the conductivity

$$\sigma(\omega) \approx i \frac{1 - \frac{c_+}{c_-}}{1 + \frac{c_+}{c_-}} \frac{\langle \mathcal{O}_1 \rangle}{\omega} \quad (4.34)$$

The ratio  $c_+/c_-$  is found by applying the boundary condition (4.32). We obtain

$$\frac{c_+}{c_-} = \frac{a-3}{a+3} e^{-2a} + \frac{2(2a^2-3)}{a(a+3)^2} e^{-2a} \frac{i\omega}{r_+} + \mathcal{O}(\omega^2) \quad , \quad a = \frac{\langle \mathcal{O}_1 \rangle}{r_+} \quad (4.35)$$

We deduce the low frequency expansion

$$\sigma(\omega) = \frac{i\langle \mathcal{O}_1 \rangle}{\omega} \left[ 1 - 2 \frac{a-3}{a+3} e^{-2a} - \frac{2(2a^2-3)}{a(a+3)^2} e^{-2a} \frac{i\omega}{r_+} + \mathcal{O}(\omega^2) \right] \quad (4.36)$$

in agreement with the leading order result (4.20). The DC conductivity is

$$\Re \sigma(0) \sim e^{-2a} = e^{-\Delta_g/T} \quad , \quad \Delta_g = \frac{3\langle \mathcal{O}_1 \rangle}{2\pi} \approx 0.48 \langle \mathcal{O}_1 \rangle \quad (4.37)$$

For  $\Delta = 2$ , at low temperatures eq. (4.31) reads

$$-3\mathcal{G}'' - \frac{2i\omega}{r_+} \mathcal{G}' + \left[ 3b^2 \tanh^2 \frac{bz}{\alpha} - \frac{8\omega^2}{r_+^2} \right] \mathcal{G} = 0 \quad (4.38)$$

whose general solution is given in terms of Legendre functions,

$$\mathcal{G}(z) \approx \left( \frac{1 - \tanh \frac{bz}{\alpha}}{1 + \tanh \frac{bz}{\alpha}} \right)^{\frac{i\omega\alpha}{6br_+}} \left[ c_+ P_{\frac{1}{2}(-1+\sqrt{1+4\alpha^2})}^{+\alpha} \left( \tanh \frac{bz}{\alpha} \right) + c_- P_{\frac{1}{2}(-1+\sqrt{1+4\alpha^2})}^{-\alpha} \left( \tanh \frac{bz}{\alpha} \right) \right] \quad (4.39)$$



We deduce the conductivity

$$\sigma(\omega) \approx i \frac{\sqrt{\langle \mathcal{O}_2 \rangle}}{\omega} \frac{0.47 - 0.66 \frac{c_+}{c_-}}{0.85 - 0.30 \frac{c_+}{c_-}} \quad (4.40)$$

The ratio  $c_+/c_-$  is found from the boundary condition at the horizon (4.32). At  $z \approx 1$  we have  $\tanh \frac{bz}{\alpha} \approx 1$ , so we may approximate

$$P_{\frac{1}{2}(-1+\sqrt{1+4\alpha^2})}^{\pm\alpha} \left( \tanh \frac{bz}{\alpha} \right) = \frac{2^{\pm\alpha/2}}{\Gamma(1 \mp \alpha)} \left( 1 - \tanh \frac{bz}{\alpha} \right)^{\mp\alpha/2} + \dots \quad (4.41)$$

We obtain

$$\begin{aligned} \mathcal{G}(1) &\approx \left[ \frac{c_+}{\Gamma(1-\alpha)} e^{+b} + \frac{c_-}{\Gamma(1+\alpha)} e^{-b} \right] e^{-\frac{i\omega}{3r_+}} \\ \mathcal{G}'(1) &\approx \left[ \frac{c_+ \left( b - \frac{i\omega}{3r_+} \right)}{\Gamma(1-\alpha)} e^{+b} - \frac{c_- \left( b + \frac{i\omega}{3r_+} \right)}{\Gamma(1+\alpha)} e^{-b} \right] e^{-\frac{i\omega}{3r_+}} \end{aligned} \quad (4.42)$$

Applying the boundary condition (4.32), we obtain

$$\frac{c_+}{c_-} = -e^{-2b} \frac{\Gamma(1-\alpha)}{\Gamma(1+\alpha)} \left[ 1 + \frac{4i\omega}{br_+} + \dots \right] \quad (4.43)$$

showing that at low frequencies,

$$\Im \sigma(\omega) \approx 0.55i \frac{\sqrt{\langle \mathcal{O}_2 \rangle}}{\omega}, \quad \Re \sigma(\omega) \sim e^{-2b} = e^{-\Delta_g/T}, \quad \Delta_g \approx \frac{3\sqrt{\alpha \langle \mathcal{O}_2 \rangle}}{2\pi} \approx 0.43 \sqrt{\langle \mathcal{O}_2 \rangle} \quad (4.44)$$

to be compared with our earlier estimate (4.25) of the imaginary part which was obtained via a different, less accurate, analytic method. The real part is exponentially small and was not detected earlier.

The above method can also be applied to other values of the dimension  $\Delta$  if one replaces the potential by its self-consistent average  $\langle V \rangle$ . Then by solving the wave equation using perturbation theory, we obtain the real part of the conductivity in

the limit  $\omega \rightarrow 0$  and therefore the gap  $\Delta_g$  ( $\Re\sigma(0) \sim e^{-\Delta_g/T}$ ) for all values of the dimension  $\Delta$ .

### 4.1.1 BF Bound

Next, we calculate the low temperature conductivity at the BF bound. For explicit analytic results, we concentrate on two cases,  $d = 3$  and  $d = 4$ . We shall obtain the conductivity  $\sigma$  as a function of the rescaled frequency

$$\hat{\omega} = \frac{\omega}{b} = \frac{\omega}{\langle q\mathcal{O}_\Delta \rangle^{1/\Delta}} \quad (4.45)$$

The function  $\sigma(\hat{\omega})$  has a well-defined limit as  $q \rightarrow \infty$  (probe limit) down to low temperatures (in the regime  $(1 \lesssim b \lesssim q^{1/\Delta})$ ) at which the condensate  $\langle \mathcal{O}_\Delta \rangle$  is large. The conductivity of physical systems can be obtained as a  $1/q^2$  expansion with the conductivity in the probe limit serving as the zeroth order term in the expansion.

### Three dimensions

Using (4.7) with  $d = 3$ , the wave equation reads

$$\frac{d}{dz} \left[ (1 - z^3) \frac{dA}{dz} \right] - \left[ b^{2\Delta} z^{2\Delta-2} F^2(z) - \frac{\omega^2}{1 - z^3} \right] A = 0 \quad (4.46)$$

To account for the boundary condition at the horizon, set

$$A = (1 - z)^{-i\omega/3} e^{-i\omega z/3} \mathcal{A}(z) \quad (4.47)$$

where we included a factor  $e^{-i\omega z/3}$  for convenience, so that only  $\mathcal{A}(z)$  will contribute to the conductivity. The wave equation becomes

$$\begin{aligned} & -3(1 - z^3)\mathcal{A}'' + z[9z - 2(1 + z + z^2)i\omega]\mathcal{A}' \\ & + [3b^{2\Delta}z^{2\Delta-2}F^2(z) \\ & - (1 + 2z + 3z^2)i\omega - \frac{(3 + 2z + z^2)(3 + z + z^2 + z^3)}{3(1 + z + z^2)}\omega^2]\mathcal{A} = 0 \end{aligned} \quad (4.48)$$

Regularity of the wavefunction  $\mathcal{A}$  at the horizon ( $z = 1$ ) implies the boundary condition

$$(3 - 2i\omega)\mathcal{A}'(1) + \left(b^{2\Delta}F^2(1) - 2i\omega - \frac{4\omega^2}{3}\right)\mathcal{A}(1) = 0 \quad (4.49)$$

At low temperatures,  $b \gg 1$ , it is convenient to rescale  $z \rightarrow z/b$ . The wave equation can be solved as a series expansion in  $1/q^2$ . For  $\Delta \leq \frac{3}{2}$ ,  $F_0(z)$  has a smooth limit (albeit unphysical) as  $b \rightarrow \infty$ . After rescaling and letting  $b \rightarrow \infty$ , we obtain the wave equation

$$-\mathcal{A}'' + [z^{2\Delta-2} - \hat{\omega}^2]\mathcal{A} = 0 \quad (4.50)$$

where we used  $F(z/b) \rightarrow F(0) = 1$ , as  $b \rightarrow \infty$ . For  $1 < \Delta \leq \frac{3}{2}$ , there are two linearly independent solutions,  $\mathcal{A}_\pm$ , distinguished by their asymptotic behavior,

$$\mathcal{A}_\pm \sim e^{\pm \frac{1}{\Delta} z^\Delta}, \quad z \rightarrow \infty \quad (4.51)$$

The general solution can be written as a linear combination,

$$\mathcal{A} = c^+ \mathcal{A}_+ + c^- \mathcal{A}_- \quad (4.52)$$

Applying the boundary condition (4.49), we deduce

$$\frac{c^+}{c^-} \sim e^{-\frac{2}{\Delta} b^\Delta} \quad (4.53)$$

so at very low temperatures,

$$c^+ = 0 \tag{4.54}$$

i.e.,  $\mathcal{A} \rightarrow 0$  as  $z \rightarrow \infty$ .

For  $\Delta = \frac{3}{2}$ , we obtain the exact explicit limit solution

$$\mathcal{A}(z) = \mathcal{A}_-(z) = \text{Ai}(bz - \hat{\omega}^2) \tag{4.55}$$

whereas  $\mathcal{A}_+(z) = \text{Bi}(bz - \hat{\omega}^2)$ , with arbitrary normalization, where we restored the scaling parameter  $b$ .

In this (unphysical) limit, the quasinormal frequencies have moved to the real axis yielding an infinite set of normal frequencies which are solutions of

$$\text{Ai}(-\hat{\omega}^2) = 0 \tag{4.56}$$

Thus we obtain an infinite tower of real frequencies given by the zeroes of the Airy function.

We deduce the limit conductivity (as  $q, b \rightarrow \infty$ )

$$\sigma(\hat{\omega}) = \frac{i}{\hat{\omega}} \frac{\text{Ai}'(-\hat{\omega}^2)}{\text{Ai}(-\hat{\omega}^2)} \tag{4.57}$$

The real frequencies that solve (4.56) are the poles of the conductivity. Notice that  $\Re\sigma = 0$ , except at the poles of  $\Im\sigma$  where  $\Re\sigma$  diverges as a  $\delta$ -function.

This expression is unphysical, as we have already explained (the probe limit breaks down in the limit  $b \rightarrow \infty$ ), but it is useful for computational purposes. We shall use it as a starting point to calculate the conductivity of a physical system at low temperatures.

At low temperatures, we can calculate the first-order correction analytically by considering the  $b \rightarrow \infty$  wave equation (4.50) as the zeroth-order equation. Then for the first-order correction  $\delta\mathcal{A}$  to the potential at low temperatures, we obtain from

(4.48),

$$-\delta\mathcal{A}'' + [z - \hat{\omega}^2]\delta\mathcal{A} = -\frac{1}{3(1 - z^3)}\mathcal{H}_1\mathcal{A} \quad (4.58)$$

where

$$\begin{aligned} \mathcal{H}_1 &= z [9z - 2(1 + z + z^2)i\omega] \frac{d}{dz} \\ &+ 3b^3 z (2F_1(z) + z^3) - (1 + 2z + 3z^2)i\omega \\ &+ \frac{z^2(1 - 15z - 12z^2 - 10z^3)}{3(1 + z + z^2)}\omega^2 \end{aligned} \quad (4.59)$$

The first-order potential leads to quasinormal modes which are zeroes of  $\mathcal{A} + \delta\mathcal{A}$ . Thus the real frequencies (4.56) of the (unphysical)  $b \rightarrow \infty$  limit get shifted at low temperatures away from the real axis. We obtain  $\hat{\omega} \rightarrow \hat{\omega} + \delta\hat{\omega}$ , where

$$\delta\hat{\omega} = \frac{\pi \text{Bi}(-\hat{\omega}^2)}{3\hat{\omega} \text{Ai}'(-\hat{\omega}^2)} \int_0^1 \frac{dz}{1 - z^3} \text{Ai}(bz - \hat{\omega}^2) \mathcal{H}_1 \text{Ai}(bz - \hat{\omega}^2) \quad (4.60)$$

This first-order expression is valid for low frequencies. As we heat up the system, most modes disappear and we are left with a finite number of quasinormal modes. Their number decreases as we increase the temperature. Conversely, as we cool down the system, (4.60) becomes increasingly accurate for an increasing number of modes. These modes shift toward the real axis ( $\delta\hat{\omega} \rightarrow 0$ ) as we lower the temperature. In the low temperature regime ( $1 \lesssim b \lesssim q^{1/\Delta}$ ), the large  $q$  is, the more spikes one obtains for  $\sigma(\omega)$ .

This shifting of quasinormal modes can be seen in plots of the conductivity. As the mode frequency approaches the real axis, the corresponding spike in the plot of the imaginary part of the conductivity becomes more pronounced. To demonstrate this, we calculated the conductivity using the first-order approximation (3.44) to the scalar field. In figure 4.2, we show the imaginary part of the conductivity at temperature  $T/T_c \approx .1$  and compare with the exact numerical solution. The agreement is very good even at such high temperature at which only one quasinormal mode is left. Unfortunately, this is the low temperature limit attained by numerical analysis as

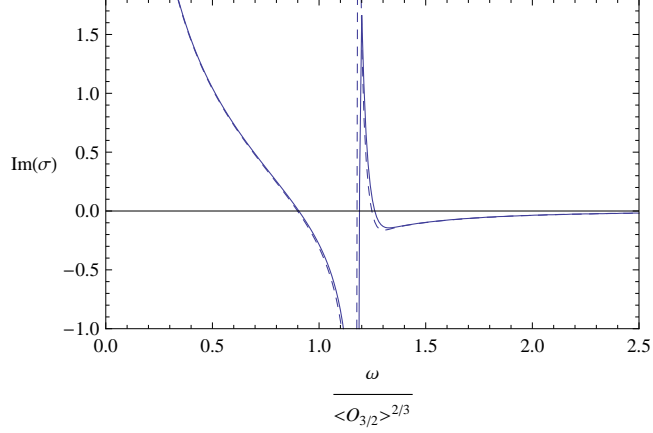


**Figure 4.2:** The imaginary part of the conductivity in  $d = 3$  using the expression (3.44) for the scalar field (dotted line) compared with the exact numerical solution (solid line) at  $\frac{T}{T_c} \approx .1$

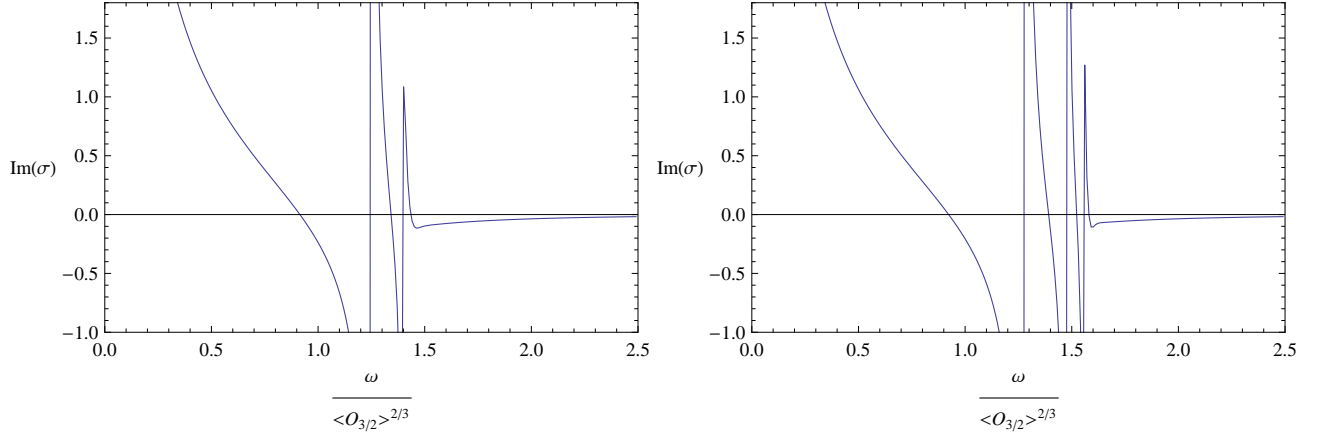


**Figure 4.3:** The imaginary part of the conductivity *vs.* frequency in  $d = 3$  using the expression (3.44) for  $F$  at  $\frac{T}{T_c} \approx .05$  (left),  $.04$  (right). As the temperature decreases, poles move toward the real axis.

numerical instabilities prohibit one from lowering the temperature further. Using our analytic results, we see in figure 4.3 the emergence of an increasing number of poles as we lower the temperature to  $T/T_c \approx .06$  and  $.04$ . Finally in figure 4.4 we compare the lower temperature ( $T/T_c \approx .01$ ) result with the  $b \rightarrow \infty$  limit analytic expression (4.57), thus demonstrating convergence.

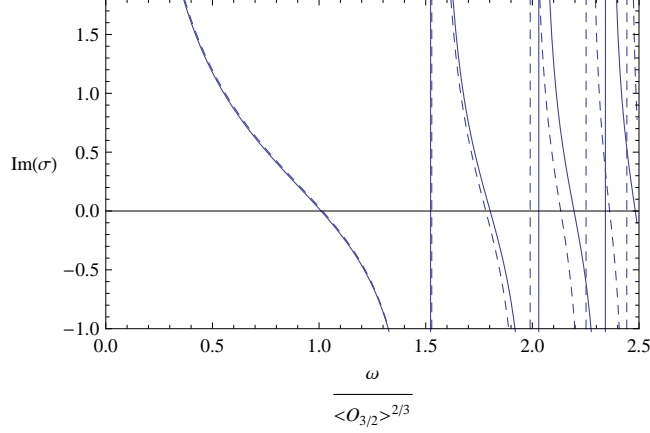


**Figure 4.4:** Comparison of the imaginary part of the conductivity in  $d = 3$  using the expression (3.44) for  $F$  at  $\frac{T}{T_c} \approx .01$  (dotted line) and the  $b \rightarrow \infty$  limit (4.57) (solid line).

For  $\Delta > 3/2$ , the potential is

$$V = b^{2\Delta} z^{2\Delta-2} (1 - z^3) F(bz) \quad (4.61)$$

with  $F$  given approximately by (3.59). It attains a maximum of order  $b^{2(2-\Delta)}$  for  $\Delta < 2$ . Therefore, at zero temperature it has infinite height. However, the width becomes infinitely narrow leading to a finite tower of poles for the conductivity (quasinormal modes). In the zero temperature limit, the number of modes increases as one approaches the BF bound and decreases away from it. For  $\Delta \geq 2$ , the height of the potential becomes finite at zero temperature. It turns out that the potential is too narrow to possess bound states, so no poles exist for  $\Delta \geq 2$ .

#### Four dimensions

The  $d = 4$  case is similar. Working as in the  $d = 3$  case, in the (unphysical)  $b \rightarrow \infty$  limit, the wave equation for  $\Delta = 2$  (at the BF bound) in the probe limit reduces to

$$A'' - \frac{1}{z} A' - [b^4 z^2 - \omega^2] A = 0 \quad (4.62)$$

whose acceptable solution can be written in terms of a Whittaker function,

$$A = W_{\frac{\hat{\omega}^2}{4}, \frac{1}{2}}(b^2 z^2) \quad (4.63)$$

(The other solution diverges as  $z \rightarrow \infty$ .) At the boundary ( $z \rightarrow 0$ ), it has a logarithmic divergence which we need to subtract before we can calculate QNMs and the conductivity (30). The conductivity is then given by

$$\sigma(\hat{\omega}) = \frac{2}{i\hat{\omega}} \frac{A_2}{A_0} + \frac{i\hat{\omega}}{2} \quad (4.64)$$

where

$$A(z) = A_0 + A_2 b^2 z^2 - A_0 \frac{\hat{\omega}^2}{2} b^2 z^2 \ln(b^2 z^2) + \dots \quad (4.65)$$

with an arbitrarily chosen cutoff.

Using the expansion for small arguments,

$$W_{\frac{\hat{\omega}^2}{4}, \frac{1}{2}}(b^2 z^2) = -\frac{2}{\hat{\omega}^2 \Gamma(-\hat{\omega}^2/4)} \left\{ 1 - [1 + \hat{\omega}^2 (2\gamma - 1 + \ln(b^2 z^2) + \psi(1 - \hat{\omega}^2/4))] \frac{b^2 z^2}{2} \right\} + \dots \quad (4.66)$$

we deduce the limit conductivity as  $q, b \rightarrow \infty$ ,

$$\sigma(\hat{\omega}) = \frac{1}{i\hat{\omega}} + i\hat{\omega} \left[ 2\gamma - \frac{1}{2} + \psi(1 - \hat{\omega}^2/4) \right] \quad (4.67)$$

We have a pole at  $\omega = 0$ , as expected and an infinite tower of real poles determined by the poles of the digamma function. The poles have real frequencies

$$\hat{\omega} = \frac{\omega_n}{\langle \mathcal{O} \rangle^{1/2}} = 2\sqrt{n} \quad , \quad n = 0, 1, 2, \dots \quad (4.68)$$

These poles are unphysical, but are good approximations to the quasinormal modes at low temperatures, in the physical regime ( $1 \lesssim b \lesssim q^{1/\Delta}$ ). As we increase the temperature, these modes move away from the real axis. At any given temperature we have a finite number of such modes. As we lower the temperature, their



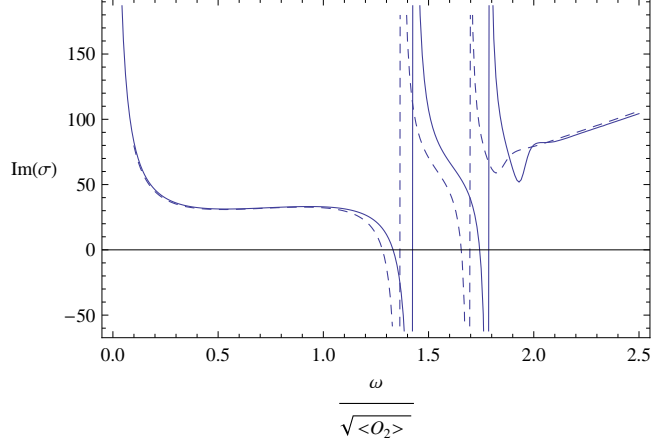


**Figure 4.5:** The imaginary part of the conductivity in  $d = 4$  using the expression (3.44) for the scalar field (dotted line) compared with the exact numerical solution (solid line) at  $\frac{T}{T_c} \approx .17$

number increases and the quasinormal modes approach the poles (4.68) on the real axis. To demonstrate this, we have calculated the conductivity using the first-order approximation (3.44) to the scalar field. In figure 4.5 we compare with numerical results at temperature  $T/T_c \approx .17$  and find good agreement. As we go to lower temperature, numerical instabilities arise and it is no longer possible to compare our analytic results with their numerical counterparts. We find convergence to the  $b \rightarrow \infty$  limit (4.67), but much slower than in  $d = 3$ . In figure 4.6 we show the imaginary part of the conductivity at  $T/T_c \approx 0.1$  and  $0.04$ . As we lower the temperature, the number of poles increases and the poles shift to the right on the real axis approaching the limit values (4.68) which correspond to the  $b \rightarrow \infty$  limit of the conductivity shown in figure 4.7.

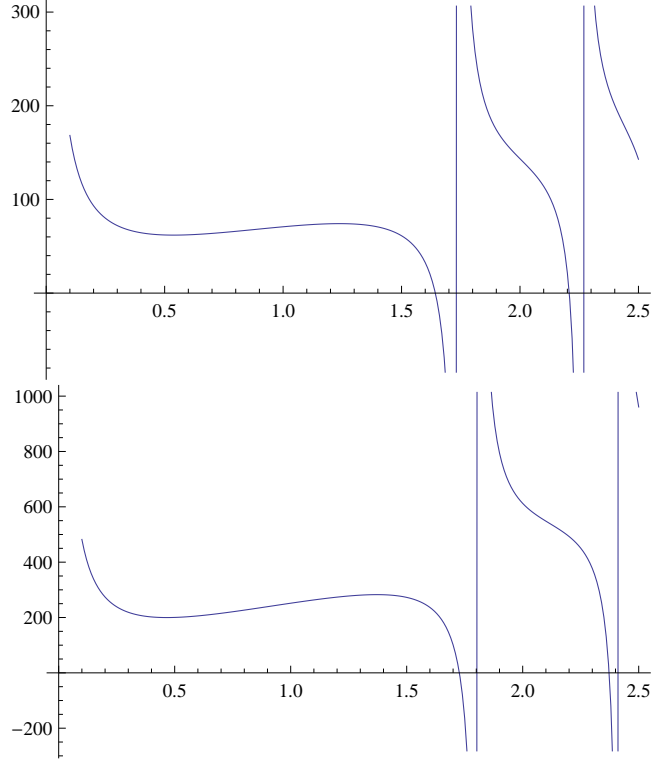


**Figure 4.6:** The imaginary part of the conductivity *vs.* frequency in  $d = 4$  using the expression (3.44) for  $F$  at  $\frac{T}{T_c} \approx .1$  (left),  $.04$  (right).

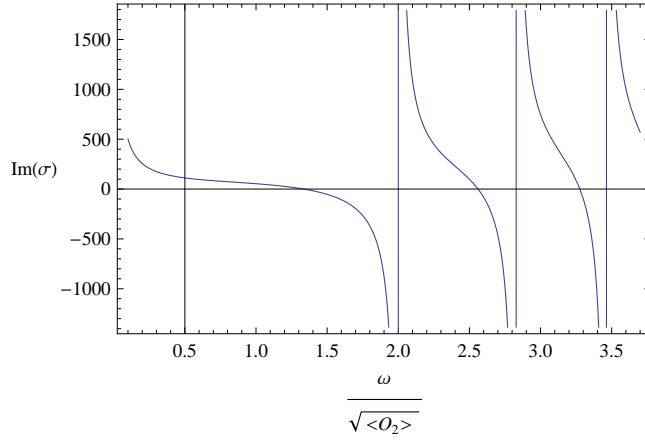


**Figure 4.7:** The imaginary part of the conductivity in the (unphysical) limit  $b \rightarrow \infty$  in  $d = 4$  (4.67).

## 4.2 as $q \rightarrow 0$

As  $q \rightarrow 0$  mean field calculations fail and we are left to find  $\mathcal{R}$  in a perturbative manner. To find  $\mathcal{R}$ , write the wave equation in integral form as

$$A_x(z_*) = e^{i\omega z_*} - \int_0^\infty dz'_* G(z_*, z'_*) V(z'_*) A_x(z'_*) , \quad (4.69)$$

where the Green function satisfies

$$-\partial_{z_*}^2 G(z_*, z'_*) - \omega^2 G(z_*, z'_*) = \delta(z_* - z'_*) . \quad (4.70)$$

Explicitly,

$$G(z_*, z'_*) = \frac{i}{2\omega} \left[ \theta(z'_* - z_*) e^{i\omega(z'_* - z_*)} + \theta(z_* - z'_*) e^{-i\omega(z'_* - z_*)} \right] . \quad (4.71)$$

The reflection coefficient is then

$$\mathcal{R} = - \int_0^\infty dz_* G(0, z_*) V(z_*) A_x(z_*) , \quad (4.72)$$

and can be calculated perturbatively,

$$\mathcal{R} = - \int_0^\infty dz_* G(0, z_*) V(z_*) e^{i\omega z_*} + \int_0^\infty dz_* G(0, z_*) V(z_*) \int_0^\infty dz'_* G(z_*, z'_*) V(z'_*) e^{i\omega z'_*} + \dots . \quad (4.73)$$

The numerical results are shown in figure 4.8. The analytic results at second order are compared with the numerical solution in figure 4.9. As expected, we have agreement at high  $\omega$ . As we go to higher perturbative orders, the agreement extends to a wider range of frequencies.

We can look at the potential to determine the behavior of the conductivity near the critical line (2.67). We shall concentrate on the case  $q^2 = 0$ , in which the system simplifies considerably. Our discussion can be extended to other values of the coupling

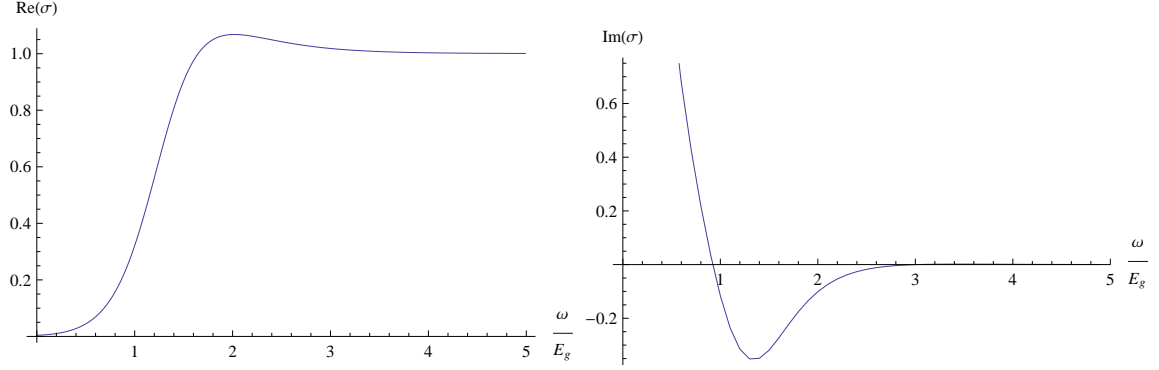


**Figure 4.8:** Real and imaginary parts of the conductivity.

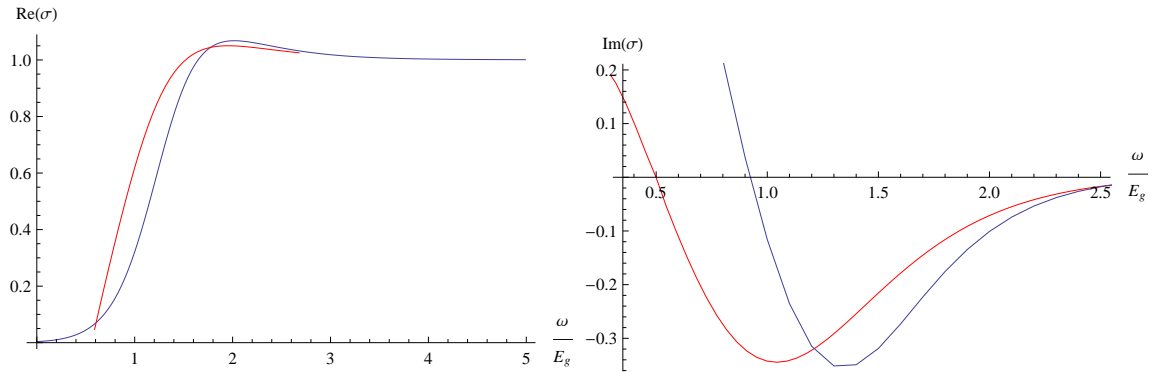


**Figure 4.9:** Comparison of analytic and numerical results on the real and imaginary parts of the conductivity (left and right panel, respectively).

constant in a straightforward, albeit tedious, manner, but no new physical insight is gained.

Regardless of the value of  $\Delta$ , the potential reaches a universal shape and never becomes large enough for spikes to form at or near the BF bound, as seen previously in the probe limit (30; 25; 28). The potential is plotted in figure 4.10 below the critical temperature. After scaling  $V$  by the charge density  $\varrho$  and  $z \rightarrow z\sqrt{\varrho}$ , the curves at various temperatures  $T \leq T_c$  are almost indistinguishable. Detail near the horizon (right panel of figure 4.10) shows the effect of lowering the temperature: the potential approaches zero faster at the horizon resulting in a longer tail. Consequently, the conductivity also approaches a universal shape (figure 4.8) below the critical temperature.

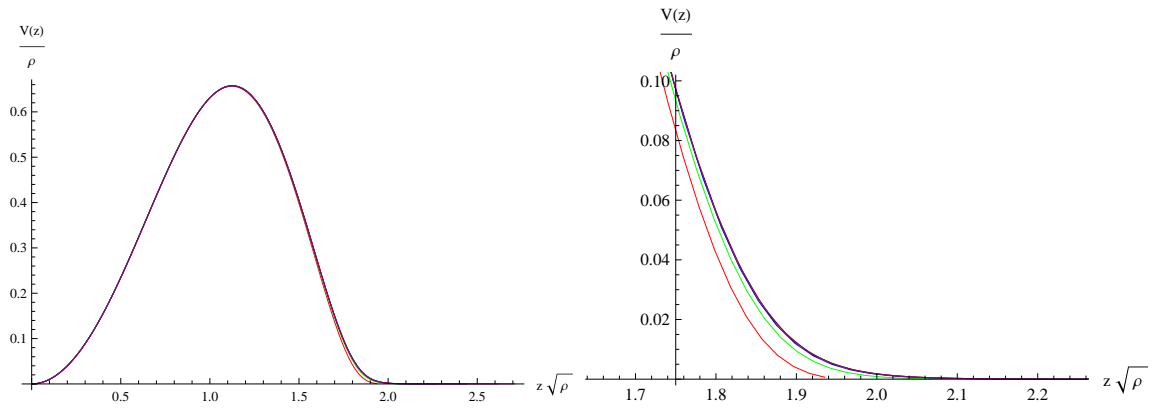


**Figure 4.10:** Left panel: the potential determining the conductivity for  $q = 0$  at various temperatures below  $T_c$ . Right panel shows detail near the horizon.

# Chapter 5

## Conclusion

In this work we have focused on producing analytical calculations of a holographic superconductor. The system was first suggested by Gubser in 2008(22) and a model was introduced soon after by (23). Since then there has been an amazing effort to explore the physics of these systems.

In my first paper we were able to show a few derive several properties of holographic superconductors analytically. Using appropriate trial functions, we were able to show that for all allowed values of  $\Delta$ , for  $d = 3$ , that a second order phase transition occurs regardless of whether we pick  $\Delta_-$  or  $\Delta_+$ . We were then able to find approximate solutions to the equations of motion in the limit that  $T \rightarrow 0$ . We then utilized these solutions to show the low temperature behavior did depend on the choice of  $\Delta$ . For  $\Delta_+$  the probe limit is well behaved, while for  $\Delta_-$  the energy gap diverges. We were then able to use our solutions to the field equations to study the transport properties. Using mean field, methods we were able to calculate the conductivity. The results obtained were in good agreement with numerics. We were then able to show that the energy gap,  $\omega_g$ , is what you would expect if our gap was caused by charged quasiparticles and was in very good agreement with (23).

We then decided to see if there was anything special about  $\Delta = \Delta_{BF}$  as  $T \rightarrow 0$  and what, if any, effect would looking at higher dimensions have. What we found

was that as  $T \rightarrow 0$   $\Delta_{BF}$  did in fact diverge, contrary to what was thought in earlier papers based on numerics. Furthermore we found that it diverged differently than  $\Delta_-$ . We were also able to see that qualitatively the theories were the same for  $d = 3$  and  $d = 4$ .

Continuing to work in the probe limit, we added anisotropy into the system. Using analytical methods, we were able to fully model the behaviour of the phase transition in these systems. Immediately one sees that the critical temperature depends on the amount of anisotropy in the system and the modulation that is introduced. We were able to show that there is a critical value of the modulation  $Q^*$ , at which  $T_c$  discontinuously goes to zero. After demonstrating that the higher order modes do not contribute significantly to the solution, we found analytical solutions that agree very well with numerics.

Moving away from the probe limit, we investigated the near extremal limit of Reissner-Nordstrom AdS black holes. In this limit the system becomes a lot more simple and we are able to offer a fully analytical treatment. We were able to show analytically that for  $m^2 = -2$  and  $q^2 = 0$  that there was a small but finite value of  $T_c$  for  $\Delta_{\pm}$ . We were able to generalize this to fully explore  $q^2$  using an approximation. We were then able to fully explore  $(q^2, m^2)$  by employing trial functions and we were able to see some interesting behavior. Most notably that for  $\Delta_-$   $q_c^2$  is no longer given by the near horizon  $AdS \times \mathbb{R}^2$  geometry like it is for  $\Delta_+$ . Instead we found that a transition occurs all the way down to the unitarity bound for  $q^2 = 0$ .

Below  $T_c$ , we were able to find perturbative solutions to the field equations. We used them to show the energy gap diverges as  $q^2 \rightarrow 0$  and conductivity, as a function of frequency, has a universal shape, when properly normalized. In the extremal limit, we found that the transport properties had no strong dependence on charge, as opposed to the probe limit where  $\omega_g \sim \langle q\mathcal{O} \rangle^{1/\Delta}$ .

## Further Work

Using the AdS/CFT Correspondence to explore superconductivity, and condensed matter in general, is still in it's infancy. There are many things that the research presented here left unanswered. While we have been able to explore the BF bound, the unitarity bound and the limit  $m \rightarrow 0$  have been largely unstudied. As demonstrated in Chapter 2, the unitarity bound doesn't behave as one would expect based on simple geometric arguments as  $q \rightarrow 0$ . The limit  $m \rightarrow 0$  was talked about in Chapter 3. In this limit our approximation breaks down. Further work has not been done on this, but it has been suggested that this may be due to the onset of a quantum phase transition.

In general there is much to be done. The biggest challenge is to find the CFT that the bulk theory is dual to. Our theory acts like superconductivity, but we have still don't know if that is what it is. The AdS/CFT is based upon the large  $N$  limit of a gauge theory. In the case of  $AdS_5$  and the study of QGPs it is obvious what  $N$  corresponds to, the color charge. However with electrodynamics and condensed matter the story isn't so clear cut. Currently work is being done on studying holographic (non) Fermi surfaces (for recent papers and review see (61; 62)). This, and work like it, will help us fully understand both sides of the AdS/CFT correspondence, so that eventually we will be able to make a direct link between a gravitational system and a condensed matter system.



# Bibliography

# Bibliography

- [1] P. Kraus, “Lectures on black holes and the AdS(3)/CFT(2) correspondence,”  
Lect. Notes Phys. **755**, 193 (2008) [arXiv:hep-th/0609074]. [2](#)
- [2] S. S. Gubser, I. R. Klebanov and A. M. Polyakov, Phys. Lett. B **428**, 105 (1998)  
[arXiv:hep-th/9802109]. [2](#)
- [3] E. Witten, “Anti-de Sitter space and holography,” Adv. Theor. Math. Phys. **2**,  
253 (1998) [arXiv:hep-th/9802150]. [2](#), [3](#)
- [4] G. 't Hooft, arXiv:gr-qc/9310026. [3](#)
- [5] L. Susskind, “The World As A Hologram,” J. Math. Phys. **36**, 6377 (1995)  
[arXiv:hep-th/9409089]. [3](#)
- [6] T. Banks, W. Fischler, S. H. Shenker and L. Susskind, “M theory as a matrix  
model: A conjecture,” Phys. Rev. D **55**, 5112 (1997) [arXiv:hep-th/9610043]. [3](#)
- [7] J. M. Maldacena, “The large N limit of superconformal field theories and  
supergravity,” Adv. Theor. Math. Phys. **2**, 231 (1998) [Int. J. Theor. Phys. **38**,  
1113 (1999)] [arXiv:hep-th/9711200]. [3](#)
- [8] G. Policastro, D. T. Son and A. O. Starinets, “The shear viscosity of strongly  
coupled N = 4 supersymmetric Yang-Mills plasma,” Phys. Rev. Lett. **87**, 081601  
(2001) [arXiv:hep-th/0104066]. [4](#)

- [9] T. Sakai and S. Sugimoto, “Low energy hadron physics in holographic QCD,” *Prog. Theor. Phys.* **113**, 843 (2005) [arXiv:hep-th/0412141]. [4](#)
- [10] T. Sakai and S. Sugimoto, “More on a holographic dual of QCD,” *Prog. Theor. Phys.* **114**, 1083 (2005) [arXiv:hep-th/0507073]. [4](#)
- [11] R. C. Myers and S. E. Vazquez, “Quark Soup al dente: Applied Superstring Theory,” *Class. Quant. Grav.* **25**, 114008 (2008) [arXiv:0804.2423 [hep-th]]. [4](#)
- [12] P. Kovtun, D. T. Son and A. O. Starinets, “Viscosity in strongly interacting quantum field theories from black hole physics,” *Phys. Rev. Lett.* **94**, 111601 (2005) [arXiv:hep-th/0405231]. [ix](#), [4](#), [5](#)
- [13] P. Romatschke and U. Romatschke, “Viscosity Information from Relativistic Nuclear Collisions: How Perfect is the Fluid Observed at RHIC?,” *Phys. Rev. Lett.* **99**, 172301 (2007) [arXiv:0706.1522 [nucl-th]]. [4](#)
- [14] S. S. Gubser and A. Karch, “From gauge-string duality to strong interactions: a Pedestrian’s Guide,” *Ann. Rev. Nucl. Part. Sci.* **59**, 145 (2009) [arXiv:0901.0935 [hep-th]]. [4](#)
- [15] D. T. Son and A. O. Starinets, “Viscosity, Black Holes, and Quantum Field Theory,” *Ann. Rev. Nucl. Part. Sci.* **57**, 95 (2007) [arXiv:0704.0240 [hep-th]]. [4](#)
- [16] C. P. Herzog, P. Kovtun, S. Sachdev and D. T. Son, “Quantum critical transport, duality, and M-theory,” *Phys. Rev. D* **75**, 085020 (2007) [arXiv:hep-th/0701036]. [5](#)
- [17] S. A. Hartnoll and P. Kovtun, “Hall conductivity from dyonic black holes,” *Phys. Rev. D* **76**, 066001 (2007) [arXiv:0704.1160 [hep-th]]. [5](#)
- [18] S. A. Hartnoll, P. K. Kovtun, M. Muller and S. Sachdev, “Theory of the Nernst effect near quantum phase transitions in condensed matter, and in dyonic black holes,” *Phys. Rev. B* **76**, 144502 (2007) [arXiv:0706.3215 [cond-mat.str-el]]. [5](#)

- [19] S. A. Hartnoll and C. P. Herzog, “Ohm’s Law at strong coupling: S duality and the cyclotron resonance,” *Phys. Rev. D* **76**, 106012 (2007) [arXiv:0706.3228 [hep-th]]. [5](#)
- [20] S. A. Hartnoll and C. P. Herzog, “Impure AdS/CFT,” *Phys. Rev. D* **77**, 106009 (2008) [arXiv:0801.1693 [hep-th]]. [5](#)
- [21] S. S. Gubser, “Phase transitions near black hole horizons,” *Class. Quant. Grav.* **22**, 5121 (2005) [arXiv:hep-th/0505189].
- [22] S. S. Gubser, “Breaking an Abelian gauge symmetry near a black hole horizon,” *Phys. Rev. D* **78**, 065034 (2008) [arXiv:0801.2977 [hep-th]]. [5](#), [13](#), [88](#)
- [23] S. A. Hartnoll, C. P. Herzog and G. T. Horowitz, “Building a Holographic Superconductor,” *Phys. Rev. Lett.* **101**, 031601 (2008) [arXiv:0803.3295 [hep-th]]. [5](#), [36](#), [88](#)
- [24] S. A. Hartnoll, C. P. Herzog and G. T. Horowitz, “Holographic Superconductors,” *JHEP* **0812**, 015 (2008) [arXiv:0810.1563 [hep-th]]. [5](#), [6](#), [25](#), [26](#), [30](#)
- [25] G. T. Horowitz and M. M. Roberts, “Zero Temperature Limit of Holographic Superconductors,” *JHEP* **0911**, 015 (2009) [arXiv:0908.3677 [hep-th]]. [x](#), [6](#), [45](#), [69](#), [86](#)
- [26] S. S. Gubser and A. Nellore, “Ground states of holographic superconductors,” *Phys. Rev. D* **80**, 105007 (2009) [arXiv:0908.1972 [hep-th]]. [6](#)
- [27] G. Siopsis and J. Therrien, “Analytic calculation of properties of holographic superconductors,” *JHEP* **1005**, 013 (2010) [arXiv:1003.4275 [hep-th]]. [6](#), [37](#), [50](#), [52](#)
- [28] G. Siopsis, J. Therrien and S. Musiri, “Holographic superconductors near the Breitenlohner-Freedman bound,” *Class. Quant. Grav.* **29**, 085007 (2012) [arXiv:1011.2938 [hep-th]].

- [29] T. Faulkner, G. T. Horowitz, J. McGreevy, M. M. Roberts and D. Vegh, “Photoemission ‘experiments’ on holographic superconductors,” arXiv:0911.3402 [hep-th]. [37](#), [86](#)
- [30] G. T. Horowitz and M. M. Roberts, “Holographic Superconductors with Various Condensates,” Phys. Rev. D **78**, 126008 (2008) [arXiv:0810.1077 [hep-th]]. [6](#)
- [31] M. Tinkham and R. A. Ferrell, “Determination of the Superconducting Skin Depth from the Energy Gap and Sum Rule,” Phys. Rev. Lett. **2**, 331 (1959) [6](#), [51](#), [82](#), [86](#)
- [32] T. Albash and C. V. Johnson, “A Holographic Superconductor in an External Magnetic Field,” JHEP **0809**, 121 (2008) [arXiv:0804.3466 [hep-th]].
- [33] T. Albash and C. V. Johnson, “Phases of Holographic Superconductors in an External Magnetic Field,” arXiv:0906.0519 [hep-th]. [6](#)
- [34] G. T. Horowitz, “Introduction to Holographic Superconductors,” arXiv:1002.1722 [hep-th]. [6](#)
- [35] arXiv:0910.1139 [cond-mat.str-el] [6](#)
- [36] J. Polchinski, “Effective Field Theory And The Fermi Surface,” arXiv:hep-th/9210046.
- [37] V. L. Ginzburg and L. D. Landau, Zh. Eksp. Teor. Fiz. **20**, 1064 (1950) [7](#)
- [38] L. P. Gorkov, “Microscopic Derivation of the Ginzburg-Landau Equations in the theory of Superconductivity” Soviet Physics JETP **36**, 1364 (1959) [7](#)
- [39] [9](#)  
G. Koutsoumbas, E. Papantonopoulos and G. Siopsis, “Exact Gravity Dual of a Gapless Superconductor,” JHEP **0907**, 026 (2009) [arXiv:0902.0733 [hep-th]].  
[13](#)

- [40] I. R. Klebanov and E. Witten, “AdS / CFT correspondence and symmetry breaking,” Nucl. Phys. B **556**, 89 (1999) [hep-th/9905104]. [13](#)
- [41] S. S. Gubser and A. Nellore, “Low-temperature behavior of the Abelian Higgs model in anti-de Sitter JHEP **0904**, 008 (2009) [arXiv:0810.4554 [hep-th]].
- [42] P. Breitenlohner and D. Z. Freedman, “Stability In Gauged Extended Supergravity,” Annals Phys. **144**, 249 (1982). [12](#)
- [43] S. A. Hartnoll, “Lectures on holographic methods for condensed matter physics,” Class. Quant. Grav. **26**, 224002 (2009) [arXiv:0903.3246 [hep-th]].
- [44] R. A. Konoplya and A. Zhidenko, “Holographic conductivity of zero temperature superconductors,” Phys. Lett. B **686**, 199 (2010) [arXiv:0909.2138 [hep-th]].
- [45] J. Bardeen, L. N. Cooper, and J. R. Schrieffer, Phys. Rev. **108**, 1175–1204 (1957).
- [46] L. N. Cooper, Phys. Rev. **104**, 1189–1190 (1954). [7](#)
- [47] T. Hertog and K. Maeda, Phys. Rev. D **71**, 024001 (2005) [arXiv:hep-th/0409314]. [13](#)
- [48] E. Dagotto, Rev. Mod. Phys. **66**, 763 (1994).
- [49] S. S. Gubser, C. P. Herzog, S. S. Pufu and T. Tesileanu, “Superconductors from Superstrings,” Phys. Rev. Lett. **103**, 141601 (2009) [arXiv:0907.3510 [hep-th]].
- [50] S. Franco, A. Garcia-Garcia and D. Rodriguez-Gomez, “A general class of holographic superconductors,” JHEP **1004**, 092 (2010) [arXiv:0906.1214 [hep-th]].
- [51] M. M. Roberts and S. A. Hartnoll, “Pseudogap and time reversal breaking in a holographic superconductor,” JHEP **0808**, 035 (2008) [arXiv:0805.3898 [hep-th]].

- [52] S. S. Gubser and S. S. Pufu, “The gravity dual of a p-wave superconductor,” *JHEP* **0811**, 033 (2008) [arXiv:0805.2960 [hep-th]].
- [53] F. Benini, C. P. Herzog, R. Rahman and A. Yarom, “Gauge gravity duality for d-wave superconductors: prospects and challenges,” arXiv:1007.1981 [hep-th].
- [54] D. Vegh, “Fermi arcs from holography,” arXiv:1007.0246 [hep-th].
- [55] J. Bardeen, L. N. Cooper, and J. R. Schrieffer, *Phys. Rev.* **108**, 1175–1204 (1957).
- [56] R. Gregory, S. Kanno and J. Soda, “Holographic Superconductors with Higher Curvature Corrections,” *JHEP* **0910**, 010 (2009) [arXiv:0907.3203 [hep-th]]. [40](#)
- [57] Q. Pan, B. Wang, E. Papantonopoulos, J. Oliveira and A. Pavan, “Holographic Superconductors with various condensates in arXiv:0912.2475 [hep-th]. [40](#)
- [58] R. Flauger, E. Pajer, and S. Papanikolaou, “A striped holographic superconductor”, *Phys. Rev. D* **83** (2011) 064009, [1010.1775](#). [19](#)
- [59] I. Martin, D. Podolsky, and S. A. Kivelson, “Enhancement of superconductivity by local inhomogeneity”, *Phys. Rev. B* **72** (2005) 060502 [19](#)
- [60] A. Aperis, P. Kotetes, E. Papantonopoulos, G. Siopsis, P. Skamagoulis and G. Varelogiannis, “Holographic Charge Density Waves,” *Phys. Lett. B* **702**, 181 (2011) [arXiv:1009.6179 [hep-th]]. [15](#)
- [61] D. Vegh, arXiv:1112.3318 [hep-th]. [90](#)
- [62] N. Iqbal, H. Liu and M. Mezei, “Lectures on holographic non-Fermi liquids and quantum phase transitions,” arXiv:1110.3814 [hep-th]. [90](#)
- [63] G. W. Gibbons and S. W. Hawking, “Classification of Gravitational Instanton Symmetries,” *Commun. Math. Phys.* **66**, 291 (1979). [102](#)

# Appendix



# Appendix A

## Operators and the AdS/CFT Correspondence

In the introduction I stated that at the heart of the AdS/CFT correspondence was the fact that the partition function of the two theories are identical

$$Z_{AdS} = Z_{CFT} \tag{1}$$

Consider the definition of a stress energy tensor from General Relativity

$$T_{\mu\nu} = \frac{\delta S}{\delta g_{\mu\nu}} \tag{2}$$

We are interested in our fields near the boundary, so we expand  $g$  near the boundary

$$g = g_{(0)} + g_{(1)} + \dots \tag{3}$$

and then we perturb  $g_{(0)}$

$$g_{(0)\mu\nu} \rightarrow g_{(0)\mu\nu} + \delta g_{(0)\mu\nu} \tag{4}$$

This perturbation changes the CFT action

$$\delta S = \int d^d x \sqrt{g_{(0)}} \delta g_{(0)\mu\nu} T^{\mu\nu} \quad (5)$$

By imposing (1) we get that

$$Z_{AdS}[g_{(0)} \rightarrow g_{(0)} + \delta g_{(0)}] = \left\langle \exp \left( i \int d^d x \sqrt{g_{(0)}} \delta g_{(0)\mu\nu} T^{\mu\nu} \right) \right\rangle_{CFT} \quad (6)$$

In other words if you perturb a field in AdS, it will source a relevant operator in the CFT. For example a gauge field sources a current because

$$J^\mu = \frac{\delta S}{\delta A_{(0)\mu}} \quad (7)$$

and a scalar field sources an expectation value because

$$\langle \mathcal{O} \rangle = \frac{\delta S}{\delta \phi_0} \quad (8)$$

# Appendix B

## Hawking Temperature

In the text we define the Hawking Temperature without giving much of an explanation. Given a metric of the form

$$ds^2 = -f(r)dt^2 + \frac{dr^2}{f(r)} + dx^2 + dy^2 \quad \text{where } f(r = r_h) = 0 \quad (9)$$

this means that we have a black hole at  $r = r_h$ . Since we are interested in looking at thermodynamics we perform a Wick rotation to euclidanize our action. As a reminder, a partition function

$$Z = \text{Tr} e^{-\beta H} = \int d\phi \int D\Phi e^{-S_E[\Phi]} \quad (10)$$

where  $S_E$  is our euclidanized action. Given a relativistic action, one simply performs a Wick rotation

$$t = -i\tau \quad (11)$$

Which gives eqn (9) a positive signature. By definition  $\tau$  is periodic, and from field theory we know  $\beta \sim \tau \sim \frac{1}{T}$ . While eqn (9) is in a curved space, even after the Wick rotation, the idea is still valid. The signature of the metric is the important part. We can perform a coordinate transformation

$$(\tau, r) \rightarrow (\theta, \rho) \text{ defined by } \rho d\theta = \sqrt{f} d\tau \text{ and } d\rho = \frac{dr}{\sqrt{f}} \quad (12)$$

Our metric then becomes

$$ds^2 = \rho^2 d\theta^2 + dR^2 \times \mathbb{R}^2 = S^2 \times \mathbb{R}^2 \quad (13)$$

This metric contains a bolt singularity (63), and it can be removed by using the fact that  $\tau$  is periodic, one arrives at

$$\begin{aligned} 2\pi &= - \lim_{r \rightarrow r_h} \sqrt{f} \Delta\tau \frac{d(\sqrt{f})}{dr} \\ \therefore \frac{1}{\tau} &= T = - \frac{f'(r_h)}{4\pi} \end{aligned} \quad (14)$$

# Vita

Jason Edward Therrien was born in Orlando Florida on June 14, 1985. In Spring 2003 he graduated from Cookeville High School and began attending the University of Tennessee that fall. In 2007 he began graduate studies at the University of Tennessee. He currently works for Halliburton as a scientist.